Russian Chemical Reviews **74** (8) 697 – 723 (2005) © 2005 Russian Academy of Sciences and Turpion Ltd

DOI 10.1070/RC2005v074n08ABEH001166

Phase equilibria, phases and compounds in the V – C system

V N Lipatnikov

Contents

I. Introduction 697
II. Phase diagrams for the V – C system at temperatures higher than 1000 K and thermodynamic properties of disordered carbides VC_y and $V_2C_{y'}$ 698
III. Ordered phases of nonstoichiometric vanadium carbides 705
IV. Nanocrystalline carbide V_8C_7 and molecular clusters V_mC_n 715
V. Phase diagram for the V – C system with consideration for ordering of VC_y 717
VI. Conclusion 720

Abstract. The review summarises the results of experimental and theoretical investigations dealing with phase equilibria and the synthesis and prediction of new compounds and phases in the vanadium – carbon system. The generalised thermodynamic characteristics of disordered cubic vanadium monocarbide VC_y and lower hexagonal vanadium subcarbide $V_2C_{y'}$, which are the most important compounds in the V – C system, are surveyed. The crystal structures of all known and possible compounds formed by vanadium and carbon, including the V_8C_{12} molecular cluster, are discussed in detail. The phase diagrams for the V – C system taking into account ordering of nonstoichiometric vanadium carbide VC_y are considered. The bibliography includes 149 references.

I. Introduction

Group IV and V d-transition metal carbides are strongly nonstoichiometric interstitial compounds.[1–4] Cubic (with the *B*1-type structure) vanadium carbide VC_y is one of the most interesting compounds of this type. This compound not only has wide practical application but also has been extensively studied by both experimental and theoretical methods.

In 1830, N Selfström isolated a black powder from metallurgical slags from Swedish blast furnaces. This powder contained an unknown element, which was later called vanadium. More recently, this powder was demonstrated to be V_2O_5. In pure form, vanadium was isolated by H Roscoe in 1869. In the early 20th century, it was found that doping of steels with vanadium (in an amount from 0.2 mass % to 0.5 mass %) increases their hardness, toughness, shock strength and resistance to abrasion and wear. Hence, vanadium-containing steels have found wide application in defence technology and engine building, in particular, in the manufacture of air engines and car motors. Detailed investigations demonstrated that the hardness properties of steels are improved because vanadium reacts with carbon dissolved in steels and forms grains of hard and refractory vanadium carbide. Initially, it was speculated that such carbide phases as V_2C_3, V_4C_3 and V_5C_4 were formed.[5–7] However, more recent studies revealed the formation of vanadium carbides, which have basic structures of lower hexagonal carbide $V_2C_{y'}$ or higher cubic carbide VC_y. Vanadium carbides are poorly soluble in iron, which hinders the growth of large crystals. This is favourable for the formation of a homogeneous fine-grained structure in steels.

Cubic vanadium carbide VC_y, like most other transition metal carbides, was synthesised for the first time by H Moissan[8] in 1893 by heating V_2O_5 with coal in the absence of air. It was believed that the composition of the carbide synthesised was close to $VC_{1.0}$. However, more recent studies demonstrated that vanadium carbide prepared by carbothermal reduction contains a large amount of oxygen.

The history of investigations of vanadium carbides and the V – C system can be arbitrarily divided into three periods.

In the first period, from the late 19th century up to 1940, vanadium carbide, like carbides and nitrides of other transition metals (titanium, zirconium, hafnium, niobium and tantalum), was considered as a usual chemical compound with constant composition. At that time, most studies were concerned with the determination of crystal structures and unit cell parameters of vanadium carbide samples prepared by one method or another. It was believed that vanadium carbide had the stoichiometric VC composition.

At the end of the first period (1930 – 1940), researchers started studies of the thermodynamic and various physical properties of carbides and nitrides and revealed numerous discrepancies in the results of investigations of the properties of vanadium carbide. These discrepancies could not be accounted for by experimental errors, the use of various experimental approaches or the presence of impurities in the samples under investigation. Detailed crystal-chemical studies demonstrated that the observed discrepancies were associated with the difference in the carbon content of carbides. It appeared that the composition of vanadium carbide (as well as of all Group IV and V transition metal carbides and nitrides) can vary over a wide range with retention of the crystal structure. The lower boundary of the homogeneity region of cubic vanadium carbide VC_y was long thought to be $VC_{0.75}$. Based on this fact, the authors of the early studies[7,9] suggested the existence of the V_4C_3 phase. Nowadays, it is known that the $VC_{0.65}$ composition corresponds to the lower boundary of the homogeneity region of cubic vanadium carbide. The precise position of the upper boundary has long remained unknown, but it was hypoth-

V N Lipatnikov Institute of Solid State Chemistry, Urals Branch of the Russian Academy of Sciences, ul. Pervomaiskaya 91, 620219 Ekaterinburg, Russian Federation. Fax (7-343) 374 44 95, tel. (7-343) 374 73 06, e-mail: lipatnikov@ihim.uran.ru

Received 9 September 2004
Uspekhi Khimii **74** (8) 768 – 796 (2005); translated by T N Safonova

esised that this boundary is most likely close to the stoichiometric composition $VC_{1.0}$.

In the second period (1940 – 1970), investigations of strongly nonstoichiometric carbides were almost completely concerned with composition – property relationships. Interest in carbides quickened in 1960s, when the influence of the composition on the crystal-chemical, thermodynamic, thermophysical, electrical, magnetic, optical, mechanical and other properties of these compounds were extensively studied. At the same time, the main qualitative views of the nature of chemical bonding in nonstoichiometric carbides were formulated. At the end of the second period, many researchers mistakenly believed that nonstoichiometric carbides had been completely studied. In 1962, the first version of the phase diagram for the V – C system was published.[10,11] In this diagram, the regions of existence of cubic VC_y and hexagonal $V_2C_{y'}$ (β-V_2C) vanadium carbides were shown (Fig. 1). This diagram has remained virtually unchanged for more than two decades.

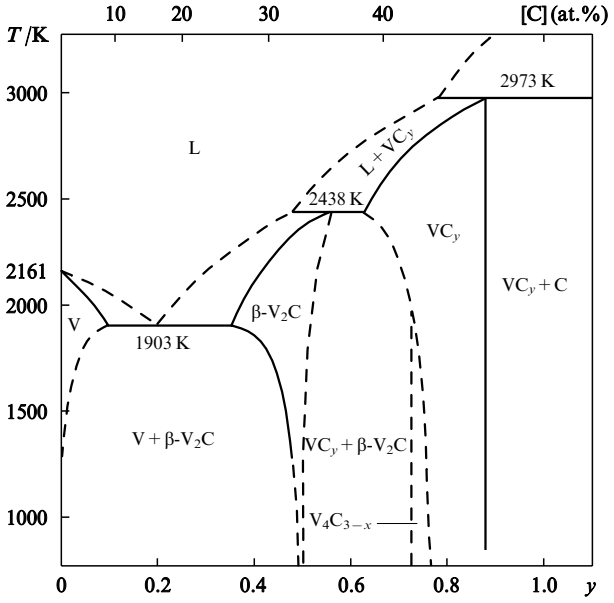


Figure 1. Phase diagram of the V – C system at temperatures higher than 800 K, which was constructed without considering ordered phases.[10]

Once wide homogeneity regions had been found for nonstoichiometric carbides, it was long thought that carbon atoms and structural vacancies (vacant interstitial sites in the metal sublattice) are randomly distributed in the lattice. However, crystallographic studies published in the late 1960s and onward demonstrated that, under particular conditions, interstitial atoms and vacancies can be redistributed over sites of the crystal lattice and form different types of ordered structures. It is nonstoichiometric vanadium carbide in which the first ordered carbide phase, *viz*., V_8C_7, was discovered in 1966.[12] More recently (in 1968), the ordered V_6C_5 phase was found.[13] These studies marked the beginning of the third period of investigations of nonstoichiometric carbides dealing with ordering and its influence on the properties of nonstoichiometric compounds. Nowadays, it is evident that, at temperatures lower than 1000 K, an ordered state of nonstoichiometric carbides is in thermodynamic equilibrium, whereas a disordered state is metastable in this temperature range.

Studies of the properties of nonstoichiometric carbides depending on the distribution of carbon atoms and vacancies demonstrated that the changes in the properties upon ordering are comparable in magnitude with the changes in these properties associated with variations in the composition of nonstoichiometric carbide within the homogeneity region of an ordered phase. Therefore, the change in the composition of carbides, on the one hand, and redistribution of atoms and vacancies in the crystal lattice of carbides, on the other hand, are two equally probable ways of controlling the properties of these substances. However, the characteristic feature of ordering as a way of providing fine control over the properties of nonstoichiometric carbides is that it changes the properties of carbides, while the chemical composition remains unchanged.

In the last decade of the 20th century, a large number of ordered phases of nonstoichiometric carbides, which have been found experimentally, and the development of methods of calculations of phase equilibria made it possible to construct the phase diagrams for the M – C systems (M = Ti, Zr, Hf, V, Nb or Ta),[1–4,14–34] which take into account not only the presence of strongly nonstoichiometric carbides MC_y ($MC_y\square_{1-y}$, where $\square$ is a structural vacancy) but also their ordering at temperatures lower than 1200 – 1300 K.

In 1992, a new class of molecular metal carbon nanoclusters M_8C_{12} was discovered (see Refs 35 and 36) and the stable molecular cluster V_8C_{12} was detected in vaporisation products of the V – C system.

Therefore, considerable information on phase equilibria and compounds in the V – C system had been accumulated by the turn of the 20th century. The phase diagram for this system appeared to be much richer and more complex than had been assumed earlier. The aim of the present review is to generalise experimental and theoretical data on compounds and phases in the V – C system published in the last 15 years with consideration for the earlier results. Emphasis is given to the phase equilibria and crystal structures of phases and compounds consisting of vanadium and carbon.

II. Phase diagrams for the V – C system at temperatures higher than 1000 K and thermodynamic properties of disordered carbides VC_y and $V_2C_{y'}$

1. Phase diagrams

The V – C system is among the best-studied systems formed by transition metals and carbon. The first version of the phase diagram for the V – C system (see Fig. 1), which takes into consideration the presence of the cubic and hexagonal carbide phases VC_y and $V_2C_{y'}$ (β-V_2C) characterised by homogeneity regions, was proposed in the study.[10] Later on, phase equilibria in this system were considered in the studies,[37–39] where 17 samples with different vanadium and carbon contents, their phase compositions and structures were studied by X-ray diffraction, differential thermal analysis and the metallographic method. The phase equilibria in the V – C system were analysed in the study.[40]

The melting point of vanadium metal determined in different studies is 2161 ± 10,[10] 2199 ± 6 (see Refs 37 – 39) or 2183 K.[40] The addition of carbon to vanadium leads to a decrease in the melting point to the eutectic temperature [1923 ± 7,[37–39] 1921 (see Ref. 40) or 1923 K (see Ref. 41)]. The $L \rightleftarrows V + V_2C_y$ eutectic mixture contains ~15 at.% carbon.[37,38,40,41] An increase in the carbon content leads to an increase in the melting point from the eutectic temperature to the temperature of the peritectoid transformation $L + VC_y \rightleftarrows V_2C_{y'}$, which was evaluated at 2438 (see Ref. 10) or 2460 ± 10 K.[37–39] Congruently melting carbide $VC_{0.74-0.77}$,[37,38] $VC_{0.81}$ (see Ref. 40) or $VC_{0.83}$ (see Ref. 41) has the highest melting point [2921 ± 12,[37–39] 2929 (see Ref. 40) or 3073 K,[41] respectively]. The temperature of the eutectic $L \rightleftarrows VC_y + C$ containing 49.5 ± 0.5 at.% or 53.5 at.% carbon is 2898 ± 12 (see Refs 37 and 38) or 2943 K,[40] respectively.

The phase diagrams for the V – C system, which were proposed in the studies[41,42] with consideration for possible ordered vanadium carbide phases, are presented in Figs 2 and 3. The first attempt to construct a region of the phase diagram for the V – C system corresponding to the co-existence of the ordered V_6C_5 and

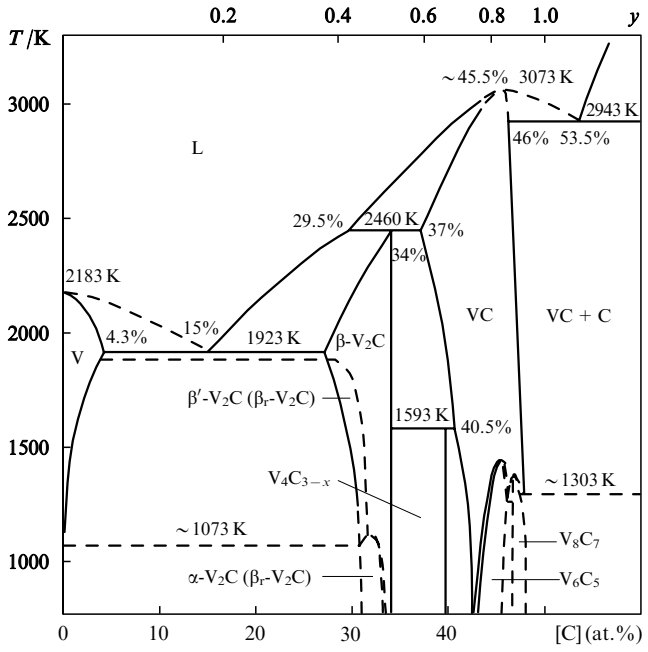


Figure 2. Phase diagram of the V – C system at temperatures higher than 800 K.[41]

α-V_2C (β_r-V_2C) and β′-V_2C (β_h-V_2C) are the low-temperature orthorhombic and high-temperature hexagonal ordered phases, respectively, of lower hexagonal disordered carbide $V_2C_{y'}$ (β-V_2C); V_6C_5 and V_8C_7 are the ordered phases of nonstoichiometric cubic carbide VC_y; V_4C_{3-x} ($x = 0.2-0.5$) is an individual compound belonging to the rhombohedral (trigonal) system, which presumably has the composition $VC_{0.67}$; the composition and the temperature range of existence of the V_4C_{3-x} compound presented in the figure are inconsistent with the most reliable experimental data.

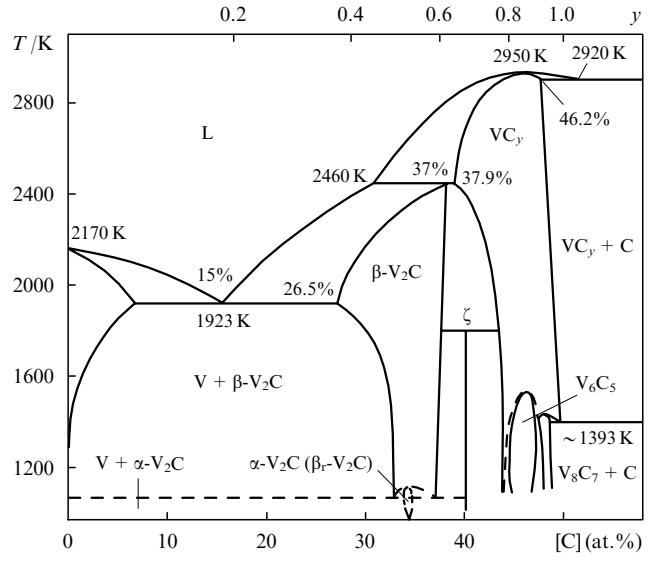


Figure 3. Phase diagram of the V – C system at temperatures higher than 1000 K.[42]

α-V_2C (β_r-V_2C) is the orthorhombic ordered phase of lower hexagonal carbide $V_2C_{y'}$ (β-V_2C); V_6C_5 and V_8C_7 are the ordered phases of nonstoichiometric cubic carbide VC_y; ζ is the rhombohedral (trigonal) phase ζ-V_4C_{3-x} ($x = 0.2-0.5$), whose composition corresponds to V_3C_2 ($VC_{0.67}$); the position of the ζ-V_4C_{3-x} phase presented in the figure is inconsistent in the composition and temperature range with experimental data.

V_8C_7 phases was made in the study.[43] In the publication,[41] an ordered region was hypothesized to exist in the phase diagram, and this region was identical to that reported in the study.[43] In the review,[40] the ordering was not discussed at all and was not reflected in the phase diagram of the V – C system.

Analysis of the phase diagram presented in Fig. 2 shows that hexagonal lower carbide $V_2C_{y'}$ (β-V_2C) has a rather extended homogeneity region from $VC_{0.45-0.46}$ to $VC_{0.52-0.56}$ at 1200 K. The homogeneity region of $V_2C_{y'}$ is expanded with increasing temperature. At 1923 K (the temperature of the eutectic $L \rightleftarrows V + V_2C_{y'}$), hexagonal carbides $VC_{0.36-0.37}$ and $VC_{0.52-0.58}$ correspond to the lower and upper boundaries of the homogeneity region, repectively. A decrease in the temperature can be accompanied by ordering of lower hexagonal carbide $V_2C_{y'}$ giving rise to the orthorhombic ordered α-V_2C (β_r-V_2C) phase.[44] The precise temperature of the disorder – order phase transition $V_2C_{y'} \rightleftarrows$ α-V_2C (β_r-V_2C) is unknown. According to the results of different studies, this temperature varies from 1100 to 1600 K. Data on the crystal structures of the β′-V_2C (β_h-V_2C) and β-V_2C ($V_2C_{y'}$) phases are also available in the literature. Both phases have a hexagonal metal sublattice, but differ in the distribution of carbon atoms. The former phase is an ε-Fe_2N-type ordered hexagonal phase, and the latter phase is a disordered hexagonal phase with the $L'3$ (W_2C) structure. From this fact it follows that the β′-V_2C (β_h-V_2C) $\rightleftarrows$ β-V_2C ($V_2C_{y'}$) transformation can occur. These hypothetical phase equilibria are shown in Fig. 2 by dashed lines.

Cubic carbide VC_y has a wide homogeneity region from $VC_{0.72}$ to $VC_{0.88}$ at 1500 K and from $VC_{0.60}$ to $VC_{0.87}$ at ~2450 K. This is the only compound among strongly nonstoichiometric carbides, which is characterised by the upper boundary of the homogeneity region most remote from the stoichiometric composition $MC_{1.0}$. At temperatures lower than 1500 K, the homogeneity region of nonstoichiometric cubic carbide VC_y has two ordered phases, *viz*., V_6C_5 with monoclinic[43,45] or trigonal[13] symmetry and the cubic V_8C_7 phase.[12,46–49] The ordered V_6C_5 phases are characterised by a rather extended homogeneity region, whereas the homogeneity region of the V_8C_7 phase is small.

The phase diagrams (see Figs 2 and 3) show also the ζ-V_4C_{3-x} phase consistent with the $VC_{0.67}$ composition (V_3C_2). This phase has a rhombohedral (trigonal) structure and is an individual compound of the V – C system, although it is sometimes erroneously called (see, for example, Ref. 42) the ordered carbide phase VC_y. The ζ-V_4C_{3-x} phase does not belong to ordered phases of cubic carbide, because its metal sublattice has trigonal rather than cubic symmetry. According to the results of the study,[10] ζ-V_4C_{3-x} exists only at temperatures lower than 1617 K and decomposes through a peritectoid reaction at $T \geqslant 1617$ K. However, the ζ-V_4C_{3-x} phase was observed at higher temperatures (up to 1870 K) in the studies.[38,50,51] According to the latest and most reliable experimental data,[52] the ζ-V_4C_{3-x} phase contains 37.9 at.% C and has a very narrow (~0.4 at.% C) homogeneity region from $VC_{0.605}$ to $VC_{0.615}$. The minimum temperature, at which this phase was detected after 78-hour annealing, is 1540 K. The temperature of peritectoid decomposition of the ζ-phase during heating is 2150 K.[52] Therefore, the composition and the temperature range of existence of the ζ-V_4C_{3-x} phase in the diagrams of the V – C system (see Figs 2 and 3) are not quite correct. Data on the crystal structures of the phases in the V – C system and the special points in its phase diagram at $T > 1000$ K are given in Tables 1 and 2.

The phase equilibria associated with ordering of nonstoichiometric vanadium carbide VC_y and occurring at temperatures lower than 1300 – 1400 K have been described in detail[1,3,4,15,19,28,47,48,53,54] and will be considered below.

Table 1. Crystal structures of the phases existing in the V–C system at temperatures higher than 1000 K.

Phase	[C] (at.%)	Space group	Pearson symbol	Lattice type
V	0–4.3	$Im\bar{3}m$ (O_h^9)	$cI2$	$A2$ (W)
α-V_2C (β_r-V_2C)	~31.0–33.0	$Pbcn$ (D_{2h}^{14})	$oP12$	ζ-Fe_2N
β-V_2C ($V_2C_{y'}$)	~27.0–34.0	$P6_3/mmc$ (D_{6h}^4)	$hP3$	$L'3$ (W_2C)
β′-V_2C (β_h-V_2C)	~27.5–31.5	$P\bar{3}m1$ (D_{3d}^3)	$hP9$	Ni_3N (ε-Fe_2N)
ζ-V_4C_{3-x}	~37.6–40.1	$R\bar{3}m$ (D_{3d}^5)	$hR20$	–
VC_y	~37.0–48.0	$Fm\bar{3}m$ (O_h^5)	$cF8$	$B1$ (NaCl)
V_6C_5	~43.0–46.0	$C2$ (C_2^3)	$mC44$	–
V_6C_5	~43.0–46.0	$P3_1$ (C_3^2)	$hP33$	–
V_8C_7	~46.0–47.0	$P4_332$ (O^6)	$cP60$	–
C	100	$P6_3/mmc$ (D_{6h}^4)	$hP4$	$A9$ (graphite)

Table 2. Parameters of the special points in the phase diagram of the V–C system at temperatures higher than 1000 K.

Reaction	Compositions of phases involved in the reaction (at.% C)			T/K	Reaction type
$L \rightleftarrows V + V_2C_{y'}$ (β-V_2C)	15.0	4.3	27.0	1923 ± 7	eutectic
$L + VC_y \rightleftarrows V_2C_{y'}$ (β-V_2C)	29.5	37.0	34.0	2460 ± 10	peritectic
$L \rightleftarrows VC_y$	–	45.5	–	3073 ± 10	congruent melting
$L \rightleftarrows VC_y + C$	53.5	46.0	~100	2943 ± 3	eutectic
$V_2C_{y'}$ (β-V_2C) + $VC_y \rightleftarrows \rightleftarrows \zeta$-$V_4C_{3-x}$	35.1	39.5	37.9	2150	peritectoid
$L \rightleftarrows V$	–	0	–	2183 ± 3	melting
$VC_y \rightleftarrows V_6C_5$	–	45.5	–	~1500	ordering
$VC_y \rightleftarrows V_8C_7$	–	46.6	–	~1400	"

2. Structures and thermodynamic properties of disordered vanadium carbides

a. Structures

Cubic ($B1$ structure type) disordered vanadium monocarbide VC_y is the most important compound existing in the V–C system at temperatures higher than 1000 K (Table 3). The width of the homogeneity region of VC_y depends on the temperature. The solid-state synthesis of vanadium monocarbide is generally carried out at ~2000 K followed by quenching to room temperature, which makes it possible to retain cubic carbide VC_y in the disordered state. At 2000 K, disordered cubic vanadium carbide has a homogeneity region from $VC_{0.65}$ to $VC_{0.88}$. This region ($0.65 \leqslant y \leqslant 0.88$) was reported in most of the published data. The unit cell of VC_y can be described as two face-centred (metal and non-metal) sublattices, which are shifted with respect to each other by one-half of the lattice period (Fig. 4). In the metal sublattice, all sites are occupied by vanadium atoms. In the non-metal (carbon) sublattice, the number of sites is larger than the number of interstitial atoms. In the disordered state (which is thermodynamically at equilibrium only at $T > 1300$–1400 K, whereas it is retained as a quenched metastable state at lower temperatures), the carbon atoms are randomly distributed over the sites, and all sites of the non-metal sublattice are occupied with the same probability equal to y (the relative carbon content of VC_y). This provides retention of cubic symmetry of the disordered non-metal sublattice and signifies that all sites of the carbon sublattice in disordered VC_y are crystallograpically equivalent. The typical X-ray diffraction pattern of homogeneous cubic vanadium carbide is shown in Fig. 5. A high degree of homogeneity of carbide $VC_{0.83}$ is evidenced by splitting of the $K_{\alpha 1}$ and $K_{\alpha 2}$ doublets observed already for the $(311)_{B1}$ reflection. The crystal

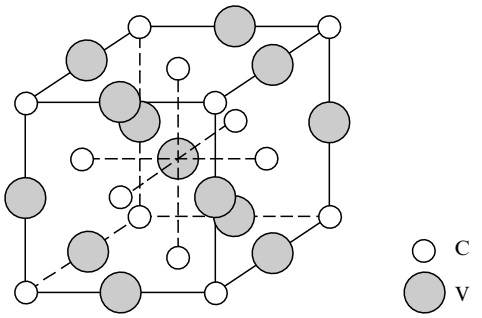


Figure 4. The unit cell of cubic disordered nonstoichiometric vanadium monocarbide VC_y [the $B1$ structure type (NaCl)].
All sites of the metal sublattices are occupied by vanadium atoms, the sites of the non-metal sublattice are randomly (with probability y) occupied by carbon atoms.

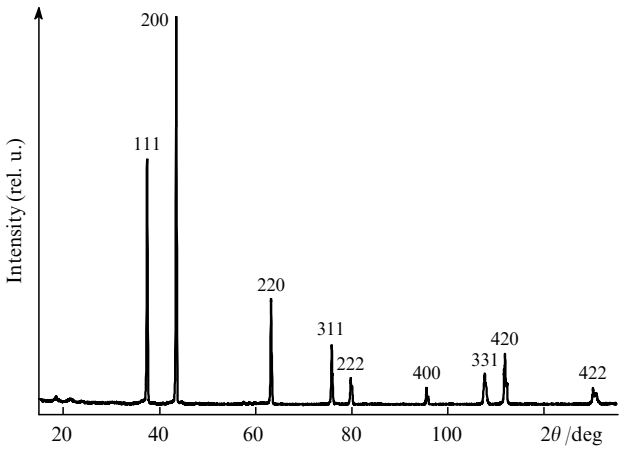


Figure 5. X-Ray diffraction pattern of disordered homogeneous carbide $VC_{0.83}$ with a $B1$-type cubic structure (Cu $K\alpha_{1,2}$ radiation).
$a_{B1} = 0.41596$ nm.[25]

Table 3. Characteristics of cubic and hexagonal disordered nonstoichiometric vanadium carbides.

Phase	Symmetry	Space group	Lattice type	Atom	Position and multiplicity	Atomic coordinates			Probability of occupancy
						x	y	z	
VC_y	cubic	$Fm3m$ (O_h^5)	$B1$ (NaCl)	V	4(a)	0	0	0	1
				C	4(b)	1/2	1/2	1/2	y
$V_2C_{y'}$	hexagonal	$P6_3/mmc$ (D_{6h}^4)	$L'3$ (W_2C)	V	2(a)	0	0	0	1
				C	2(c)	1/3	2/3	1/4	$y'/2$

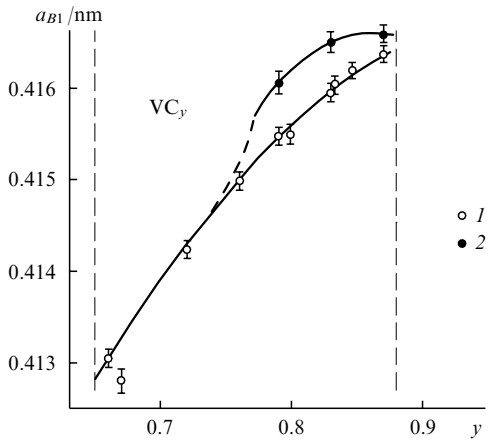


Figure 6. Plot of the parameter a_{B1} of the basic cubic crystal lattice *vs*. the composition of carbide VC_y in quenched disordered (*1*) and annealed ordered (*2*) states.[25]
The boundaries of the homogeneity region of carbide VC_y are shown by vertical bars.

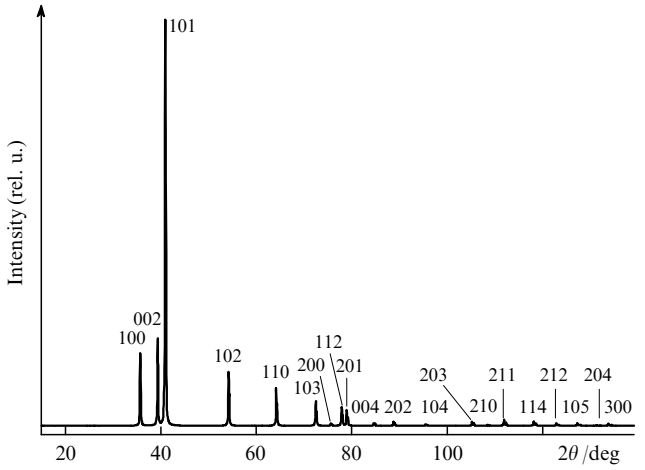


Figure 8. X-Ray diffraction pattern of disordered homogeneous lower vanadium carbide V_2C ($VC_{0.50}$) with a $L'3$-type hexagonal structure (Cu $K\alpha_{1,2}$ radiation).
$a = 0.2902$ nm, $c = 0.4577$ nm.

lattice period of both disordered and ordered VC_y increases with increasing carbon content (Fig. 6).

Lower vanadium carbide $V_2C_{y'}$ (β-V_2C), which is also called semicarbide or subcarbide, has a hexagonal structure of the $L'3$ (W_2C) type. In this structure, carbon atoms randomly occupy no more than one-half of all octahedral interstitial sites in the metal sublattice (Fig. 7). Since it cannot be unambiguously determined which sites of the non-metal sublattice are occupied by carbon atoms, and which sites are, on the contrary, vacant, the probability of finding a carbon atom in each site of the non-metal sublattice of lower vanadium carbide $V_2C_{y'}$ is $y'/2$ (see Table 3). The width of the homogeneity region of disordered lower vanadium carbide quenched to high temperatures is small, from $VC_{0.42-0.45}$ to $VC_{0.50}$. The volume of its unit cell enriched in carbon slightly increases. The unit cell parameters of the carbide of stoichiometric composition V_2C ($VC_{0.50}$) are larger than those of $V_2C_{0.94}$ ($VC_{0.47}$) ($a = 0.2902$ and $c = 0.4577$ nm as opposed to $a = 0.2885$ and $c = 0.4571$ nm). The X-ray diffraction pattern of disordered lower vanadium carbide V_2C ($VC_{0.50}$) with a hexagonal lattice of the $L'3$ (W_2C) type is shown in Fig. 8.

The thermodynamic properties of nonstoichiometric vanadium carbides vary substantially within their homogeneity regions. Hence, investigations, in which the measured thermodynamic characteristics were assigned to a particular composition of carbide in the known structural (disordered or ordered) state, are of great interest. The temperature and concentration dependences of the thermodynamic characteristics of disordered carbides allow the quantitative description of high-temperature phase equilibria involving VC_y and $V_2C_{y'}$. Besides, disorder – order phase transformations and transitions between ordered phases can be directly studied with the use of these data. However, available results of experimental thermodynamic investigations of nonstoichiometric vanadium carbides, whose compositions and crystal structures were well characterised, are scarce.

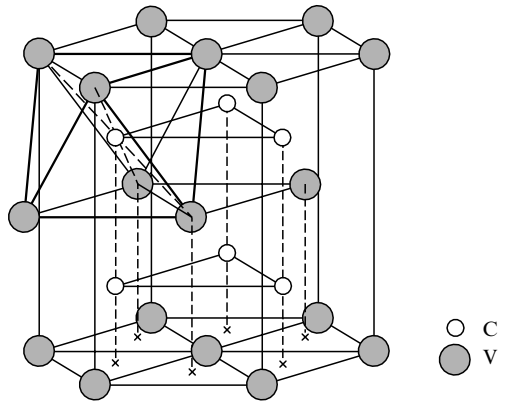


Figure 7. Hexagonal (space group $P6_3/mmc$) structure of the $L'3$ (W_2C) type of lower vanadium carbide $V_2C_{y'}$.
Metal atoms form a hexagonal close-packed lattice, in which one-half or less than one-half of octahedral interstitial sites are randomly occupied by carbon atoms.

b. Enthalpy of formation

The enthalpies of formation of cubic carbide VC_y with different carbon contents were determined [55, 56] by calorimetry from the thermal effects of combustion in oxygen:

Carbide	$\Delta H^\circ_{f\,298}$ /kJ mol^{-1}	Carbide	$\Delta H^\circ_{f\,298}$ /kJ mol^{-1}
$VC_{0.72}$	-90.5 ± 5.6	$VC_{0.82}$	-111.7 ± 4.1
$VC_{0.76}$	-108.2 ± 7.0	$VC_{0.84}$	-98.9 ± 4.2
$VC_{0.77}$	-101.6 ± 5.4	$VC_{0.88}$	-100.3 ± 5.9 (see Ref. 55)
$VC_{0.80}$	-96.7 ± 12.0	$VC_{0.88}$	-112.2 ± 4.7 (see Ref. 56)

The empirical dependence of the enthalpy of formation on the composition of cubic carbide VC_y for the range $0.72 \leqslant y \leqslant 0.88$ was described [56] by a linear function

$$\Delta H^\circ_{f\,298}(y) = -48.3 - 66.3y \pm 6.7 \text{ (kJ mol}^{-1}\text{)}.$$

In the study,[57] the enthalpy of formation of carbide $VC_{0.88}$ was estimated at -100.9 ± 2.9 kJ mol^{-1}.

However, analysis of the experimental results [55–57] taking into account experimental errors demonstrated [58] that the enthalpy of formation of cubic VC_y is square function of the carbon content and, for the range $0.70 \leqslant y \leqslant 0.88$, takes the form

$$\Delta H^\circ_{f\,298}(y) = 104.78 - 437.73y + 224.02y^2 \text{ (kJ mol}^{-1}\text{)}. \quad (1)$$

As mentioned above, the characteristic feature of cubic carbide VC_y is that the upper boundary of its homogeneity region corresponds to $VC_{0.875}$ and is far from the equiatomic composition $VC_{1.0}$. All attempts to synthesise stoichiometric carbide $VC_{1.0}$ failed. However, the thermodynamic characteristics were theoretically estimated. The enthalpy of formation of hypothetical carbide $VC_{1.0}$ was evaluated [59] at -117.2 ± 41.9 kJ mol^{-1}. In the study,[60] the energy of formation of structural vacancies in cubic carbide VC_y was calculated from the experimental data [56] and the

standard enthalpy of formation $\Delta H^{\circ}_{f\,298}$ of the stoichiometric compound $VC_{1.0}$ was estimated at -105.9 ± 2.9 kJ mol^{-1}. According to the results of the study,[60] the enthalpy of formation linearly depends on the composition of cubic carbide VC_y in the composition region from $VC_{0.65}$ to $VC_{1.0}$.

$$\Delta H^{\circ}_{f\,298}(y) = -91.4 - 14.5y \text{ (kJ mol}^{-1}\text{)}. \quad (2)$$

It should be noted that the enthalpy difference between carbide $VC_{0.88}$ and hypothetical $VC_{1.0}$ calculated by Eqns (1) and (2) is small (2.0 and 1.7 kJ mol^{-1}, respectively). The small enthalpy difference corresponds to the small difference in the free energy of formation of these compounds, which can be compensated by the contribution of the configurational entropy of non-stoichiometric carbide. As a result, carbide $VC_{0.88}$ can have a lower free energy than stoichiometric carbide $VC_{1.0}$, due to which imperfect carbide $VC_{0.88}$ rather than stoichiometric carbide $VC_{1.0}$ exists in equilibrium with carbon. This situation cannot occur, for example, in the case of carbide TiC_y, because its free energy depends more strongly on the composition compared to vanadium carbide. This is evident from the enthalpy differences. For titanium carbides $TiC_{0.88}$ and $TiC_{1.0}$, this difference is 16.5 kJ mol^{-1},[28] *i.e.*, it is 7–8 times larger than that for carbides $VC_{0.88}$ and $VC_{1.0}$.

The dependence of the enthalpy of formation (in kJ mol^{-1}) on the composition of lower carbide $V_2C_{y'} \equiv VC_y$ ($y \leqslant 0.5$) determined in the study[61] can be described by the following function:

$$\Delta H^{\circ}_{f\,298}(y) = -42.2 - 53.7y \pm 2.6,$$

according to which the enthalpy of formation of carbide V_2C ($VC_{0.5}$) is

$$\Delta H^{\circ}_{f\,298\ V_2C} = 2\,\Delta H^{\circ}_{f\,298\ VC_{0.5}} = -138.1 \text{ kJ mol}^{-1}.$$

Apparently, this value is underestimated in magnitude. In the study,[57] the enthalpy of formation of V_2C was estimated at -147.4 ± 21.0 kJ mol^{-1}, which is more realistic.

c. Enthalpy (heat content)

The enthalpies $(H^{\circ}_T - H^{\circ}_{298})$ of cubic VC_y with different carbon contents were measured at 500–1500,[62] 1300–2500 (see Ref. 63) and 400–1100 K (see Ref. 64) and approximated by the polynomials

$$H^{\circ}_T - H^{\circ}_{298} = A + BT + CT^2 + DT^{-1}. \quad (2a)$$

In the study,[62] the enthalpies of several samples of lower vanadium carbide $V_2C_{y'}$ (VC_y for $y \leqslant 0.5$) with different carbon contents were also measured.The measured temperature dependences $(H^{\circ}_T - H^{\circ}_{298})$ show a jump increase in the enthalpy at $\sim$1385 K associated with the disorder–order transition. The polynomials proposed in this study, can be considered as suitable for the description of the enthalpy in the temperature range from 300 to 1385 K. The polynomials reported in the studies[62,63] do not quite satisfy the evident normalisation condition at $T = 298$ K

$$H^{\circ}_T - H^{\circ}_{298} \equiv 0.$$

Hence, in the present review, the preliminary results of measurements[62,63] were processed taking into account this condition. The polynomial coefficients are given in Table 4.

The enthalpies of vanadium carbides containing small amounts of oxygen and nitrogen, for example, of $V(C_{0.995}O_{0.002}N_{0.003})_{0.813}$, were measured in the study.[64] The composition of the latter carbide was written as $VC_{0.813}$. However, the carbon content in this formula is overestimated. Hence, the index for carbon presented in Table 4 is written according to its actual content.

The empirical temperature and concentration dependence of the enthalpy (in kJ mol^{-1}) of disordered cubic carbide was obtained from the data given in Table 4,

$$\begin{aligned}(H^{\circ}_T - H^{\circ}_{298})_{VC_y} = {} & (-7.69 + 26.95\times10^{-3}T + \\ & + 11.84\times10^{-6}T^2 - 416T^{-1}) + \\ & + (0.24 - 18.29\times10^{-3}T - 11.75\times10^{-6}T^2 + 1864T^{-1})y + \\ & + (-12.66 + 42.47\times10^{-3}T)y^2.\end{aligned} \quad (3)$$

This dependence allows one to estimate the enthalpy of VC_y for all y in the temperature range from 300 to 2000 K.

The enthalpy $(H^{\circ}_T - H^{\circ}_{298})_{V_2C}$ (in kJ mol^{-1}) of hexagonal carbide V_2C (β-V_2C) is twice as high as the enthalpy of hexagonal $VC_{0.5}$

$$(H^{\circ}_T - H^{\circ}_{298})_{V_2C} = 2\,(H^{\circ}_T - H^{\circ}_{298})_{VC_{0.5}}.$$

The temperature dependence, which was determined from the results of the study[62] and refined taking into account the normalisation condition $(H^{\circ}_T - H^{\circ}_{298}) \equiv 0$ at $T = 298$ K, takes the form

$$\begin{aligned}(H^{\circ}_T - H^{\circ}_{298})_{V_2C} = {} & -33.58 + 83.12\times10^{-3}T + \\ & + 1.7\times10^{-6}T^2 + 2580T^{-1}.\end{aligned} \quad (4)$$

This dependence is valid for the temperature range from 300 to 1600 K.

Table 4. Coefficients of the temperature dependence of enthalpy for hexagonal ($VC_{0.42}$, $VC_{0.45}$, $VC_{0.51}$) and cubic vanadium carbides VC_y [see Eqn (2a)].

VC_y	A /kJ mol^{-1}	$10^3\,B$ /kJ mol^{-1} K^{-1}	$10^6\,C$ /kJ mol^{-1} K^{-2}	D /kJ K mol^{-1}	T /K	Ref.
$VC_{0.42}$	−15.283	38.573	0.716	1109.9	300–1385	62
$VC_{0.45}$	−15.883	40.017	0.572	1164.3	300–1585	62
$VC_{0.51}$	−16.790	41.562	0.849	1290.0	300–1585	62
$VC_{0.70}$	−17.589	43.702	1.214	1328.5	300–1585	62
$VC_{0.72}$	−9.397	29.051	8.366	0	1300–2000	63
$VC_{0.75}$	−9.613	29.470	9.355	0	1300–2000	63
$VC_{0.75}$ (see [a])	−15.422	45.043	5.091	460.9	300–1100	64
$VC_{0.76}$	−17.591	43.756	1.549	1315.5	300–1585	62
$VC_{0.81}$ (see [a])	−14.778	43.132	6.746	395.0	300–1100	64
$VC_{0.84}$ (see [a])	−17.156	47.473	4.043	789.8	300–1100	64
$VC_{0.84}$	−17.630	43.827	2.093	1306.3	300–1385	62
$VC_{0.86}$	−17.822	43.999	2.412	1339.8	300–1385	62
$VC_{0.86}$	−12.378	39.851	5.656	0	1300–2000	63
$VC_{0.87}$ (see [a])	−18.056	50.062	2.158	877.8	300–1100	64
$VC_{0.88}$ (see [a])	−16.775	46.186	4.064	789.8	300–1100	64
$VC_{0.88}$	−16.908	42.324	2.730	1207.9	300–1385	62

[a] The compositions of carbides VC_y determined in the study[64] are given in accordance with the real carbon content.

The enthalpies of hexagonal carbide $VC_{0.46}$ and cubic carbides $VC_{0.71}$, $VC_{0.83}$ and $VC_{0.86}$ in the temperature range of 400 – 1300 K were also experimentally determined in the studies.[65,66] These enthalpies are apparently slightly underestimated.

d. Heat capacity and entropy

The heat capacities of hexagonal and cubic vanadium carbides $VC_{0.46}$, $VC_{0.53}$, $VC_{0.71}$, $VC_{0.83}$ and $VC_{0.86}$ were measured [65,67] in the temperature range from 10 to 300 K by adiabatic calorimetry. The preliminary results of measurements were described in the publication.[67] The tabulated heat capacities, enthalpies and entropies of these carbides (Tables 5 and 6) were published in the study.[65] The experimental error was no higher than 1%.

Table 5. Heat capacities C_p (J g-atom^{-1} K^{-1}), $\Delta S_T^\circ = S_T^\circ - S_{10}^\circ$ (J g-atom^{-1} K^{-1}) and $H_T^\circ - H_{10}^\circ$ (J g-atom^{-1}) for hexagonal carbides $VC_{0.46}$ and $VC_{0.53}$ in the temperature range of 10 – 300 K.[65,67]

T/K	$VC_{0.46}$			$VC_{0.53}$		
	C_p	$H_T^\circ - H_{10}^\circ$	ΔS_T°	C_p	$H_T^\circ - H_{10}^\circ$	ΔS_T°
10	0.008	–	–	0.008	–	–
50	1.629	21.0	0.544	1.390	17.0	0.461
100	7.360	268.8	3.475	6.720	219.8	3.056
150	11.70	753.6	6.783	11.02	674.1	6.615
200	14.82	1419.3	10.59	14.28	1310.5	10.26
250	17.16	2223.2	14.19	16.78	2089.2	13.73
273	17.99	2625.1	15.70	17.72	2487.0	15.24
298	18.80	3085.7	17.33	18.54	2939.1	16.87
300	18.86	3127.5	17.46	18.62	2976.8	17.00

The temperature dependence of the heat capacity (in J mol^{-1} K^{-1}) of hypothetical stoichiometric vanadium carbide $VC_{1.0}$ was calculated.[60]

$$C_p(T) = 38.4 + 0.017T - 1351.5T^{-1}. \quad (5)$$

The heat capacity of this carbide determined at 300 K (39.0 J mol^{-1} K^{-1}) is, apparently, overestimated. For comparison, the heat capacities of carbides $VC_{0.71}$, $VC_{0.83}$ and $VC_{0.86}$ were evaluated at 30.50, 31.95 and 32.10 J mol K^{-1}, respectively.[65]

The heat capacities of ordered carbides $VC_{0.79}$, $VC_{0.83}$ and $VC_{0.87}$ were measured [25,26,68,69] in the temperature range from 300 to 1570 K by differential scanning calorimetry. The temperature dependences of the heat capacity at $T > 1300$ K show peaks characteristic of order – disorder phase transitions.

The heat capacities of $VC_{0.76}$, $VC_{0.80}$, $VC_{0.85}$ and $VC_{0.87}$ in the temperature range of 1 – 20 K were measured in the study.[70] At $T < 5$ K, the heat capacity is described by the dependence

$$C_p(T) = \gamma T + \alpha T^3 + \beta T^5.$$

Taking into account the method used for the synthesis, the obtained carbides were, apparently, disordered. Nevertheless, with the reference to optical anisotropy of $VC_{0.85}$ observed in reflected white light, the authors of the study [70] hypothesised that this sample can contain the ordered V_6C_5 phase.

According to the results of the investigation,[65] the entropies S_{298}° of nonstoichiometric cubic carbides $VC_{0.71}$, $VC_{0.83}$ and $VC_{0.86}$ are 14.99, 13.57 and 13.31 J g-atom^{-1} K^{-1} (see Tables 5 and 6) or 25.62, 24.83 and 24.76 J mol^{-1} K^{-1}, respectively. These values were used to calculate the dependence of the entropy (J mol^{-1} K^{-1}) on the composition of cubic vanadium carbide

$$S_{298}^\circ(y) = 40.21 - 32.77y + 17.22y^2. \quad (6)$$

The entropy S_{298}° of hexagonal $VC_{0.53}$ is 16.87 J g-atom^{-1} K^{-1} (see Table 5) or 25.81 J mol^{-1} K^{-1}. Hence, the entropy of lower carbide V_2C (β-V_2C) of stoichiometric composition can be estimated at 51 – 52 J mol^{-1} K^{-1}. This entropy of hexagonal carbide β-V_2C is, apparently, underestimated. In the study,[71] the change in the entropy upon the formation of β-V_2C was evaluated at -4.2 J mol^{-1} K^{-1}. Hence it follows that

$$S_{298\ V_2C}^\circ = 2S_{298\ V}^\circ + S_{298\ C}^\circ + \Delta S_{298}^\circ.$$

Taking into account the entropies of vanadium metal ($S_{298\ V}^\circ = 28.67$ J mol^{-1} K^{-1}) [72] and carbon ($S_{298\ C}^\circ = 5.39$ J mol^{-1} K^{-1}),[73] $S_{298\ V_2C}^\circ$ for lower vanadium carbide is 58.53 J mol^{-1} K^{-1}.

e. Free energy

It was demonstrated [28,74] that the part of the free energy (F) of the disordered MX_y compound, which does not include components accounting for the contribution of the configurational entropy $S_c(y,0)$, is

$$F_0(T) + yF_1(T) + y^2F_2(T) = \Delta H_{f\,298}^\circ(y) + (H_T^\circ - H_{298}^\circ)_{MX_y} - (7)$$
$$-T\left[S_{298}^\circ(y) + \int_{298}^{T} \frac{1}{T} d(H_T^\circ - H_{298}^\circ)_{MX_y}\right].$$

The free energy (in kJ mol^{-1}) of disordered vanadium carbide can be calculated with the use of dependences (1), (3) and (6) according to Eqn (7). The calculations carried out in the studies [2,25–27] demonstrated that the following dependence is valid for disordered cubic carbide VC_y:

$$F_0(T) + yF_1(T) + y^2F_2(T) = (97.09 + 145.0\times10^{-3}T - \quad (8)$$
$$-11.84\times10^{-6}T^2 - 208T^{-1} - 26.95\times10^{-3}T\ln T) +$$
$$+(-437.49 - 86.23\times10^{-3}T + 11.75\times10^{-6}T^2 +$$
$$+ 932T^{-1} + 18.29\times10^{-3}T\ln T)y +$$
$$+ (211.36 + 267.21\times10^{-3}T - 42.47\times10^{-3}T\ln T)y^2.$$

The energy parameters $F_0(T)$, $F_1(T)$ and $F_2(T)$ of the free energy determined for disordered cubic carbide VC_y are

Table 6. Heat capacities C_p (J g-atom^{-1} K^{-1}), $\Delta S_T^\circ = S_T^\circ - S_{10}^\circ$ (J g-atom^{-1} K^{-1}) and $H_T^\circ - H_{10}^\circ$ (J g-atom^{-1}) for cubic carbides $VC_{0.71}$, $VC_{0.83}$ and $VC_{0.86}$ in the temperature range of 10 – 300 K.[65,67]

T, K	$VC_{0.71}$			$VC_{0.83}$			$VC_{0.86}$		
	C_p	$H_T^\circ - H_{10}^\circ$	ΔS_T°	C_p	$H_T^\circ - H_{10}^\circ$	ΔS_T°	C_p	$H_T^\circ - H_{10}^\circ$	ΔS_T°
10	0.008	–	–	0.004	–	–	0.042	–	–
50	1.005	12.0	0.293	0.712	9.0	0.251	0.670	8.0	0.209
100	5.610	172.0	2.386	4.815	139.0	1.758	4.690	135.0	1.675
150	9.839	561.0	5.485	8.960	485.7	4.522	8.834	473.1	4.396
200	13.15	1138.8	8.792	12.43	1025.8	7.620	12.27	1004.8	7.453
250	15.78	1863.1	12.02	15.28	1720.8	10.72	15.07	1691.5	10.47
273	16.79	2269.2	13.44	16.37	2085.0	12.10	16.16	2051.5	11.85
298	17.75	2671.2	14.99	17.38	2507.9	13.57	17.17	2466.0	13.31
300	17.84	2704.7	15.07	17.46	2512.1	13.69	17.25	2503.7	13.40

applicable for the temperature range of 298 – 2000 K. Analogous calculations performed in these studies for hexagonal carbide β-V_2C without consideration for its homogeneity region gave the following dependence of the free energy (in kJ mol^{-1}) for the temperature range of 298 – 1600 K

$$F(T)_{V_2C} = -180.96 + 513.67\times10^{-3}T - 1.70\times10^{-6}T^2 + 1290T^{-1} - 83.12\times10^{-3}T\ln T. \quad (9)$$

With a knowledge of the parameters $F_0(T)$, $F_1(T)$ and $F_2(T)$ and the free energy $F(T)_{V_2C}$, it is possible to perform thermodynamic calculations of phase equilibria involving hexagonal and cubic nonstoichiometric vanadium carbides.

f. High-temperature vaporisation of vanadium carbide

In studies of the thermodynamic properties of nonstoichiometric carbides, vapour pressure measurements over a vaporising solid compound are used along with adiabatic, differential scanning and bomb calorimetry. From the viewpoint of determining the thermodynamic properties of nonstoichiometric carbides, congruent vaporisation (sublimation), *i.e.*, vaporisation, which occurrs in equilibrium conditions without changes in the composition of the solid phase, is of most interest.

According to the kinetic theory of gases, the rate of vaporisation from the surface existing in equilibrium with vapour is equal to the condensation rate proportional to the equilibrium vapour pressure p. Under non-equilibrium conditions (for example, in the case of vacuum vaporisation from the open surface), the vaporisation rate is independent of the condensation rate but is equal to the equilibrium vaporisation rate at this temperature T.[75] This is true if the residual pressure in a vacuum chamber is no higher than 10 Pa (~0.1 mmHg). Therefore, the equilibrium parameter, *viz.*, the saturated vapour pressure, can be found from the rate of stationary vacuum vaporisation, after which many thermodynamic characteristics can be calculated. If the transition of the condensed phase into vapour is accompanied by its dissociation, the observed vaporisation rate and the partial pressures are smaller than the equilibrium values. This fact can be taken into account by introducing the vaporisation coefficient $\alpha \leqslant 1.0$.

The kinetic and thermodynamic conditions of congruent vaporisation of disordered nonstoichiometric interstitial compounds have been considered in detail in the monograph.[1] The thermodynamics of congruent vaporisation of nonstoichiometric compounds was investigated also in the studies.[76, 77]

The vapour composition over the V–C system in the temperature range of 2417 – 2603 K was studied by mass spectrometry.[78] Judging from the X-ray diffraction data and the lattice parameter, the authors used a sample containing carbide $VC_{0.88}$ along with free carbon. The vapour pressure was not measured and only data on the $V : VC_2$ ratio in the gas phase were reported.

The studies [79, 80] were concerned with vaporisation of vanadium carbide by the Knudsen effusion method in the temperature range of 2346 – 2545 K. Taking into account the method of the synthesis, the composition of the resulting carbide is $VC_{0.99}$. Hence, the study was, apparently, performed with the use of carbide $VC_{0.88}$ containing a large amount of free carbon. The vaporisation rate was determined from the mass change upon vaporisation. Vaporisation did not lead to a change in the composition of vanadium carbide, and the condensate consisted of pure vanadium. The temperature dependence of the vapour pressure of vanadium p_V (in atm) over the V–C system is described by the equation

$$\log p_V = 7.63 - \frac{30\,700}{T}. \quad (10)$$

Investigation of the phase equilibria in the V–C system demonstrated [10] that heating of vanadium carbide of any composition *in vacuo* leads to the predominant loss of the metal. Vaporisation of vanadium carbide becomes noticeable at temperatures higher than 1800 K.

Storms [11] found the temperature dependence of the vapour pressure of vanadium (in atm) based on the thermochemical characteristics of dissociation of carbide $VC_{0.88}$ in equilibrium with carbon

$$\log p_V = 7.56 - \frac{31\,210}{T}. \quad (11)$$

Vaporisation of carbide $VC_{0.84}$ in the temperature range from 2073 to 2423 K under vacuum of 0.0013 Pa (1×10^{-5} mmHg) was investigated [81] by the Langmuir method based on the determination of the vaporisation rate from the open surface of a sample heated *in vacuo*. The total time of vacuum vaporisation varied from 42 h at 2073 K to 12 h at 2423 K. During vaporisation, the crystal lattice parameter on the sample surface slightly increases. Taking into account the changes in the chemical composition and the lattice parameter, the vaporisation rate of vanadium atoms during vacuum heating of carbide VC_y was initially larger than the vaporisation rate of carbon atoms, *i.e.*, $V_V/V_C > 1/y$. As a result, the samples were depleted in metal and enriched in carbon, and their compositions became close to the upper boundary of the homogeneity region of cubic carbide ($VC_{0.88}$). Vacuum heating of vanadium carbide leads to vaporisation of not only vanadium but also of carbon, because elimination of free carbon was observed neither on the surface nor in the bulk of the samples. At 2000 – 2400 K, vaporisation of vanadium carbide occurs according to the reaction [81]

$$VC_y\,(\text{sol.}) \longrightarrow V\,(\text{gas}) + y\,C\,(\text{gas}), \quad (12)$$

the composition of the congruently vaporising carbide varied from $VC_{0.85}$ to $VC_{0.87}$ and was shifted to the upper boundary of the homogeneity region with increasing temperature. A similar conclusion about the predominant loss of the metal and the shift of the composition of vanadium carbide to the upper boundary of the homogeneity region as a result of vaporisation has been drawn earlier in the study.[10]

An increase in the temperature from 2073 to 2423 K led to an increase in the total rate of vacuum vaporisation of vanadium carbides by a factor of almost 300, and the mass loss through vaporisation at 2423 K for one hour was 6% – 7%. The experimental data on the vaporisation rate of vanadium carbide (in kg m^{-2} s^{-1}) at 2000 – 2500 K can be described by the equation [81]

$$\ln V = 25.117 - \frac{80\,900}{T} \pm 0.015. \quad (13)$$

The partial pressures of vanadium and carbon over congruently vaporising vanadium carbides were estimated from the measured vaporisation rate and assuming that the vaporisation coefficient of vanadium is 1.[81] At 2073, 2273 and 2423 K, congruent vaporisation of carbides $VC_{0.85}$, $VC_{0.86}$ and $VC_{0.87}$, respectively, was demonstrated to occur. The estimated partial pressures of vanadium and carbon were as follows: 1.1×10^{-3} and 0.9×10^{-3} Pa over carbide $VC_{0.85}$ at 2073 K; 0.035 and 0.030 Pa over carbide $VC_{0.86}$ at 2273 K; and 0.34 and 0.30 Pa over carbide $VC_{0.87}$ at 2423 K, respectively.

Vaporisation in the V–C system was thoroughly investigated [50] by mass spectrometry using a Knudsen effusion cell. The vapour was ionised and the ion current rather that its absolute pressure was measured. Several samples of vanadium metal and 18 samples of vanadium carbides of different compositions were used in measurements. The measurements for the samples of different compositions were carried out in the temperature ranges of 1445 – 1819, 1740 – 2226 and 1809 – 2173 K. The activity of vanadium (a_V) was determined as the ratio of the ion currents of vanadium metal and vanadium carbide vaporised under comparable conditions. In these calculations, the heat of vaporisation of vanadium metal (532.1 kJ mol^{-1}) was used as the basic value. The plots of $\log a_V$ *vs* y for 1700 and 2000 K were constructed, and the carbon activity a_C was calculated by numerical integration

according to the Gibbs – Duhem equation. In the investigation,[50] the equation was not given in an explicit form. However, the carbon activity was, apparently, determined by integration of the following equation:

$$d \ln a_C = -\frac{1}{y} d \ln a_V . \quad (14)$$

The partial enthalpies of vaporisation of vanadium and carbon were calculated by the equation

$$\Delta \bar{H}_{V(C)} = \Delta H^{\circ}_{V(C)} - RT \ln a_{V(C)} \quad (15)$$

using the enthalpies of vaporisation of vanadium and carbon at 1650 K: $\Delta H^{\circ}_V = 525.4$ and $\Delta H^{\circ}_C = 713.8$ kJ mol^{-1}.

The free energies of formation of vanadium carbides VC_y with different carbon contents at 1700 K were calculated [50] according to the formula

$$\Delta F_f(y,T) = RT(\ln a_V + y \ln a_C) + \quad (16)$$
$$+ RT[y \ln y + (1-y)\ln(1-y)].$$

At 1700 K, $\Delta F_f(y,1700)$ varied from -19.9 for $VC_{0.74}$ to -21.3 kJ mol^{-1} for $VC_{0.88}$. The enthalpy of formation $\Delta H^{\circ}_{f\,298}$ of carbide $VC_{0.88}$ is -104.6 ± 1.8 J mol^{-1}. It should be noted that the results published in the study [50] were obtained for the temperature range higher than the temperature of the order – disorder transition $VC_y - V_8C_7$, *i.e.*, for the disordered state of vanadium carbide.

III. Ordered phases of nonstoichiometric vanadium carbides

Cubic vanadium carbide VC_y is the first transition metal carbide, in which ordering was observed,[12] and is one of a few strongly nonstoichiometric carbides, in which atom-vacancy ordering was studied in detail. Let us consider the main concepts related to this ordering.

Atomic or atom-vacancy ordering is a synonym of a disorder – order structural phase transition (magnetic ordering in the case of magnetic phase transitions). Ordering as a phase transition is a result of atomic redistribution over sites of the crystal lattice of a substitutional solid solution. In the disordered state, components of the solid solution, which can replace each other, are randomly distributed over the sites of the crystal lattice and the probability of occupancy of a particular site by an atom of a particular type is equal to its concentration in solution. A decrease in the temperature leads to ordering, with the result that the crystal lattice sites of a disordered solution are divided into several sublattices. Sublattices of an ordered solution differ from each other in the probability of occupancy of the sites by atoms of a particular type. Ordered phases generated by dividing the lattice of a disordered crystal into several sublattices are called superstructures.

Ordering can also occur in interstitial solid solutions, if the number of interstitial sites is larger than the number of atoms occupying these sites. In the ordering process in interstitial solutions, vacancies and interstitial atoms serve as components of substitutional solutions, whereas solvent atoms form a stationary atomic framework, within which the interstitial atoms and vacancies are redistributed.

In disordered nonstoichiometric compounds, all sites of the non-metal sublattice are crystallographically equivalent. Ordering is accompanied by redistribution of interstitial atoms and structural vacancies over the non-metal sublattice sites. As a result, the crystal lattice sites of the disordered solution become non-equivalent and are divided into at least two sublattices, which differ in the probability of occupancy of the sites by atoms of one and the same type. From the above it is evident that nonstoichiometry is a prerequisite for ordering in imperfect interstitial compounds, because it is responsible for the fact that the number of interstitial sites is larger than the number of atoms. Hence, the presence of structural vacancies in nonstoichiometric interstitial compounds leads, under certain conditions, to ordering. In the simplest case, ordering in a non-metal sublattice consists in dividing the system formed by octahedral interstitial sites of the metal sublattice into two new sublattices. All sites in the first superstructure sublattice are occupied by interstitial atoms, whereas the sites in the second sublattice are vacant. Hence, it is safe to assume that ordering in nonstoichiometric compounds gives rise to a vacancy sublattice.

Ordering in non-metal sublattices of nonstoichiometric compounds is accompanied by lowering of crystal symmetry. Actually, some symmetry transformations of a disordered non-metal sublattice, which relate the occupied sites to the vacancies, are not involved in the symmetry group of the ordered crystal, because these sites are crystallographically non-equivalent.

Over many years, the positions of interstitial atoms in lattices of nonstoichiometric compounds were determined primarily by X-ray diffraction methods. However, X-ray scattering amplitudes for interstitial atoms are small compared to those for metal atoms, due to which it is not always possible to determine the positions of interstitial atoms by analysing the intensities of diffraction lines. Hence, it is a wide spread opinion that interstitial atoms in non-metal sublattices of nonstoichiometric compounds are always randomly distributed.

The development of experimental techniques and, particularly, the use of neutron diffraction, made it possible to reveal that, under certain conditions, an ordered distribution of interstitial atoms can occur in nonstoichiometric compounds. The neutron diffraction technique is one of the most informative methods for studying nonstoichiometric interstitial compounds, because neutron scattering intensities of transition metal nuclei are comparable with those of light elements. Ordering of interstitial atoms in these compounds was detected also by other diffraction methods, such as electron diffraction, high-resolution X-ray diffraction and various physicochemical methods.

Ordering of interstitial atoms has been experimentally observed in most nonstoichiometric carbides of Group IV and V transition metals.

Vanadium carbides VC_y and $V_2C_{y'}$ are rather convenient to study. Since the X-ray scattering amplitude for the vanadium atom differs not very much (by a factor of ~ 5) from that for carbon, superstructure reflections can be observed in X-ray diffraction patterns. The neutron scattering amplitude for the vanadium atom is negative and small in magnitude compared to that for the carbon atom (-0.038×10^{-12} and 0.665×10^{-12} cm, respectively).[82] For this reason, the ordered non-metal (carbon) sublattice makes the major contribution to neutron diffraction from vanadium carbide, and the most intense superstructure reflections are weaker than the structure reflections $(111)_{B1}$ and $(200)_{B1}$ by only a factor of 11 – 20, *i.e.*, these reflections are quite observable. Besides, vanadium carbide can be studied by NMR spectroscopy, because the ^{51}V nuclei have the nonzero spin $I = 7/2$. The structures of ordered phases of nonstoichiometric vanadium carbides VC_y and $V_2C_{y'}$ were studied by X-ray, neutron and electron diffraction, NMR spectroscopy and electron and optical microscopy. However, in spite of the fact that ordering in vanadium carbides was studied more thoroughly compared to other transition metal carbides, many experimental data on the compositions and structures of ordered phases of carbide VC_y were not confirmed in later studies. These phases are not mentioned in the present review.

1. NMR spectroscopic studies of vanadium carbide

NMR spectroscopy provides information on the mutual arrangement of interstitial atoms and structural vacancies in non-metal sublattices of nonstoichiometric compounds, *i.e.*, information on the short-range order in such compounds. As a rule, no more than three – four types of the nearest environment of metal atoms formed by carbon atoms and vacancies are observed in ordered phases of nonstoichiometric carbides.[3,4] Hence data on the short-

range order in non-metal sublattices of carbides obtained by NMR spectroscopy provide indirect evidence for the presence of a particular ordered phase in samples.

The nearest environment of the vanadium atom in carbide VC_y with the $B1$ structure involves three coordination spheres (see Fig. 4). The first coordination sphere is formed by six occupied or partially vacant sites of the non-metal sublattice. The second ordered coordination sphere consists of 12 metal atoms. The third coordination sphere is formed by eight sites of the non-metal sublattice occupying the vertices of the cubic unit cell. It is convenient to describe the environment of the metal atoms with the use of superscripts and subscripts indicating the numbers of vacancies in the first and third non-metal coordination spheres, respectively. For example, the vanadium position V_0^2 signifies that the first coordination sphere of vanadium is complete (contains no vacancies), whereas the second non-metal coordination sphere has two vacancies.

Carbides VC_y with $y = 0.66$, 0.70, 0.80, 0.84 and 0.875 were studied by NMR spectroscopy throughout the homogeneity region of the cubic phase.[83] The ^{51}V NMR spectra of carbides $VC_{0.875}$, $VC_{0.84}$ and $VC_{0.70}$ show several resonance lines, whose intensities depend on the composition of VC_y. The intensities of two lines rapidly decrease, whereas the intensity of the third line increases as the carbon content decreases. The spectrum of carbide $VC_{0.70}$ shows an additional weak line. All observed lines and their satellites in the ^{51}V NMR spectra of VC_y were compared with the positions of the vanadium atoms, whose first coordination spheres have different numbers of vacancies: V_0 (without vacancies), V_1 (with one vacancy), V_2 and V_3. The following expression relating the jump in the Knight shift (K) to the number of vacancies (n) in the nearest environment of the vanadium atom was derived:

$$K_n - K_{n-1} \approx nK_0, \tag{17}$$

where $K_0 \approx 0.07\% - 0.09\%$, *i.e.*, the jump in the Knight shift is proportional to the number of vacancies in the first coordination sphere of the vanadium atom in VC_y.

To elucidate the character of distribution of vacancies in vanadium carbide, the experimental distribution of probabilities $P(n)$ of vanadium sites was compared with the random distribution of probabilities calculated by the formula

$$P(n) = C_6^n (1-y)^n y^{6-n}. \tag{18}$$

For all VC_y samples under consideration, the experimental distributions differed from the random distribution. For example, a decrease in the carbon content leads to a much more rapid decrease in the probability of existence of the V_0 positions with the complete (without vacancies) environment in the first coordination sphere compared to the random distribution, and the V_3 positions are observed much more rarely. A small number of the V_3 positions and the absence of vanadium atom positions, whose first coordination spheres have four or more vacancies, were attributed to repulsion between the adjacent vacancies. Therefore, according to the results of the study,[82] cubic vanadium carbide has a short-range order.

The ^{51}V NMR spectrum of carbide $VC_{0.875}$ differs substantially from the spectra of other vanadium carbides. In particular, the intensity ratio of the lines corresponding to the V_0 and V_1 positions is 1 : 3. Assuming that the relative intensity of each line is proportional to the relative number of the corresponding positions, three-fourths of all vanadium atoms in carbide $VC_{0.875}$ have one vacancy in the first coordination sphere, whereas the rest of the vanadium atoms have a complete environment. This distribution of vacancies is indicative of the presence of the V_8C_7-type superstructure with the space group $P4_332$ or $P4_132$.[12] However, the authors of the publication [83] cast doubt that this model of distribution of vacancies is quite consistent with the real lattice. Actually, this superstructure characterised by a helicoidal arrangement of vacancies has only the V_0^1 and V_1^1 positions, whereas analysis of satellites in the NMR spectrum suggested the existence of three types of positions V_1, which could not be resolved.

Interesting results were obtained in the study of an annealed single crystal of $VC_{0.84}$.[13, 84] The ^{51}V NMR spectra of this carbide were resolved into lines corresponding to the V_0 and V_1 positions. Investigation of the satellites made it possible to resolve the intense band of V_1 into lines corresponding to the V_1^0, V_1^1 and V_1^2 positions which have no vacancies, one vacancy and two vacancies in the second coordination sphere, respectively. In the spectra, the intensity ratio of the V_1^1 and V_1^2 lines is 2 : 1. Hence, it is reasonable to assume that the number of the V_1^1 positions in the carbide under study is twice as large as the number of the V_1^2 positions. Taking into account high intensities of the lines, the corresponding V_1^1 and V_1^2 positions can be considered as positions of an ordered structure of vanadium carbide.

In the study of $VC_{0.84}$ by electron diffraction,[13] the authors suggested the trigonal symmetry for the ordered phase V_6C_5. The available NMR data made it possible to describe the distribution of carbon atoms and vacancies in the trigonal unit cell, *i.e.*, to determine the structure of V_6C_5, taking into account the ratio of the number of the V_1^1 positions to the number of the V_1^2 positions. The trigonal superstructure of V_6C_5 with the space group $P3_1$ can be represented as helical chains composed of $V_6C_5\square$ quasimolecules. The presence of weak lines corresponding to the V_0 and V_1^0 positions was attributed to the deviation of the composition of vanadium carbide $VC_{0.84}$ from the ideal composition of the ordered phase V_6C_5 ($VC_{0.83}$). It should be noted that the presence of these lines can be associated also with the violation of the long-range order in the sample under investigation.

Attempts to obtain quantitative data on the short-range order in carbide VC_y by minimisation of the ^{51}V NMR spectra were made in the studies.[85, 86] The experimental ^{51}V NMR spectra of carbides $VC_{0.75}$, $VC_{0.84}$, $VC_{0.85}$, $VC_{0.86}$ and $VC_{0.87}$ are analogous to the spectra described in the study [83] and have resonance lines corresponding to the V_0, V_1 and V_2 vanadium atom positions. Assuming that the lines in the spectra are associated with the fact that the crystals contain nuclei in different local environments (different positions of metal atoms), and the intensity of the line is proportional to the number of positions of a particular type, the theoretical intensity of the line was represented as

$$I_{\text{theor}}(v) = \sum_i \lambda_i P_i I_i(v), \tag{19}$$

where P_i is the probability of existence of a cluster characterised by the ith configuration of the nearest environment of the resonating nucleus formed by non-metal atoms, λ_i is the multiplicity of the ith configuration; and $I_i(v)$ is the mathematical model of the ideal spectral line for this configuration. (In the study,[85] the lines were described by the Gaussian distribution; the octahedron composed of six sites of the non-metal sublattice containing a metal atom in the centre was chosen as the basic cluster.) The probabilities P_i were represented as an expansion in series of pair and multiparticle correlation parameters, which were determined by minimisation of the functional $\sum[I_{\text{theor}}(v) - I_{\text{exp}}(v)]^2$. The spectra were best described taking into account pair and triple correlations. The consideration of higher-order correlation moments did not lead to a substantial change in the spectra.

According to the results of the studies,[85, 86] the pair correlations ε_{21} describing the distribution of carbon atoms (or vacancies) between two adjacent vertices of the octahedron, which are located relative to each other in the first coordination sphere, are negative throughout the homogeneity region of vanadium carbide. This fact indicates that the probability of finding vacancies in the nearest proximity to each other is lower than that in the case of random distribution throughout the homogeneity region of VC_y. The short-range order parameter α_1 for the first coordination sphere is approximately equal to -0.1. This parameter slowly increases in magnitude and passes through a minimum in the vicinity of the $VC_{0.83}$ composition as the deviation from the stoichiometry increases.

The results of calculations [85, 86] for the correlations and the short-range order parameter in vanadium carbide are on the whole consistent with the results of the publications.[13, 83, 84] The latter data provide evidence that there is the short-range order in carbide VC_y due to repulsions between vacancies. In the monograph,[86] the presence of ordered phases of vanadium carbide was erroneously attributed to a particular short-range order. In the studies,[3, 4, 19, 87, 88] it was demonstrated that the long-range order does not necessarily appear in nonstoichiometric compounds with the *B*1 structure even in the presence of the highest short-range order in the first and second coordination spheres. Hence, the presence of the short-range order in strongly nonstoichiometric carbides is a necessary but not sufficient condition for the presence of the long-range order.

2. Diffuse electron scattering

Ordering in nonstoichiometric vanadium carbides was studied also by diffuse electron scattering. The short-order range parameters α_{hkl} for eight nearest coordination spheres of non-metal sublattices were calculated [89, 90] using experimental data [45] on the intensities of diffuse electron scattering by vanadium carbide $VC_{0.75}$. The vacancy was chosen as the centre of the coordination spheres. For nonstoichiometric carbide MC_y, the number of carbon atoms n_C and the number of vacancies $n_\square$ in the jth sphere with coordination number z_j are

$$n_C = z_j(1-\alpha_j)y, \qquad (20)$$
$$n_\square = z_j[1-(1-\alpha_j)y].$$

With a knowledge of the short-range order parameter (including $\alpha_j = 0$), the number of carbon atoms and the number of vacancies in the corresponding coordination sphere can be calculated by these equations.

The calculated parameters α and the numbers n_C and $n_\square$ in each coordination sphere are given in Table 7. For comparison, these values were calculated for the ordered phase V_6C_5 with monoclinic (space group $C2/m$ or $C2$) or trigonal (space group $P3_1$) superstructures (ideal M_6X_5-type superstructures do not differ in the short-range order) and disordered carbide $VC_{0.75}$.

As can be seen from Table 7, the distribution of carbon atoms and vacancies in the non-metal sublattice of carbide $VC_{0.75}$ determined in the studies [45, 89, 90] differs substantially from the random distribution in disordered carbide $VC_{0.75}$. In the first two coordination spheres, the numbers of vacancies are much smaller than those observed for the random distribution. The parameter α oscillates and decreases in magnitude with increasing radius of the coordination sphere. The data on the distribution of carbon atoms and vacancies were interpreted [89, 90] as a consequence of mutual repulsion between the vacancies, and it was noted that an analogous short-range order should be observed in niobium and tantalum carbides. A conclusion about the same type of short-range order in nonstoichiometric Group V transition metal monocarbides was drawn also in the study.[91] The authors of the cited paper believed that it is impossible to prepare completely disordered (without short-range order) VC_y samples with $y > 0.78$.

Diffuse electron scattering was also used to study the short-range order in lower hexagonal carbides $V_2C_{y'}$ and $Nb_2C_{y'}$.[92] It was demonstrated that the short-range order and the long-range order in these carbides are associated with the distribution of carbon atoms and structural vacancies in regular $C-\square-C-\square-\ldots$ rows parallel to the c axis. A comparison of the experimental and calculated diffuse scattering intensities revealed the possible types of ordering in carbides V_2C and Nb_2C.

3. Crystal structures of ordered phases of nonstoichiometric vanadium carbides

Most precise and detailed information on the crystal structures of ordered phases of nonstoichiometric compounds can be obtained by diffraction methods. Principal structural characteristics of both experimentally observed and calculated ordered phases of nonstoichiometric lower hexagonal $V_2C_{y'}$ and cubic VC_y vanadium carbides are given in Table 8.

In disordered lower vanadium carbide $V_2C_{y'}$ (β-V_2C) with a hexagonal structure of the $L'3$ (W_2C) type, the hexagonal ε-Fe_2N-type ordered phase β'-V_2C (β_h-V_2C) initially appears due to ordering caused by lowering of the temperature. At temperatures lower than 1100 K, the orthorhombic ζ-Fe_2N-type ordered phase β_r-V_2C (α-V_2C) is formed. The existence of the hexagonal ordered phase β'-V_2C (β_h-V_2C) was documented.[37, 44, 47, 93, 94, 105–109] The orthorhombic ordered phase β_r-V_2C (α-V_2C) was found in the studies.[44, 46, 93, 94, 105, 108–113] However, the refined data on the structures and crystal lattice parameters, the conditions of formation, concentrations and temperature ranges of existence of these phases obtained by different (and sometimes the same) research groups are not quite consistent with each other. Instability of the hexagonal ε-Fe_2N-type ordered phase β'-V_2C (β_r-V_2C) was noted in the investigation.[107] This high-temperature ordered phase was not observed in quenched samples of lower vanadium carbide.[92, 113] However, the results of experimental studies [108, 109] performed by high-temperature neutron diffraction demonstrated that the orthorhombic ζ-Fe_2N-type phase β_r-V_2C (α-V_2C) is a low-temperature ordered phase of lower vanadium carbide. An increase in the temperature leads to the transformation of the latter phase into the high-temperature ordered ε-Fe_2N-type hexagonal phase β'-V_2C (β_h-V_2C). The authors of these studies hypothesised that samples of lower vanadium carbide, whose composition differs from stoichiometric V_2C, undergo a polymorphic transformation

$$\beta_r\text{-}V_2C\ (\alpha\text{-}V_2C) \rightleftharpoons \beta'\text{-}V_2C\ (\beta_h\text{-}V_2C)$$

Table 7. Short-range order parameters (α), numbers of carbon atoms (n_C) and vacancies ($n_\square$) in the coordination spheres (hkl) of carbide $VC_{0.75}$, the ideal ordered phase V_6C_5 and disordered carbide $VC_{0.75}$ (see Ref. 89).

CS [a]	CN [b]	$VC_{0.75}$			Ideal superstructure of V_6C_5 (space group $C2/m$, $C2$, $P3_1$)			Disordered carbide		
		α	n_C	$n_\square$	α	n_C	$n_\square$	α	n_C	$n_\square$
110	12	−0.178	10.6	1.4	−0.2	12	0	0	9	3
200	6	−0.260	5.7	0.3	−0.2	6	0	0	4.5	1.5
211	24	0.176	14.8	9.2	0.2	16	8	0	18	6
220	12	0.008	8.9	3.1	0	10	2	0	9	3
310	24	0.041	17.3	6.7	0	20	4	0	18	6
222	8	−0.171	7.0	1.0	−0.2	8	0	0	6	2
321	48	−0.070	38.5	9.5	−0.1	44	4	0	36	12
400	6	0.143	3.8	2.2	0.2	4	2	0	4.5	1.5

[a] CS is the coordination sphere (hkl) with the radius $R_j = (a_{B1}/2)(h^2 + k^2 + l^2)^{1/2}$ (a_{B1} is the lattice parameter of disordered carbide VC_y with the *B*1 structure; a vacancy is located in the centre of the coordination sphere). [b] CN is the coordination number of the sphere (hkl).

Table 8. Ordered phases of strongly nonstoichiometric vanadium carbides.

Ordered phase					Basic phase		Note	Ref.
composition	non-metal content (at.%)	symmetry	space group	unit cell parameters (lattice parameters in nm)	composition	lattice type		
β_r-V_2C (α-V_2C)	~33.0 ($VC_{0.5}$)	orthorhombic, ζ-Fe_2N type	*Pbcn*	$a = 0.4567 = c_0$, $b = 0.5744 = 2a_0$, $c = 0.5026 \approx a_0\sqrt{3}$	$VC_{y'}$	*L*′3	$T_{tr} < 1100$ K	93, 94
β'-V_2C (β_h-V_2C)	~33.0 ($VC_{0.5}$)	hexagonal	–	$a = 0.4997 \approx a_0\sqrt{3}$, $c = 0.4568 = c_0$	$VC_{y'}$	*L*′3	prepared by quenching from 1800 K	93, 94
V_3C_2	$VC_{0.667}$–$VC_{0.710}$ ($VC_{0.67}$–$VC_{0.72}$ at 300 K)	–	–	–	VC_y	*B*1	calculation; $T_{tr} < 1155$ K; the homogeneity region corresponds to 800 K	27, 32
V_6C_5	$VC_{0.745}$–$VC_{0.831}$	–	–	–	VC_y	*B*1	calculation; $T_{tr} < 1485$ K; the homogeneity region corresponds to 1100 K	27, 32
V_6C_5	~45.5 ($VC_{0.83}$)	trigonal	$P3_1$, $P3_2$	$a = 0.509$, $c = 1.44$	VC_y	*B*1	according to the results of the studies,[95–97] the trigonal phase is intermediate between the disordered phase VC_y and the monoclinic phase V_6C_5	13, 25, 26, 69, 95, 96
V_6C_5	~45.5 ($VC_{0.83}$)	monoclinic	*C*2	$a = 0.509$, $b = 1.018$, $c = 0.882$, $\gamma = 109.8°$	VC_y	*B*1	$T_{tr} < 1420$ K	43, 45, 96, 97
V_6C_5	~45.5 ($VC_{0.83}$)	monoclinic	*C*2/*m*	–	VC_y	*B*1	Nb_6C_5 structure type (see Refs 99–102)	98
δ'-VC_y	~45.5 ($VC_{0.83}$)	trigonal	–	$a = 0.5885 \approx a_0\sqrt{2}$, $c = 1.443 \approx 2a_0\sqrt{3}$	VC_y	*B*1	$T_{tr} < 1300$ K	93
δ''_M-VC_y	45.0–47.0	monoclinic	–	$a = (a_0\sqrt{3})/2$, $b = a_0\sqrt{6}$, $c = 8a_0\sqrt{2}$, $\gamma = 109.47°$	VC_y	*B*1	$T_{tr} < 1500$ K	93
V_8C_7	~46.6 ($VC_{0.87}$)	cubic	$P4_332$	$a = 0.8332 \approx 2a_0$	VC_y	*B*1	first-order phase transition; $T_{tr} < 1500$ K	12, 43, 46–49, 69, 98–104

in a two-phase region (β_r-V_2C + β_h-V_2C). For example, only orthorhombic ordered ζ-Fe_2N-type phase was observed [108] in neutron diffraction patterns of lower carbide $VC_{0.47}$ at temperatures up to 1373 K inclusive. At 1393 K, the neutron diffraction pattern has reflections of the orthorhombic and hexagonal ordered phases. At 1413 K, the diffraction pattern shows superstructure reflections corresponding only to the high-temperature ordered ε-Fe_2N-type phase.

As can be seen from Table 8, M_3C_2-, M_6C_5- and M_8C_7-type ordered phases can exist in nonstoichiometric cubic vanadium carbide. In carbide VC_y, the first of these phases has not been experimentally detected. However, the possibility of its existence is supported by thermodynamic calculations. The phase V_8C_7 was experimentally found only in vanadium carbide and was not observed in carbides of other transition metals. The existence of this phase is associated with the specific position of the upper boundary of the homogeneity region of vanadium monocarbide for $VC_{0.875}$.

As for the symmetry of the ordered phases, the trigonal (space group $P3_1$) [13, 25, 69] and monoclinic (space group *C*2) [43, 45] V_6C_5-type ordered phases and the cubic (space group $P4_332$) ordered phase V_8C_7 were found in VC_y.[12, 46–49, 69, 103, 104] It should be noted that V_8C_7 (see Ref. 12) is the first ordered phase experimentally found in nonstoichiometric carbides. Hardening of high-vanadium cast iron was demonstrated [98] to be accompanied by the formation of the disperse ordered carbide phases V_6C_5 and V_8C_7. The phase V_6C_5 is monoclinic (space group *C*2/*m*) and is structurally similar to monoclinic ordered niobium carbide Nb_6C_5 (space group *C*2/*m*).[99–102] In high-carbon cast iron, monoclinic carbide V_6C_5 is located in the centre of eutectic grains, whereas the cubic (space group $P4_332$) ordered phase V_8C_7 can occur in the outer layer of the grains.[98] The formation of the ordered phase V_6C_5 was observed in the study [114] of vanadium-containing steel annealed at 1000 K for 50–150 h by transmission electron microscopy and electron diffraction. Data on the symmetry of the V_6C_5 phase found in this study are lacking. Calculations demonstrated that the ordered phase V_3C_2 can exist,[25–27, 32] and this phase can have orthorhombic (space group *Immm* or $C222_1$) or monoclinic symmetry (space group *P*2).

Investigations of the trigonal ordered phase V_6C_5 by electron diffraction and electron miscroscopy [13, 115] showed that this phase is stable at temperatures close to the transition temperature to the disordered state, because this phase is disordered as a result of its heating with electron beam.[115] The monoclinic ordered phase V_6C_5 is, apparently, formed at temperatures lower than the temperature of formation of the trigonal phase V_6C_5.[43] Actually, neutron diffraction studies demonstrated [95–97] that the monoclinic phase is stable in the temperature range of 1050–1370 K, and the trigonal phase exists in the range of 1140–1520 K. According to the average experimental estimates, the lower

boundary of the homogeneity region of the ordered phase V_6C_5 corresponds to carbide $VC_{0.75-0.77}$, and the upper boundary corresponds to carbide $VC_{0.82-0.86}$. An ambiguity of the boundaries, particularly, of the upper boundary, is associated with the difference in the conditions of annealing of carbide VC_y used in different experiments. Annealed samples of carbide VC_y with $y \geqslant 0.83$ contained already two ordered phases, *viz*., V_6C_5 and V_8C_7. The single-phase region of existence of the cubic superstructure of V_8C_7 is very narrow (no broader than from $VC_{0.863}$ to $VC_{0.875}$, *i.e*., to the upper boundary of the homogeneity region of disordered VC_y). The precise determination of the chemical composition of vanadium carbide, as well as of other refractory carbides, is a rather complicated problem. However, taking into account the errors in the determination of the composition, it can be assumed that vanadium carbides containing only the ordered phase V_8C_7 have the composition $VC_{0.870\pm0.005}$. This may be evidence that the ordered phase V_8C_7 has no homogeneity region and is formed only upon annealing of carbide $VC_{0.875}$. If the carbon content of carbide is smaller, the phase V_8C_7 is present along with the ordered phase V_6C_5.

Therefore, several ordered M_6C_5-type phases of different symmetry and the ordered cubic M_8C_7-type phase were found in nonstoichiometric carbide VC_y. Let us consider their structures in more detail using such concepts as the disorder – order transition channel and the distribution function $n(\boldsymbol{r})$ of atoms between the sites $\boldsymbol{r}$ in an ordered crystal lattice. The distribution function $n(\boldsymbol{r})$ has the symmetry of the ordered crystal lattice and reflects the probability of finding an atom of this type in the site r. In a disordered crystal, the probabilities $n(\boldsymbol{r})$ are equal for all sites and coincide with the fraction of lattice sites occupied by atoms of this type. For example, the distribution function $n(\boldsymbol{r})$ of the atoms X in the disordered nonstoichiometric compound $MX_y\square_{1-y}$ is equal to the fraction of lattice sites occupied by these atoms, *i.e*., $n(\boldsymbol{r}) = y$.

The space-periodic modulation of the atom distribution (the deviation of the probability $n(\boldsymbol{r})$ from its value for the random distribution) resulting in the formation of an ordered phase can be represented as a superposition of several plane concentration waves.[116] The wave vectors of the latter are the superstructure vectors $\boldsymbol{k}_s^{(j)}$ of the reciprocal lattice in the first Brillouin zone of the disordered lattice. In the static concentration wave method,[116] the distribution function of atoms of this type is described through a fraction of sites occupied by these atoms and the superposition of the static concentration waves

$$n(\boldsymbol{r}) = y + \sum_s \sum_{j\in s} \Delta(\boldsymbol{k}_s^{(j)}, \boldsymbol{r}), \qquad (21)$$

where $\Delta(\boldsymbol{k}_s^{(j)}, \boldsymbol{r})$ is the standing plane static concentration wave generated by the superstructure vector $\boldsymbol{k}_s^{(j)}$ of the star $\{\boldsymbol{k}_s\}$.† The equation for this wave takes the form

$$\Delta(\boldsymbol{k}_s^{(j)}, \boldsymbol{r}) = \frac{1}{2}\left[Q(\boldsymbol{k}_s^{(j)})\exp(i\boldsymbol{k}_s^{(j)}\boldsymbol{r}) + Q^*(\boldsymbol{k}_s^{(j)})\exp(-i\boldsymbol{k}_s^{(j)}\boldsymbol{r})\right], \qquad (22)$$

where $Q(\boldsymbol{k}_s^{(j)})$ is the concentration wave amplitude

$$Q(\boldsymbol{k}_s^{(j)}) = \eta_s\gamma(\boldsymbol{k}_s^{(j)}), \qquad (23)$$

η_s is the long-range order parameter and $\gamma(\boldsymbol{k}_s^{(j)}) = \gamma_s\exp(i\varphi_s^{(j)})$ is the coefficient taking into account the crystal symmetry. The coefficient $\gamma(\boldsymbol{k}_s^{(j)})$ is chosen so that the long-range order parameters equal to unity correspond to a completely ordered crystal of stoichiometric composition. Taking into account Eqn (23), the expression (22) can be represented as follows

$$\Delta(\boldsymbol{k}_s^{(j)}, \boldsymbol{r}) = \frac{1}{2}\eta_s\left[\gamma(\boldsymbol{k}_s^{(j)})\exp(i\boldsymbol{k}_s^{(j)}\boldsymbol{r}) + \gamma^*(\boldsymbol{k}_s^{(j)})\exp(-i\boldsymbol{k}_s^{(j)}\boldsymbol{r})\right]. \qquad (24)$$

From Eqns (21) and (24) it follows that the long-range order parameter η_s corresponds to each star of the wave vector $\{\boldsymbol{k}_s\}$. In the sites $\boldsymbol{r}$ located in the crystallographically equivalent positions, the distribution function takes the same value because it is invariant with respect to rotation and reflection involved in the point symmetry group of an ordered crystal. The number of values assumed by the distribution function at the sites of an ordered lattice is one unit larger than the number of long-range order parameters.

Summation in Eqn (21) is carried out over all non-equivalent superstructure vectors of the first Brillouin zone of the disordered lattice, *i.e*., over all superstructure vectors involved in the disorder – order phase transition channel.[3,4,117]

Analysis of the symmetry of the M_6C_5-type ($M_6C_5\square$-type) superstructures formed in nonstoichiometric transition metal carbides was carried out in the studies.[117,118]

The unit cell of the monoclinic (space group $C2/m$) superstructure of M_6C_5 is shown in Fig. 9. The translation vectors of this unit cell and the coordinates of atoms and vacancies are given in Table 9.

The translation of all superstructure sites of the reciprocal lattice of the monoclinic ordered phase M_6C_5 shows that the first

Table 9. Monoclinic [space group $C2/m$ (C_{2h}^3)] superstructure of M_6C_5 (V_6C_5).

Atom	Position and multiplicity	Atomic coordinates in ideal ordered structure [a]			Distribution function $n(x_I, y_I, z_I)$
		x/a_m	y/b_m	z/c_m	
C 1 (vacancy)	2(*a*)	0	0	0	$n_1 = y - \eta_9/6 - \eta_4/3 - \eta_3/3$
C 2	2(*d*)	0	1/2	1/2	$n_2 = y + \eta_9/6 - \eta_4/3 + \eta_3/3$
C 3	4(*g*)	0	1/3	0	$n_3 = y - \eta_9/6 + \eta_4/6 + \eta_3/6$
C 4	4(*h*)	0	1/6	1/2	$n_4 = y + \eta_9/6 + \eta_4/6 - \eta_3/6$
M 1	4(*i*)	1/4	0	3/4	
M 2	8(*j*)	1/4	2/3	3/4	

[a] Parameters of the monoclinic unit cell:

$$\boldsymbol{a}_m = \frac{1}{2}\langle 1\bar{1}\bar{2}\rangle_{B1},\ \boldsymbol{b}_m = \frac{3}{2}\langle 110\rangle_{B1},\ \boldsymbol{c}_m = \frac{1}{2}\langle 1\bar{1}2\rangle_{B1}.$$

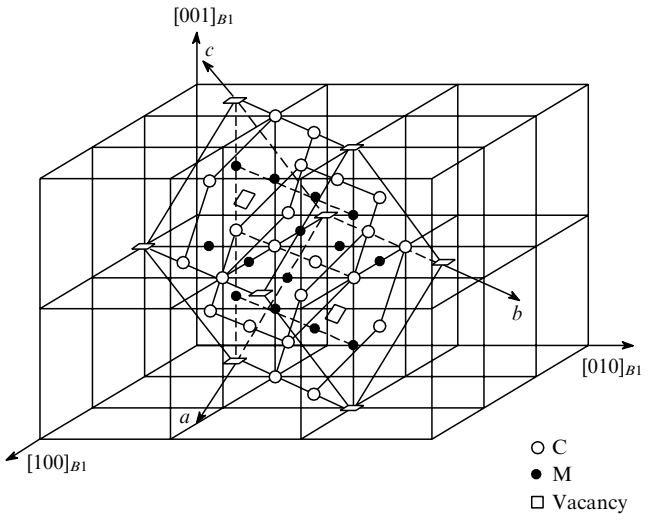


Figure 9. Position of the monoclinic (space group $C2/m$) unit cell of the superstructure M_6C_5 in the lattice with the $B1$ structure.

† The wave vector star is a set of all nonequivalent vectors generated from the vector $\boldsymbol{k}$ by rotation elements of the point symmetry group of the crystal. The wave vector star is denoted by $\{\boldsymbol{k}\}$, and the individual vectors involved in this set are called the arms of the star. The detailed definition of the wave vector star was given in publications.[3,4]

Brillouin zone of the disordered face-centred cubic (FCC) lattice contains five non-equivalent superstructure vectors belonging to three stars $\{\boldsymbol{k}_9\}$, $\{\boldsymbol{k}_4\}$ and $\{\boldsymbol{k}_3\}$.‡ These five vectors are involved in the phase transition channel associated with the formation of the ordered phase M_6C_5 (space group $C2/m$).

Calculations demonstrated [3, 4, 53, 117] that the distribution function describing the superstructure of M_6C_5 takes the form

$$n(x_I, y_I, z_I) = y - \frac{\eta_9}{6}\cos[\pi(x_I - y_I + z_I)] - \qquad (25)$$
$$- \frac{\eta_4}{3}\cos\frac{4\pi(x_I + y_I)}{3} - \frac{\eta_3}{3}\cos\frac{\pi(x_I - 5y_I - 3z_I)}{3},$$

where x_I, y_I, z_I are the coordinates of the nodes of the ordered non-metal FCC sublattice, $\boldsymbol{r} \equiv x_I, y_I, z_I$.

The distribution function (25) at all sites of the basic non-metal FCC sublattice takes four values (see Table 9). This indicates that, in the case of the above ordering, the non-metal sublattice of disordered nonstoichiometric carbide MC_y is divided into four non-equivalent sublattices. The probability of occupancy of the sites of the first sublattice by interstitial atoms is n_1, the probability of occupancy of the sites of the second sublattice is n_2, *etc*. The resulting distribution function is a superposition of three concentration waves related to three long-range order parameters, η_9, η_4 and η_3, respectively.

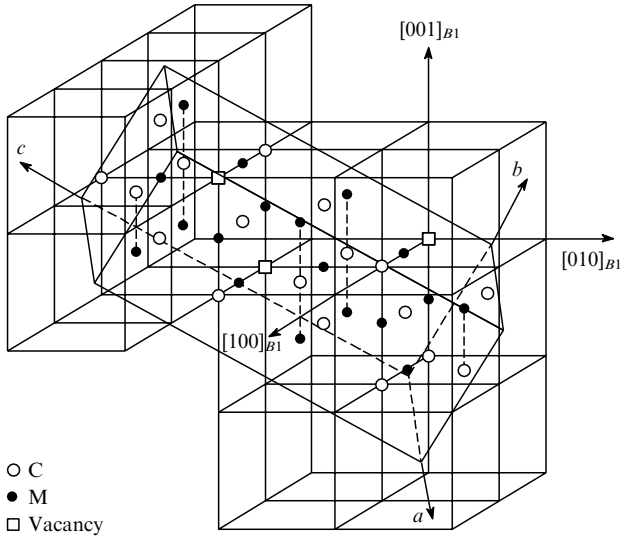


Figure 10. Position of the trigonal (space group $P3_1$) unit cell of the superstructure M_6C_5 in the lattice with the $B1$ structure.

The trigonal (space group $P3_1$) unit cell of the superstructure of M_6C_5 is shown in Fig. 10. The translation vectors of this unit cell and the coordinates of atoms and vacancies in the ideal trigonal superstructure of M_6C_5 are given in Table 10. The disorder – order phase transition channel giving rise to the trigonal superstructure of M_6C_5 includes 13 arms belonging to three stars $\{\boldsymbol{k}_9\}$, $\{\boldsymbol{k}_4\}$ and $\{\boldsymbol{k}_3\}$. Hence, the distribution function, as in the above-considered case, depends on three long-range order parameters

‡ Hereinafter, the numbering of the wave vector stars $\{\boldsymbol{k}_s\}$ of the first Brillouin zone of the FCC crystal and the arms of the stars are given in accordance with the monographs,[3, 4] where all $\{\boldsymbol{k}_s\}$ stars were described in detail.

Table 10. Trigonal [space group $P3_1$ (C_3^2)] superstructure of M_6C_5 (V_6C_5).

Atom	Position and multiplicity	Atomic coordinates in ideal ordered structure [a]			Distribution function $n(x_I, y_I, z_I)$
		x/a_{tr}	y/b_{tr}	z/c_{tr}	
C 1 (vacancy)	3(*a*)	1/9	8/9	1/6	$n_1 = y - \eta_9/6 - \eta_4/3 - \eta_3/3$
C 2	3(*a*)	4/9	5/9	1/6	$n_3 = y - \eta_9/6 + \eta_4/6 + \eta_3/6$
C 3	3(*a*)	7/9	2/9	1/6	$n_3 = y - \eta_9/6 + \eta_4/6 + \eta_3/6$
C 4	3(*a*)	1/9	5/9	1/3	$n_4 = y + \eta_9/6 + \eta_4/6 - \eta_3/6$
C 5	3(*a*)	4/9	2/9	1/3	$n_4 = y + \eta_9/6 + \eta_4/6 - \eta_3/6$
C 6	3(*a*)	7/9	8/9	1/3	$n_2 = y + \eta_9/6 - \eta_4/3 + \eta_3/3$
M 1	3(*a*)	1/9	5/9	1/12	
M 2	3(*a*)	4/9	2/9	1/12	
M 3	3(*a*)	7/9	8/9	1/12	
M 4	3(*a*)	1/9	2/9	1/4	
M 5	3(*a*)	4/9	8/9	1/4	
M 6	3(*a*)	7/9	5/9	1/4	

[a] Parameters of the trigonal unit cell:

$\boldsymbol{a}_{tr} = \frac{1}{2}\langle 21\bar{1}\rangle_{B1}$, $\boldsymbol{b}_{tr} = \frac{1}{2}\langle \bar{1}12\rangle_{B1}$, $\boldsymbol{c}_{tr} = 2\langle 1\bar{1}1\rangle_{B1}$.

$$n(x_I, y_I, z_I) = y - \frac{\eta_9}{6}\cos[\pi(x_I - y_I + z_I)] - \qquad (26)$$
$$- \frac{\eta_4}{6}\left[\cos\frac{4\pi(x_I + y_I)}{3} - \frac{\sqrt{3}}{3}\sin\frac{4\pi(x_I + y_I)}{3} - \right.$$
$$\left. - \frac{2\sqrt{3}}{3}\sin\frac{4\pi(x_I - z_I)}{3} + \cos\frac{4\pi(y_I + z_I)}{3} + \frac{\sqrt{3}}{3}\sin\frac{4\pi(y_I + z_I)}{3}\right] -$$
$$- \frac{\eta_3}{6}\left[\cos\frac{\pi(x_I - 5y_I - 3z_I)}{3} - \frac{\sqrt{3}}{3}\sin\frac{\pi(x_I - 5y_I - 3z_I)}{3} + \right.$$
$$+ \frac{2\sqrt{3}}{3}\sin\frac{\pi(5x_I + 5y_I + z_I)}{3} + \cos\frac{\pi(3x_I + y_I - 5z_I)}{3} +$$
$$\left. + \frac{\sqrt{3}}{3}\sin\frac{\pi(3x_I + y_I - 5z_I)}{3}\right].$$

This distribution function describing the trigonal superstructure of M_6C_5 takes the same four values, n_1, n_2, n_3 and n_4, as the distribution function (25), which describes the monoclinic (space group $C2/m$) superstructure of M_6C_5. However, the mutual arrangement of the sites of four sublattices in the trigonal ordered structure differs from that observed in the monoclinic superstructure. The values of the distribution function (26) are given in Table 10.

The unit cell of the monoclinic (space group $C2$) superstructure of M_6C_5 is shown in Fig. 11. The translation vectors of this unit cell and the coordinates of atoms and vacancies in the ideal monoclinic M_6C_5-type superstructure are given in Table 11. The monoclinic ordered phase of M_6C_5 is formed through the transition channel involving nine superstructure vectors of the reciprocal lattice belonging to four stars $\{\boldsymbol{k}_9\}$, $\{\boldsymbol{k}_4\}$, $\{\boldsymbol{k}_3\}$ and $\{\boldsymbol{k}_0\}$. Calculations demonstrated [3, 4, 53, 117] that this monoclinic superstructure of M_6C_5 is described by the distribution function, which depends on four long-range order parameters

$$n(x_I, y_I, z_I) = y - \frac{\eta_9}{6}\cos[\pi(x_I - y_I + z_I)] - \qquad (27)$$
$$- \frac{\eta_4}{12}\left[\cos\frac{4\pi(x_I + y_I)}{3} - \sqrt{3}\sin\frac{4\pi(x_I + y_I)}{3}\right] -$$
$$- \frac{\eta_3}{12}\left[\cos\frac{\pi(x_I - 5y_I - z_I)}{3} - \sqrt{3}\sin\frac{\pi(x_I - 5y_I - 3z_I)}{3}\right] -$$

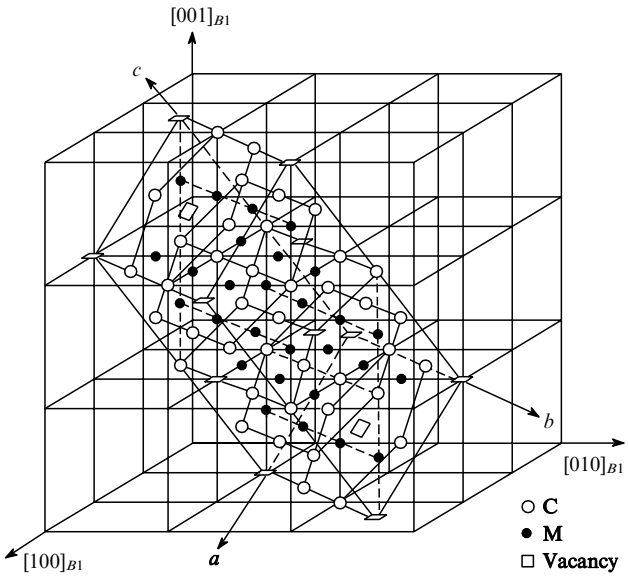


Figure 11. Position of the monoclinic (space group $C2$) unit cell of the superstructure M_6C_5 in the lattice with the $B1$ structure.

$$-\frac{\eta_0}{12}\left[3\cos\frac{\pi(x_I+7y_I+9z_I)}{6}-\sqrt{3}\sin\frac{\pi(x_I+7y_I+9z_I)}{6}+\right.$$
$$\left.+3\cos\frac{\pi(7x_I+y_I-9z_I)}{6}-\sqrt{3}\sin\frac{\pi(7x_I+y_I-9z_I)}{6}\right].$$

At all sites of the basic non-metal FCC sublattice, the distribution function (27) takes five values (see Table 11). Hence, as a result of the above-described ordering, the non-metal sublattice of disordered nonstoichiometric carbide is divided into five non-equivalent sublattices, which differ in the probabilities of occupancy of their sites by interstitial atoms.

For all the completely ordered M_6C_5-type phases under consideration, the relative stoichiometric concentration of carbon atoms is $y_{st} = 5/6$. If only non-metal sublattices of these superstructures are considered, the complete atomic planes $(1\bar{1}1)_{B1}$, in which all sites are occupied by carbon atoms, alternate with the imperfect $(1\bar{1}1)_{B1}$ planes, in which one-third of sites are vacant, along the $[1\bar{1}1]_{B1}$ direction (see Figs 9 – 11). In the imperfect planes, one-third of all sites are vacant, and each vacancy is surrounded by interstitial atoms, which form a regular hexagon.

In the completely ordered monoclinic (space group $C2/m$ and $C2$) and trigonal (space group $P3_1$) M_6C_5-type carbide structures, the metal atoms are in the same environment formed by non-metal sublattice sites (see Table 6, which gives the short-range order parameters and the distributions of carbon atoms and vacancies from the first to the eighth coordination spheres in the non-metal sublattice for the ideal superstructures of V_6C_5 crystallising in these space groups). If consideration is restricted to the first and second coordination spheres, these completely ordered structures have only two types of metal atom positions (Fig. 12), M_1^1 or V_1^1 (a metal atom with one vacancy in the first coordination sphere and one vacancy in the second coordination sphere) and M_1^2 (V_1^2) (a metal atom with one vacancy in the first coordination sphere and two vacancies in the second coordination sphere). In the ideal completely ordered structures of V_6C_5 (space group $C2/m$, $P3_1$ and $C2$), two-thirds of all vanadium atoms occupy the V_1^1 positions and one-third of vanadium atoms occupy the V_1^2 positions. Actually, the ^{51}V NMR spectra of annealed single crystals of vanadium carbide $VC_{0.84}$ show lines corresponding to the V_1^0, V_1^1 and V_1^2 positions with the intensity ratio of the V_1^1 and V_1^2 lines equal to 2 : 1.[13,84] Taking into account high intensities of these lines, V_1^1 and V_1^2 were considered[13,84] as positions of an ordered structure of V_6C_5 (see Section III.1).

The identity of the short-range order in three superstructures of V_6C_5 does not allow one to distinguish them based on the NMR spectroscopic data. It is also difficult to distinguish these superstructures with the use of diffraction data. That is why the results obtained in different studies of the structures of ordered phases V_6C_5 are so contradictory. In the study,[117] a procedure was developed for calculations of diffraction spectra of superstructures using the data on the disorder – order phase transition channel, and the diffraction spectra of all $M_{2t}X_{2t-1}$-type superstructures (X = C, N, O; t = 1, 1.5, 2, 3, 4), which can exist in strongly nonstoichiometric compounds, were calculated.

The calculated neutron diffraction spectra of the superstructures of V_6C_5 are presented in Fig. 13. It can be seen that the theoretical diffraction patterns of the ideal monoclinic (space

Table 11. Monoclinic [space group $C2$ (C_2^3)] superstructure of M_6C_5 (V_6C_5).

Atom	Position and multiplicity	Atomic coordinates in ideal ordered structure [a]			Distribution function $n(x_1, y_1, z_1)$
		x/a_m	y/b_m	z/c_m	
C 1 (vacancy)	2(*a*)	0	0	0	$n_1 = y - \eta_9/6 - \eta_4/12 - \eta_3/12 - \eta_0/2$
C 2 (vacancy)	2(*b*)	0	1/3	1/2	$n_1 = y - \eta_9/6 - \eta_4/12 - \eta_3/12 - \eta_0/2$
C 3	2(*a*)	0	1/3	0	$n_5 = y - \eta_9/6 - \eta_4/12 - \eta_3/12 + \eta_0/2$
C 4	2(*a*)	0	2/3	0	$n_3 = y - \eta_9/6 + \eta_4/6 + \eta_3/6$
C 5	2(*b*)	0	0	1/2	$n_5 = y - \eta_9/6 - \eta_4/12 - \eta_3/12 + \eta_0/2$
C 6	2(*b*)	0	2/3	1/2	$n_3 = y - \eta_9/6 + \eta_4/6 + \eta_3/6$
C 7	4(*c*)	0	1/6	1/4	$n_4 = y + \eta_9/6 + \eta_4/6 - \eta_3/6$
C 8	4(*c*)	0	1/2	1/4	$n_2 = y + \eta_9/6 - \eta_4/12 + \eta_3/12$
C 9	4(*c*)	0	5/6	1/4	$n_4 = y + \eta_9/6 + \eta_4/6 - \eta_3/6$
M 1	4(*c*)	1/4	1/6	1/8	
M 2	4(*c*)	1/4	1/2	1/8	
M 3	4(*c*)	1/4	5/6	1/8	
M 4	4(*c*)	1/4	0	3/8	
M 5	4(*c*)	1/4	1/3	3/8	
M 6	4(*c*)	1/4	2/3	3/8	

[a] Parameters of the monoclinic unit cell:

$$\boldsymbol{a}_m = \frac{1}{2}\langle 1\bar{1}\bar{2}\rangle_{B1},\ \boldsymbol{b}_m = \frac{3}{2}\langle 110\rangle_{B1},\ \boldsymbol{c}_m = \langle 1\bar{1}2\rangle_{B1}.$$

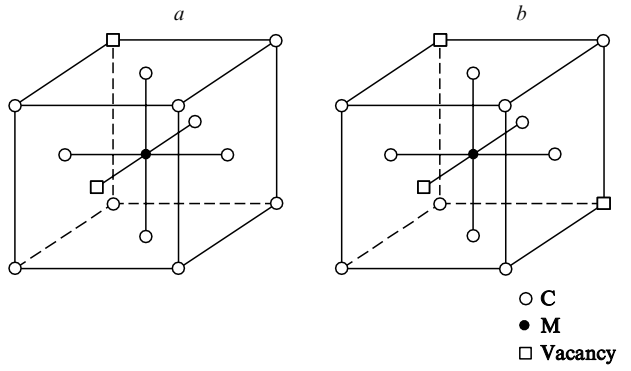


Figure 12. The M_1^1 (*a*) and M_1^2 (*b*) sites occupied by metal atoms in ideal completely ordered M_6C_5-type structures (space group $C2/m$, $P3_1$ and $C2$).
Two-thirds of all metal atoms occupy the M_1^1 sites and one-third of metal atoms occupy the M_2^1 sites.

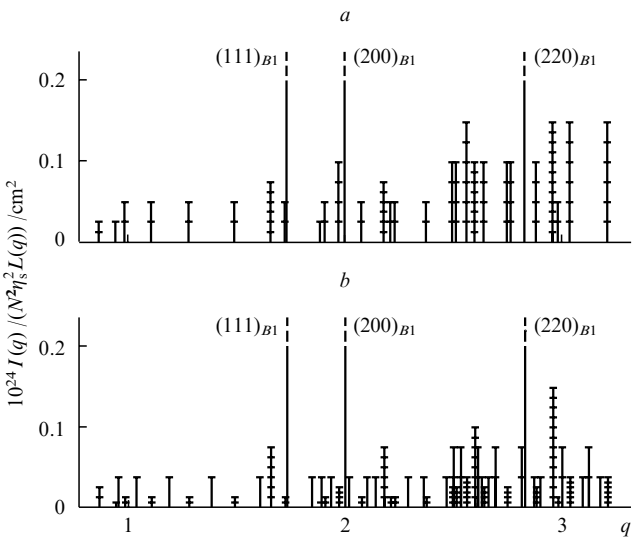


Figure 13. Theoretical neutron diffraction spectra of the ideal superstructures V_6C_5 (space group $C2/m$ and $P3_1$) (*a*) and V_6C_5 (space group $C2/m$) (*b*) constructed depending on the magnitude of the diffraction vector $q = (2a_{B1}\sin\theta)/\lambda$.
The intensities of reflections were calculated for the neutron scattering factors of vanadium and carbon atoms, $f_V = -0.038 \times 10^{-12}$ and $f_C = 0.665 \times 10^{-12}$ cm. The number of unit segments along the vertical lines representing the intensities of superstructure reflections is equal to the repetition factor of the corresponding reflection. For comparison, the intensities of the $(111)_{B1}$ and $(200)_{B1}$ structure reflections are 2.806 and 1.598 in units of the y axis, *i.e.*, these intensities are 10–20 times higher than the intensities of the strongest superstructure reflections.

group $C2/m$) superstructure of V_6C_5 is identical to the trigonal (space group $P3_1$) superstructure, which is reasonable taking into account that the disorder–order phase transition channel corresponding to each superstructure includes the arms of the same stars $\{\boldsymbol{k}_9\}$, $\{\boldsymbol{k}_4\}$ and $\{\boldsymbol{k}_3\}$, and the parameters determining the length of the arms $\boldsymbol{k}_4^{(j)}$ and $\boldsymbol{k}_3^{(l)}$ are equal for both superstructures. If these superstructures are characterised by the equal long-range order parameters η_s, there are no differences in the intensity of the superstructure reflections determined by the same star $\{\boldsymbol{k}_s\}$.[4,117] Therefore, if the corresponding long-range order parameters are equal, the diffraction spectra of these ideal superstructures of V_6C_5 (space group $C2/m$ and $P31$) have superstructure reflections identical in both position and intensity.

However, the intensities of superstructure diffraction reflections in the spectra of real ordered phases of V_6C_5 (space group $C2/m$ and $P31$) will be different because the static atomic displacements differ in direction and magnitude. Analysis of diffraction spectra taking into account possible static atomic displacements allows one to determine whether ordered V_6C_5-type phases have monoclinic or trigonal symmetry.

The diffraction pattern of the monoclinic (space group $C2$) superstructure of V_6C_5 is more complex than those of the above two superstructures of V_6C_5 (space group $C2/m$ and $P3_1$) (see Fig. 13), because the diffraction spectrum of this ordered phase has superstructure reflections associated with four stars $\{\boldsymbol{k}_9\}$, $\{\boldsymbol{k}_4\}$, $\{\boldsymbol{k}_3\}$ and $\{\boldsymbol{k}_0\}$. Therefore, it is easier to distinguish the monoclinic (space group $C2$) phase of V_6C_5 in studies of ordered V_6C_5 phases by diffraction methods.

The relation between three superstructures of V_6C_5 is illustrated by Fig. 14.[1,4,118] If only the non-metal sublattice is considered, complete planes containing only carbon atoms alternate with partially imperfect planes containing carbon atoms and vacancies along the $[1\bar{1}1]_{B1}$ direction in these superstructures. In the imperfect planes, vacancies occupy one-third of carbon sites. In the plane, the vacancies form regular hexagons. The mutual arrangement of the imperfect planes giving rise to three different

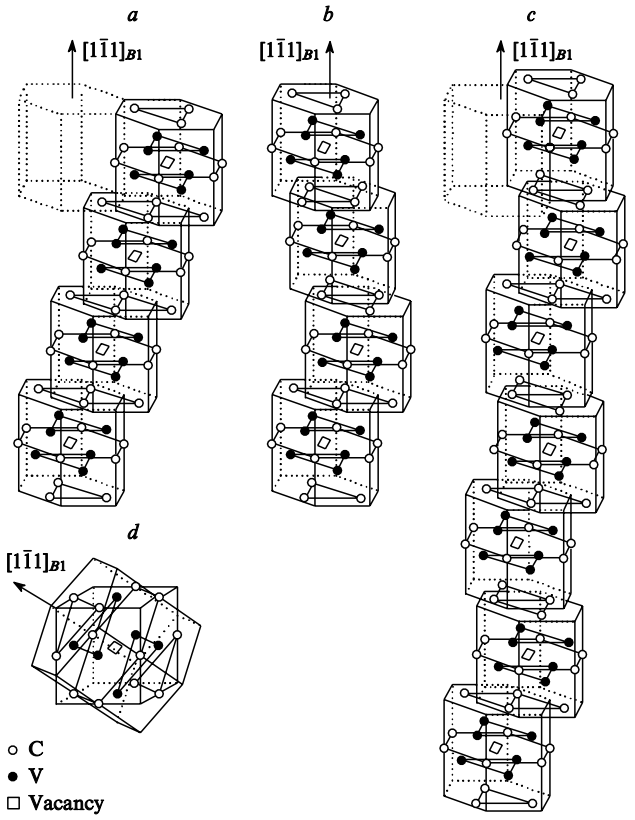


Figure 14. Models of related structures of the ordered carbide phases V_6C_5 (M_6C_5);[1,117]
(*a*) the monoclinic (space group $C2/m$) structure of V_6C_5, (*b*) the trigonal (space group $P3_1$) structure of V_6C_5, (*c*) the monoclinic (space group $C2$) structure of V_6C_5, (*d*) the position of the $V_6C_5\square$ quasimolecule in $B1$-type lattice.

M_6C_5-type structures is presented in Fig. 14. The successive threefold shift of the atoms with respect to the vacancies located in the equidistant imperfect planes along the $\{1/2\ -1/2\ 1\}_{B1}$ direction gives rise to the monoclinic (space group $C2/m$) structure of V_6C_5 (see Fig. 14 *a*). The successive helical shift along the $\{1/2\ -1/2\ 1\}_{B1}$, $\{1/2\ -1\ 1/2\}_{B1}$ and $\{1\ -1/2\ 1/2\}_{B1}$ vectors gives rise to the trigonal (space group $P3_1$) structure of V_6C_5 (see Fig. 14 *b*). Alternate shifts of the atoms and vacancies located in the imperfect planes along the $\{1/2\ -1/2\ 1\}_{B1}$ and $\{1/2\ -1\ 1/2\}_{B1}$ vectors (see Fig. 14 *c*) give rise to the monoclinic (space group $C2$) superstructure.

All superstructures of V_6C_5 can be represented as a set of $V_6C_5\square$ quasimolecules (see Fig. 14 *d*) arranged in a certain order. These superstructures differ only in the mutual arrangement of partially imperfect planes. Since such superstructures are identical in character of the short-range order, they have similar energies of formation. This is responsible for mixing of the sequences of the mutual arrangement of partially imperfect planes typical of each structure. As a result, the regular alternation of the planes along the *c* axis can be distorted, resulting in weakening of particular superstructure reflections.

The cubic ordered phase V_8C_7 with the space group $P4_332$ is observed only in the vicinity of the upper boundary of the homogeneity region of carbide VC_y corresponding to $VC_{0.875}$. The translation vectors of the unit cell of this ordered phase (Fig. 15) are twice as large as those of the basic structure $B1$, $\boldsymbol{a}_1 = \{2\ 0\ 0\}_{B1}$, $\boldsymbol{a}_2 = \{0\ 2\ 0\}_{B1}$ and $\boldsymbol{a}_3 = \{0\ 0\ 2\}_{B1}$.

The cubic (space group $P4_332$) superstructure of V_8C_7 is formed through the transition channel including all arms belonging to three stars $\{\boldsymbol{k}_9\}$, $\{\boldsymbol{k}_8\}$ and $\{\boldsymbol{k}_4\}$.[117] The corresponding

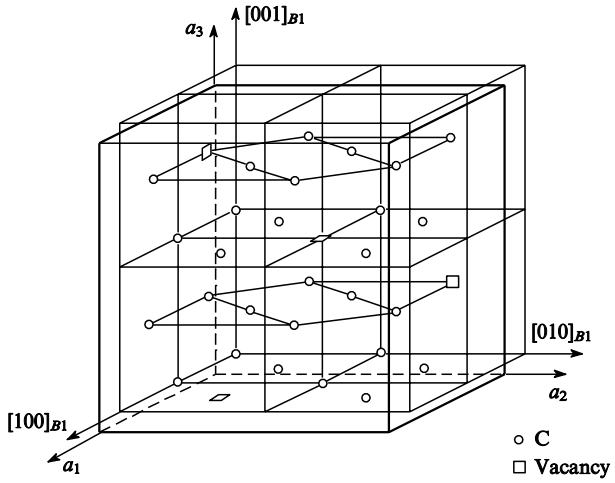


Figure 15. Position of the cubic (space group $P4_332$) unit cell of the superstructure V_8C_7 in the lattice with the $B1$ structure.

distribution function depends on three long-range order parameters

$$n(x_I, y_I, z_I) = y - \frac{\eta_9}{16}\left[\cos\pi(x_I + y_I + z_I) - \cos\pi(x_I - y_I + z_I) - \right. \quad (28)$$
$$\left. - \cos\pi(x_I + y_I - z_I) - \cos\pi(-x_I + y_I + z_I)\right] -$$
$$- \frac{\eta_8}{8}\left[-\cos\pi(2x_I + z_I) + \sin\pi(2x_I + z_I) - \cos\pi(y_I + 2z_I) + \right.$$
$$\left. + \sin\pi(y_I + 2z_I) - \cos\pi(x_I + 2y_I) + \sin\pi(x_I + 2y_I)\right] -$$
$$- \frac{\eta_4}{8}\left[\cos\pi(x_I + y_I) + \cos\pi(x_I + z_I) + \cos\pi(y_I + z_I) + \right.$$
$$\left. + \sin\pi(x_I - y_I) - \sin\pi(x_I - z_I) + \sin\pi(y_I - z_I)\right].$$

For this function, $y_{st} = 7/8$. In the case of the above-considered ordering, the non-metal sublattice of disordered nonstoichiometric carbide VC_y is divided into four non-equivalent sublattices. The probability of occupancy of the sites in these sublattices by carbon atoms [values of the distribution function (28)] are given in Table 12. In the ideal ordered cubic (space group $P4_332$) phase V_8C_7, three-fourths of all metal atoms occupy the V_1^1 positions, and the other atoms occupy the V_1^0 positions.

The structures of ordered phases of carbide VC_y determined by X-ray diffraction [49, 69] were refined [25, 26] taking into account the data on disorder – order transition channels. In the latter studies, samples of nonstoichiometric carbide VC_y containing different amounts of carbon (y = 0.66, 0.79, 0.83 and 0.87) were prepared by hot pressing of a mixture of powders of vanadium metal and carbide $VC_{0.875}$ at ~2200 K and a pressure of 35 MPa under an atmosphere of argon of special purity. Graphite foil was placed between the powder mixture and a graphite press-mould to avoid cracking. The hot-pressing time was 30 min. All samples had a porosity of < 3%, were homogeneous and contained only one VC_y phase with the $B1$ structure.

To prepare ordered carbides VC_y, compact samples synthesised as described above were annealed in evacuated sealed quartz tubes. Disordered carbide $VC_{0.875}$ was prepared by water quenching of a sample, which was pre-annealed at 1450 K and sealed in a quartz tube. Free carbon in the VC_y samples was absent. The nitrogen content was no higher than 0.09 mass %, and the oxygen content was 0.1 mass % – 0.3 mass %.

X-Ray diffraction studies (Cu $K\alpha_{1,2}$ radiation) were carried out in the angle range 2θ = 14 – 120° in a step-scan mode with a step of 0.02°. The exposure time per step was 10 s. Metallographic studies were performed in reflected light using polished samples of sintered and annealed carbides. Before study, the surface of metallographic sections was subjected to etching.

X-Ray diffraction patterns of $VC_{0.79}$, $VC_{0.83}$ and $VC_{0.87}$ samples prepared by annealing nonstoichiometric vanadium carbide had not only intense reflections but also additional peaks, whose intensities were no higher than 5% of the intensities of structure lines. The appearance of low-intensity additional reflections is indicative of the formation of ordered phases in thermally treated samples. In the X-ray pattern of carbide $VC_{0.66}$ subjected to thermal treatment, no additional reflections were observed.

Figure 16 shows fragments of X-ray diffraction patterns of annealed samples of carbides $VC_{0.79}$, $VC_{0.83}$ and $VC_{0.87}$.[25, 26] The intense lines observed in all X-ray diffraction patterns in the angle ranges 2θ = 37.4° and 43.4° are the $(111)_{B1}$ and $(200)_{B1}$ structure reflections. The X-ray diffraction patterns of all annealed carbides have diffuse peaks in the 2θ angle ranges of 21.2 – 22.0° and ~30.0 – 31.0°. These peaks are absent in the X-ray diffraction

Table 12. Characteristics of the cubic [space group $P4_332$ (O^6)] superstructure of M_8C_7 (V_8C_7).

Atom	Position and multiplicity	Atomic coordinates in ideal ordered structure [a]			Distribution function $n(x_I, y_I, z_I)$
		x/a_1	y/a_2	z/a_3	
C 1 (vacancy)	4(b)	5/8	5/8	5/8	$n_1 = y - \eta_9/8 - 3\eta_8/8 - 3\eta_4/8$
C 2	4(a)	1/8	1/8	1/8	$n_2 = y + \eta_9/8 + 3\eta_8/8 - 3\eta_4/8$
C 3	12(d)	1/8	5/8	5/8	$n_3 = y + \eta_9/8 - \eta_8/8 + \eta_4/8$
C 4	12(d)	1/8	3/8	7/8	$n_4 = y - \eta_9/8 + \eta_8/8 + \eta_4/8$
M 1	8(c)	3/8	3/8	3/8	
M 2	24(e)	1/8	3/8	1/8	

[a] Parameters of the cubic unit cell: $\boldsymbol{a}_1 = \langle 200\rangle_{B1}$, $\boldsymbol{a}_2 = \langle 020\rangle_{B1}$, $\boldsymbol{a}_3 = \langle 002\rangle_{B1}$.

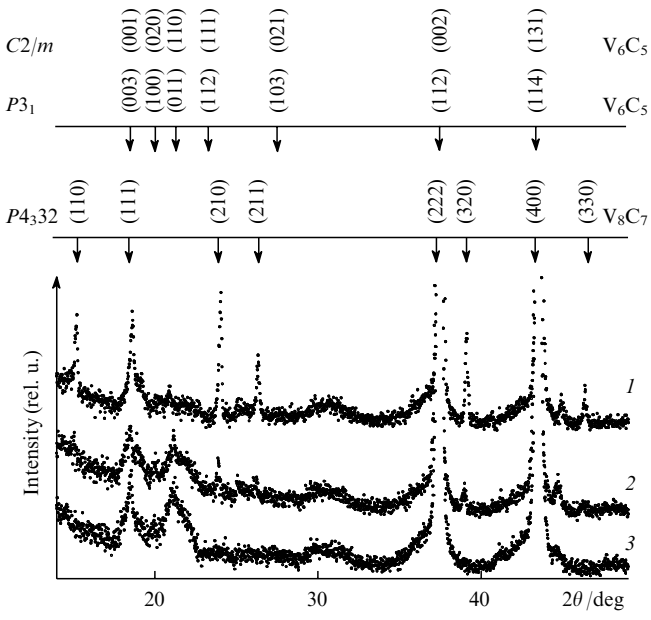


Figure 16. Fragments of X-ray diffraction patterns of annealed nonstoichiometric vanadium carbides $VC_{0.87}$ (*1*), $VC_{0.83}$ (*2*) and $VC_{0.79}$ (*3*).[25, 26] The positions of superstructure reflections for the ordered V_6C_5 and V_8C_7 phases are indicated by arrows; for all reflections, the Miller indices corresponding to the space group of the ordered phase are given.

patterns of disordered carbides. They are parasitic reflections from radiation with the wavelength $\lambda/2$ and correspond to the $(200)_{B1}$ and $(220)_{B1}$ structure reflections. The appearance of these peaks is associated with large accumulation of the signal during measurements of X-ray diffraction patterns of annealed carbides.

In the X-ray diffraction pattern of annealed carbide $VC_{0.87}$, the first superstructure reflection with the following diffraction vector

$$|\boldsymbol{q}| = 2a_{B1}\frac{\sin\theta}{\lambda} \approx 0.710$$

is observed for the angle $2\theta = 15.14^\circ$ (see Fig. 16). This reflection corresponds to the $\{1/2\ 1/2\ 0\}$ superstructure vector with a length $|\boldsymbol{q}| \approx 0.707$ belonging to the star $\{\boldsymbol{k}_4\}$ with the running index $\mu_4 = 1/4$. The next reflection with $|\boldsymbol{q}| \approx 0.871$ is observed at $2\theta = 18.55^\circ$ and corresponds to the $\{1/2\ 1/2\ 1/2\}$ vector of the star $\{\boldsymbol{k}_9\}$. The intensity of the third reflection ($2\theta = 24.04^\circ$) corresponding to the $\{1\ 1/2\ 0\}$ vector of the star $\{\boldsymbol{k}_8\}$ is the highest of all superstructure peaks. The next three superstructure reflections in the X-ray diffraction pattern of an annealed $VC_{0.87}$ sample (see Fig. 16) are observed at the angles $2\theta = 26.34$, 39.14 and 46.34° and correspond to the $\{1\ 1/2\ 1/2\}$ vector of the star $\{\boldsymbol{k}_4\}$, the $\{3/2\ 1\ 0\}$ vector of the star $\{\boldsymbol{k}_8\}$ and the $\{3/2\ 3/2\ 0\}$ vector of the star $\{\boldsymbol{k}_4\}$. The X-ray diffraction spectrum of annealed carbide $VC_{0.87}$ has 19 superstructure reflections corresponding to three stars $\{\boldsymbol{k}_9\}$, $\{\boldsymbol{k}_8\}$ and $\{\boldsymbol{k}_4\}$ in the 2θ angle range from 14° to 110°.

Analysis of the positions and intensities of the observed superstructure reflections demonstrated that thermal treatment of carbide $VC_{0.87}$ afforded the cubic ordered phase V_8C_7 (space group $P4_332$). The disorder–order phase transition channel $VC_{0.87} \rightarrow V_8C_7$ includes all arms of the Lifshitz stars $\{\boldsymbol{k}_9\}$ and $\{\boldsymbol{k}_8\}$ and the non-Lifshitz star $\{\boldsymbol{k}_4\}$ (at $\mu_4 = 1/4$). The Landau group-theoretical criterion for the occurrence of the second-order phase transition is not fulfilled, because the transition channel involves arms of the non-Lifshitz star $\{\boldsymbol{k}_4\}$, the sum $(\boldsymbol{k}_4^{(1)} + \boldsymbol{k}_4^{(5)} + \boldsymbol{k}_4^{(9)})$ being equal to the (111) structure vector of the reciprocal lattice. Even from symmetry considerations, it is evident that the formation of the ordered V_8C_7 phase can occur only as the first-order phase transition. This is consistent with the conclusions drawn in the studies.[4, 117]

Metallographic analysis of annealed carbide $VC_{0.87}$ confirmed the presence of an ordered phase belonging to the cubic system. As a result of ordering, each grain of the basic disordered phase is divided into domains of an ordered phase of isometric shape (Fig. 17). In reflected polarised white light, the ordered domains give no interference, which indicates that the ordered V_8C_7 phase is isotropic. Microstructural studies demonstrated also that the disorder–order phase transition in carbide $VC_{0.87}$ starts at the grain boundaries of the disordered phase. In disordered carbide, grains of the basic phase have distinct straight boundaries (see Fig. 17 *a*). After annealing, these boundaries become broken due to ordering (see Fig. 17 *b*). The domains intergrow with grains of the basic phase from the boundaries to the centres of the grains and penetrate into crystallites with time. Due to small domain sizes and the same cubic symmetry of the disordered and ordered phases, the domain boundaries cannot be observed by optical microscopy.

Analysis of the X-ray diffraction pattern of annealed carbide $VC_{0.83}$ (see Fig. 16) demonstrated that the sample contained two ordered phases. The X-ray pattern has superstructure reflections of the ordered phase V_8C_7 along with lines of the phase V_6C_5 with trigonal (space group $P3_1$) or monoclinic (space group $C2/m$) symmetry. In the X-ray pattern of annealed carbide $VC_{0.83}$, the ordered V_6C_5 phase is characterised by the $\{1/2\ 1/2\ 1/2\}$ superstructure reflection ($2\theta = 18.54^\circ$), which belongs to the star $\{\boldsymbol{k}_9\}$ and whose position is identical to that of the analogous reflection for the cubic ordered phase V_8C_7, and the $\{2/3\ 2/3\ 0\}$ ($2\theta = 20.11^\circ$), $\{1/6\ -5/6\ -1/2\}$ ($2\theta = 21.14^\circ$), $\{-1/3\ -1/3\ 1\}$ ($2\theta = 23.74^\circ$) and $\{7/6\ 1/6\ 1/2\}$ ($2\theta = 27.34^\circ$) reflections belonging to the stars $\{\boldsymbol{k}_4\}$ (with $\mu_4 = 1/3$) and $\{\boldsymbol{k}_3\}$ (with $\mu_3 = 1/6$).

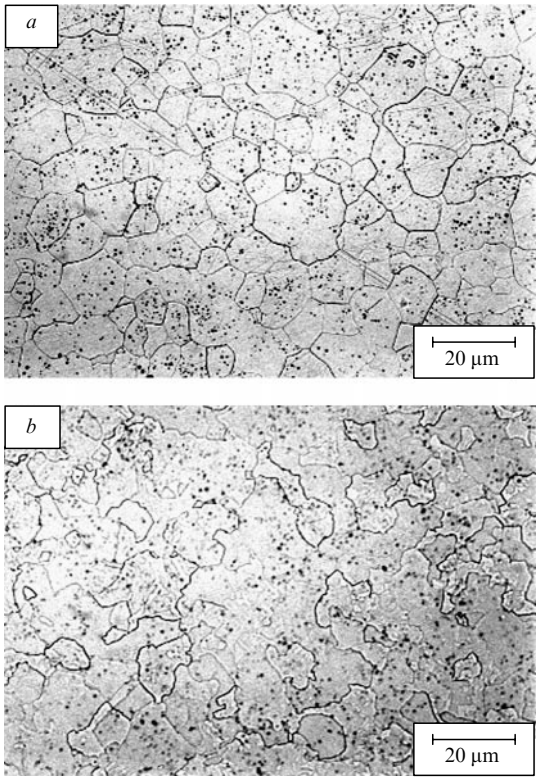


Figure 17. Changes in the microstructure of compact nonstoichiometric vanadium carbide $VC_{0.87}$ upon ordering;
(*a*) in disordered carbide $VC_{0.87}$, grains have distinct linear boundaries, (*b*) in ordered carbide V_8C_7 ($VC_{0.87}$), the grain boundaries of the basic phase are corroded due to formation of domains of the ordered phase V_8C_7.

Therefore, the disorder–order phase transition channel associated with the formation of the superstructure of V_6C_5 involves the arms of the Lifshitz star $\{\boldsymbol{k}_9\}$ and the non-Lifshitz stars $\{\boldsymbol{k}_4\}$ and $\{\boldsymbol{k}_3\}$. From symmetry considerations, the formation of the ordered phase V_6C_5 should occur as the first-order phase transition.

A set of the observed superstructure wave vectors giving rise to the transition channel $VC_{0.83} \rightarrow V_6C_5$ can correspond to either trigonal (space group $P3_1$) or monoclinic (space group $C2/m$) superstructures of the V_6C_5 type.

Investigation of the microstructure of annealed carbide $VC_{0.83}$ in reflected polarised white light demonstrated that the sample contained domains of two ordered phases. One phase is composed predominantly of isometric grains and gives no interference, *i.e.*, it is isotropic. Hence, this phase is apparently the cubic ordered phase V_8C_7 and comprises 15%–20% of the sample. The second phase comprises 80%–85% of the sample. Domains of the second phase are of platelet-like and prismatic shape characteristic of crystals belonging to the monoclinic and trigonal systems and show an interference colour, *i.e.*, they are anisotropic. In reflected polarised white light, the domains of the second phase are blue and yellow in colour. These facts suggest that the second phase is carbide V_6C_5. Therefore, the results of microstructural studies are consistent with the conclusions drawn from X-ray diffraction data.

The X-ray diffraction pattern of annealed carbide $VC_{0.79}$ has superstructure reflections of only the ordered V_6C_5-type structure (see Fig. 16). Its microstructure contains domains of only an anisotropic ordered phase. Consequently, prolonged annealing of vanadium carbide $VC_{0.79}$ afforded the only ordered V_6C_5 phase.

The X-ray diffraction pattern of annealed carbide $VC_{0.66}$ have reflections of only the basic cubic phase with the $B1$ structure and

shows no additional reflections, although reflections of the rhombohedral (trigonal) phase ζ-V_4C_{3-x} would be expected to appear. Carbides ζ-M_4C_{3-x} ($x \leqslant 0.33$) have an imperfect carbon sublattice and are formally (without consideration for the crystal structure) identical in composition to M_3C_2 ($MC_{0.67}$). Carbide ζ-V_4C_{3-x} is not an ordered phase of cubic carbide VC_y because it has the trigonal rather that the FCC metal sublattice.[119] According to the results of the study,[52] the rhombohedral phase ζ-V_4C_{3-x} contains 37.9 at.% carbon, has a very narrow homogeneity region ($VC_{0.605}$–$VC_{0.615}$), is generated by a peritectoid reaction at 2150 K and is observed up to 1540 K. The absence of the ζ-V_4C_{3-x} phase in annealed carbide $VC_{0.66}$ (see Refs 25 and 69) is, apparently, associated with the fact that annealing was carried out starting from a lower temperature (1200 K). It should be noted that the composition of carbide $VC_{0.66}$ corresponds to the lower boundary of the homogeneity region of the ζ-V_4C_{3-x} phase.

Additional analysis of the X-ray diffraction spectral patterns of ordered carbide V_8C_7 (Fig. 18) led authors of the publication [49] to the conclusion that this superstructure is characterised by large static atomic displacements. The vanadium atoms, which form an octahedral environment of the structural non-metal vacancy, are shifted toward the vacancy by 0.003–0.006 nm. The carbon atoms are also shifted toward the vacancies, but these shifts are substantially larger (as large as 0.05 nm). In disordered carbide $VC_{0.87}$ with the period $a_{B1} = 0.4172$ nm, the V–V and V–C interatomic distances are 0.295 and 0.209 nm, respectively, whereas these distances in the vacant $\square V_6$ octahedron in ordered carbide V_8C_7 are smaller (0.282–0.293 and 0.180–0.209 nm), which is indicative of contraction of the octahedron. In the filled CV_6 octahedron of ordered carbide V_8C_7, the V–V and V–C distances are 0.295–0.311 and 0.209–0.258 nm, respectively. Such large shifts of the metal atoms can give rise to additional reflections, which are absent in the X-ray diffraction pattern of the ideal (without consideration for atomic displacements) ordered V_8C_7-type cubic (space group $P4_332$) phase.

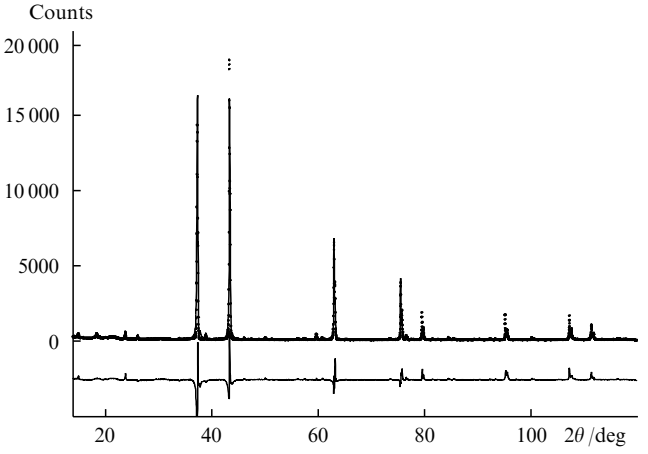


Figure 18. Experimental (dotted line) and calculated (solid line) X-ray diffraction patterns (Cu $K\alpha_{1,2}$ radiation) of the ordered phase V_8C_7.[49] The intensity differences between the experimental and calculated X-ray diffraction patterns are shown at the bottom of the figure.

IV. Nanocrystalline carbide V_8C_7 and molecular clusters V_mC_n

In the last 15–20 years, methods for the preparation of nanostructured substances and materials were extensively developed, and the influence of the particle (grain) size on the properties of nanocrystalline compounds was actively studied.[120–126] For example, vanadium carbide $VC_{0.875}$ was prepared in the nanocrystalline state by atom-vacancy ordering as a result of the disorder–order transformation $VC_{0.875} \rightarrow V_8C_7$.[127–131]

1. Nanocrystalline vanadium carbide

A coarse-grained powder (with a particle size of 1–2 μm) of vanadium carbide $VC_{0.875}$ was subjected to long-term ageing at an environmental temperature in a closed vessel (to avoid penetration of water vapour from air). An aged vanadium carbide powder appeared to be very hygroscopic. Immediately after withdrawal from the vessel, the powder contained no more than 0.2 mass % of physically adsorbed water. After storage under environmental conditions for several months, the water content reached 2.0 mass % and then remained unchanged. Generally, coarse-grained vanadium carbide powders do not possess such a high hygroscopicity.

Chemical analysis of an aged vanadium carbide powder demonstrated that it has the composition $VC_{0.875}$ corresponding to the upper boundary of the homogeneity region of the cubic phase with the $B1$ structure.

A vanadium carbide powder was studied by the microscopic method. Discrete irregularly shaped agglomerates with sizes of 5–50 μm are observable under ~100 magnification. These agglomerates consist of particles with sizes of ~1 μm. Under higher magnification, it is seen that these particles have a complex structure and are composed of a large number of very small, nanometre-size, particles (hereinafter, these particles will be referred to as nanoparticles or nanocrystallites). Figure 19 shows a photomicrograph taken with a high-resolution DSM 982 Gemini scanning electron microscope. Each particle with a size of ~1 μm looks like an opened rosebud or a loose head of cabbage and consists of nanocrystallites. Under 50 000 magnification it can be seen that the observed nanocrystallites appear as curved leaves, which, as a first approximation, can be modelled by disks with a diameter of ~400–600 nm and a thickness of ~15–20 nm. The volume of these disks corresponds to that of a rather large spherical particle with a diameter of 150–220 nm. However, due to the small thickness of the disk, the ratio of its surface area to the volume is 0.107–0.143 nm^{-1}, which corresponds to the specific surface area of the powder of 19–26 $m^2\ g^{-1}$.

The crystal structure of vanadium carbide was studied by X-ray diffraction using Cu $K\alpha_{1,2}$ radiation. The X-ray diffraction patterns of disordered carbide $VC_{0.875}$, annealed coarse-grained ordered carbide $VC_{0.875}$ (V_8C_7) and nanostructured carbide $VC_{0.875}$ are shown in Fig. 20. The X-ray pattern of the $VC_{0.875}$ nanopowder (see Fig. 20 *c*) has structure reflections of the basic $B1$ phase along with superstructure reflections corresponding to the cubic ordered phase V_8C_7 with the space group $P4_332$. The

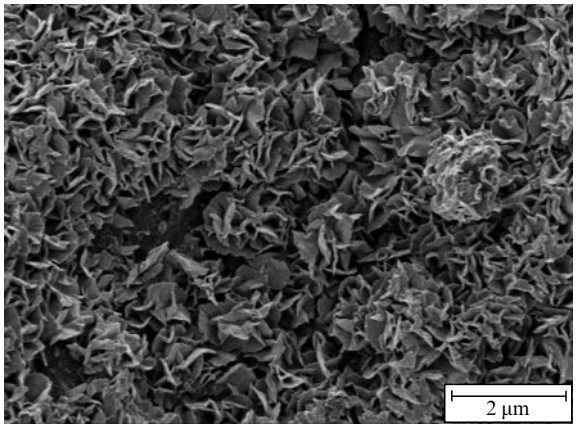


Figure 19. Microstructure of a powder of vanadium carbide $VC_{0.875}$ subjected to long-term ageing at environmental temperature and under an environmental atmosphere (10 000 magnification).[127, 131]

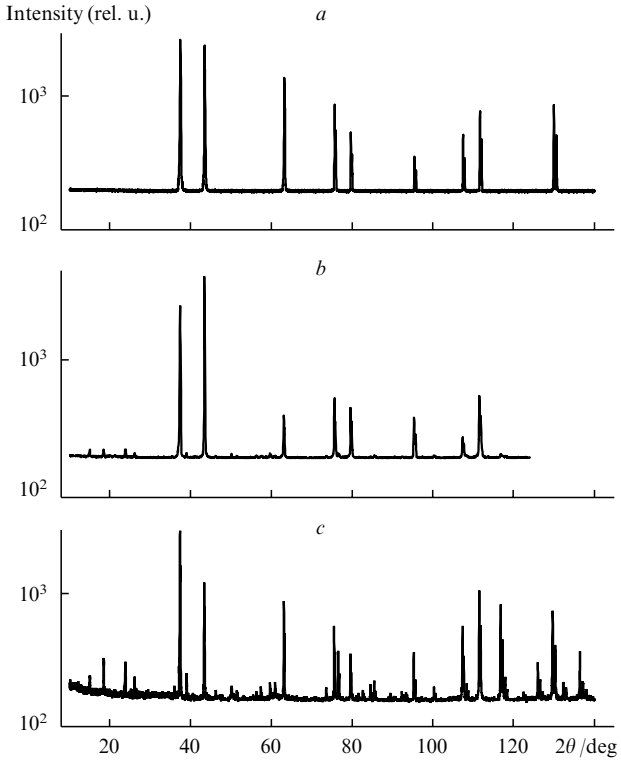


Figure 20. Powder X-ray diffraction patterns of disordered carbide $VC_{0.875}$ (a_{B1} = 0.41638 nm) (*a*), ordered coarse-grained carbide $VC_{0.875}$ (V_8C_7) (a_{B1} = 0.41682 nm) (*b*) and nanostructured carbide $VC_{0.875}$ (a_{B1} = 0.41685 nm) (*c*) (Cu $K\alpha_{1,2}$ radiation).[127, 130, 131]
Superstructure reflections observed in the X-ray diffraction patterns of *b* and *c* correspond to the cubic (space group $P4_332$) ordered phase V_8C_7. High intensities of superstructure reflections for a $VC_{0.875}$ nanopowder and an anomalous increase in their intensity in the region $2\theta > 100^\circ$ can be a consequence of large static displacements of vanadium atoms.

lattice parameter of the ordered phase is 0.8337 ± 0.0001 nm. The ideal cubic M_8C_7-type superstructure with the space group $P4_332$ (see Fig. 15) has the doubled (compared to the disordered basic *B*1 phase) lattice parameter.[17, 117] Hence, the lattice parameter of the basic phase of the vanadium carbide under consideration is a_{B1} = 0.41685 nm. This parameter is substantially (by 0.00047 nm) larger than the lattice parameter of disordered carbide $VC_{0.875}$. The authors speculated [17, 25, 26, 55] that this large difference in the lattice parameter of ordered and disordered carbides $VC_{0.875}$ can be observed only in the case of the highest or near-highest degree of ordering.

The intensity ratio of the structure and superstructure reflections supports the conclusion that the degree of long-range order in vanadium carbide is close to the maximum value. Besides, this ratio indicates that the ordered phase occupies the whole volume of the substance, *i.e.*, the latter is a single-phase powder.

The intensities of superstructure reflections of coarse-grained ordered carbide $VC_{0.875}$ (I_{super}) decrease with increasing diffraction angle 2θ (see Fig. 20 *b*), whereas the intensities of superstructure reflections of a vanadium carbide nanopowder at $2\theta > 100^\circ$ even increase (see Fig. 20 *c*). This is probably attributable to large relaxation static displacements of vanadium atoms in the vicinity of carbon vacancies. These displacements were actually observed in ordered carbide V_8C_7.[49]

Defects in a nanostructured vanadium carbide powder were studied [127, 130] by positron lifetime measurements using a powder of carbide $VC_{0.875}$, which was precalcinated at 400 K to remove adsorbed water. For comparison, the positron lifetime in coarse-grained sintered vanadium carbide with the same composition $VC_{0.875}$ was measured. The spectrum of coarse-grained vanadium carbide has only a short-lifetime component at 157 ± 2 ps, which corresponds to positron annihilation at a structural vacancy of the carbon sublattice.[132–134] Quantitative analysis of the spectrum of the nanostructured powder demonstrated that this spectrum has a short-lifetime component along with a long-lifetime component at 500 ps with a relative intensity of 7% associated with positron annihilation at defects on the particle surface. The thickness of the surface layer in a vanadium carbide nanopowder was estimated [127–131] at 0.5–0.7 nm by comparing the relative intensities of the short- and long-lifetime components. Therefore, the results of positron lifetime measurements demonstrated that only nonmetal structural vacancies are present in the interior of vanadium carbide nanocrystallites, whereas their surface layer contains vacancy agglomerates as defects.

The microhardness of a nanostructured powder of $VC_{0.875}$, which was cold pressed at 10 MPa and then sintered under vacuum (1×10^{-3} Pa) with a rise in temperature from 400 to 2000 K, was measured under a load of 200 and 500 g. The microhardness was H_V = 60–80 GPa, which is $\sim$3 times larger than that of macrocrystalline vanadium carbide (29 GPa under a load of 0.1 and 0.2 kg) and approaches to the microhardness of diamond. The substantially higher microhardness of carbide $VC_{0.875}$, which was prepared by sintering a nanopowder, can be explained taking into account the Hall–Petch law, according to which H_V is proportional to $d^{-1/2}$ (*d* is the grain size).

Based on the results of investigations of the structure and properties of vanadium carbide powders, the following model of the nanocrystallite structure was proposed.[127, 129–131] Nanocrystallites have a shape of strongly curved disks with a diameter of 400–600 nm and a thickness of 15–20 nm. Their interior consists of ordered carbide V_8C_7 with a high degree of long-range order and contains a negligible amount of dissolved oxygen. The surface layer of nanocrystallites contains chemisorbed oxygen in an amount of 3.1 mass % and a substantial amount of vacancy agglomerates, which is indicative of its loose structure. The thickness of the surface phase is no larger than 0.7 nm or four atomic monolayers.

The observed morphology of the nanocrystalline vanadium carbide powder may be a consequence of grain cracking at the interface between disordered and ordered phases. Actually, a jump increase in the FCC-sublattice parameter by 0.0004 nm (as a result of the disorder–order phase transition $VC_{0.875} \rightarrow V_8C_7$; the domain size of the ordered phase is $\sim$20 nm) was observed at 1413 ± 20 K by high-temperature X-ray diffraction.[48] At 300 K, the parameter a_{B1} of the basic crystal lattice of quenched disordered carbide $VC_{0.875}$ differs from that of ordered carbide with the same carbon content, but this difference (published data) is 0.0002 nm. The difference in the volumes of the disordered and ordered phases is responsible for strains followed by cracking.

Strains can occur also due to the mismatch between the atomic structures of antiphase domains in ordered vanadium carbide. In any case, the formation of a nanostructure of a powder of nonstoichiometric vanadium carbide $VC_{0.875}$ is caused by the disorder–order phase transition $VC_{0.875} \rightarrow V_8C_7$.

2. Metallocarbohedrene V_8C_{12}

In 1992, the V_8C_{12} molecular cluster was detected in the V–C system by mass-spectrometric study of the products of the plasma-chemical gas-phase synthesis from hydrocarbons and vanadium vapour, which was prepared by laser heating of the metal. This cluster along with Ti_8C_{12} and analogous compounds belong to metallocarbohedrenes (metallocarbons, metcars) M_8C_{12}.[35, 36] In the synthesis, helium was used as an inert gas.

The molecular cluster of stoichiometric composition V_8C_{12} presumably has a pentagondodecahedral shape (Fig. 21 *a*). In the ideal molecule, all atoms are located on the sphere, and its surface is formed by linking the adjacent atoms and consists of 12 regular pentagons. In this molecule, all vanadium and carbon atoms have

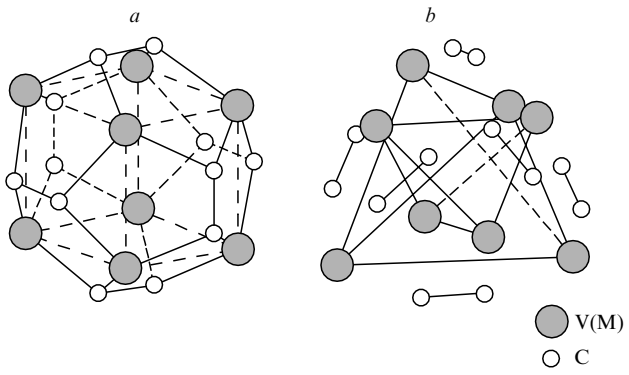


Figure 21. Dodecahedral structure of the molecular cluster V_8C_{12} (M_8C_{12}) with symmetry T_h (*a*) and T_d (*b*).

identical (as in fullerene C_{60}) coordination (the coordination number is three), occupy identical positions and are distributed between the vertices of the dodecahedron so that the vanadium atoms are bound only to the carbon atoms and six C_2 fragments alternate with eight vanadium atoms. The dodecahedral structure of V_8C_{12} can be represented as a cube formed by vanadium atoms, the C_2 fragment being bound to each face of the cube. The point symmetry group T_h of this ideal structure includes 24 symmetry elements (rotations and reflections).

The electronic structure of V_8C_{12} with symmetry T_h was calculated [135] with the use of the following bond lengths:

Bond	C – C	V – C	V – V
Length /nm	0.144	0.189	0.285

The electronic energy spectrum of V_8C_{12} was demonstrated to be similar to the spectrum of Ti_8C_{12}, but it is slightly shifted to negative energies due to a larger electronegativity of vanadium compared to titanium. The populations of the atomic orbitals corresponding to M – C interactions involving vanadium are ~9% lower than those involving titanium because the atomic orbitals of vanadium are more localised. The V_8C_{12} molecular cluster is chemically less stable than Ti_8C_{12}.

In another structure of the V_8C_{12} cluster with the point symmetry group T_d (see Fig. 21 *b*), the vanadium atoms occupy two types of positions, and the sites belonging to positions of each type form a tetrahedron. The smaller tetrahedron is rotated with respect to the larger tetrahedron by 90°. The vanadium atoms differ in the arrangement relative to the C_2 dimers. Six C_2 fragments are parallel to the edges of the larger tetrahedron formed by the V(1) atoms and perpendicular to the edge of the smaller tetrahedron formed by the V(2) atoms. The V(1) atoms are bound to three nearest carbon atoms, and the V(2) atoms are bound to six carbon atoms.

The question as to which of these two structures (with symmetry T_h or T_d) actually exists remains open, because molecular crystals of metallocarbons are unavailable.

Initially, the plasma-chemical gas-phase synthesis of titanium, zirconium, hafnium and vanadium molecular clusters have afforded predominantly the M_8C_{12} and M_mC_n cluster particles with a ratio of C : M ≈ 1.5 – 2.0.[35, 36, 136] Nanoparticles of carbides TiC, ZrC, HfC and VC with a metal FCC sublattice were absent. At the same time, only monocarbide nanoparticles can be prepared by the conventional plasma-chemical synthesis (without laser heating of the plasma). More recently, particles with cubic ($M_{14}C_{13}$) and dodecahedral (M_8C_{12}) structures were simultaneously prepared by the plasma-chemical gas-phase synthesis in the V – C and Ti – C systems.[137] The synthesis with the use of low-power laser heating afforded a larger amount of 'cubic' $M_{14}C_{13}$ nanoparticles compared to M_8C_{12}. An increase in the power of laser radiation and an increase in the hydrocarbon concentration lead to the predominant formation of dodecahedral particles with the metal-to-carbon ratio varying from 1 : 1.5 to 1 : 2, which was demonstrated in the study of the Nb – C and Zr – C systems.[138, 139] Therefore, a decrease in the carbon concentration in the plasma due to a decrease in the hydrocarbon concentration or a decrease in the power of laser radiation results in a relative carbon deficiency and the predominant formation of monocarbide nanoparticles, whereas an increase in the carbon concentration in the plasma makes it possible to synthesise the M_mC_n clusters varying from M_8C_{12} to $M_{11}C_{21}$ and $M_{13}C_{22}$.[138, 139]

Such facts, as the synthesis of the V_8C_{12} molecular cluster in the V – C system and the formation of cubic $V_{14}C_{13}$ nanoparticles in the plasma,[137] provide indirect evidence that it is possible to synthesise stoichiometric monocarbide $VC_{1.0}$ with the *B*1 structure.

V. Phase diagram for the V – C system with consideration for ordering of VC_y

Ordering of nonstoichiometric cubic vanadium carbide VC_y has been studied for many years. However, until recently, a reliable phase diagram of the V – C system, which takes into account the formation of ordered phases, has been lacking in the literature. The first attempt to construct a fragment of the phase diagram, where the ordered phases V_6C_5 and V_8C_7 co-exist, has been made in the publication.[43] Later on, an attempt was made [48] to take into account phase equilibria in VC_y in the narrow composition range $0.84 \leqslant y \leqslant 0.93$ at $1273 < T < 1473$ K. The main problem associated with the construction of the phase diagram of the V – C system is that $VC_{0.875}$ rather than the $MC_{1.0}$ compound of stoichiometric composition serves as the upper boundary of the homogeneity region of disordered cubic vanadium carbide VC_y, as opposed to other transition metal carbides. The unusual position of the upper boundary of the homogeneity region of carbide VC_y is responsible for the edge effect, which is manifested in the formation of the ordered phase V_8C_7, which is absent in other carbides.

As mentioned above, disordered vanadium carbide VC_y ($VC_y\square_{1-y}$) has a rather extended homogeneity region, within which the carbon atoms and structural vacancies form a substitutional solution in the non-metal sublattice. Depending on the composition and the conditions of the synthesis and thermal treatment, carbide VC_y can exist in the disordered or ordered state. The disordered state is in thermodynamic equilibrium at temperatures higher than 1300 – 1400 K, whereas the ordered state is in thermodynamic equilibrium at $T < 1300$ K. However, due to low diffusion mobility of atoms, the disordered state of nonstoichiometric vanadium carbide is easily retained upon quenching from $T > 1400$ K to lower temperatures (~300 K) and exists as a metastable state at $T < 1000$ K.

In the studies,[27, 32] the phase equilibria in the ordering region of nonstoichiometric cubic carbide VC_y were calculated by the order parameter functional method.[1 – 4, 16, 53, 140 – 142]

In the first version of calculations, it was assumed that the ordered phase V_8C_7 has no homogeneity region. Actually, single-phase samples with the cubic superstructure V_8C_7 are formed only in the case of carbide $VC_{0.87-0.875}$, whereas at lower carbon concentrations ($0.83 < y < 0.87$), the phase V_6C_5, which has an extended homogeneity region,[2] is always present in samples containing the ordered phase V_8C_7.[5, 47, 68, 69, 143] In the studies,[62, 144, 145] the temperature of the $V_8C_7 \rightleftharpoons VC_y$ transition was demonstrated to be virtually independent (within experimental error) of the composition of carbide VC_y (Fig. 22). To take into account the specific features of the ordered phase V_8C_7 ($VC_{0.875}$), where no homogeneity region was observed, its free energy was represented as follows

$$F_{V_8C_7\ (VC_{0.875})}(T) = F(T) - TS_c + \frac{\Delta H_{tr}}{T_{tr}}(T - T_{tr}), \qquad (29)$$

where

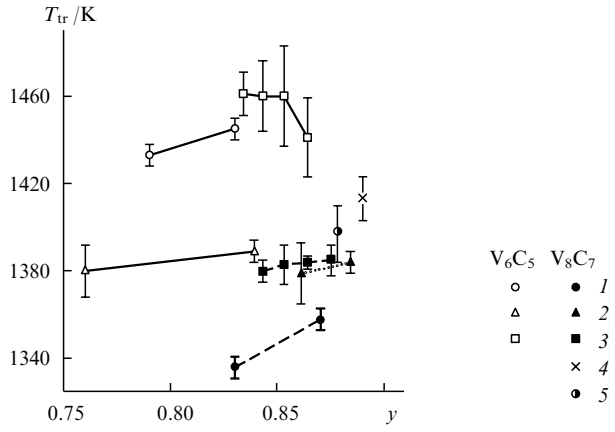


Figure 22. Dependence of the temperature of the phase transitions $V_6C_5 \rightleftarrows VC_y$ (empty balls) and $V_8C_7 \rightleftharpoons VC_y$ (solid balls) on the composition of vanadium carbide VC_y;
(*1–5*) the results of the studies,[25, 62, 48, 144, 145] respectively.

$$F(T) = F_0(T) + x\,F_1(T) + x^2F_2(T)$$

at $x = 0.875$ [$F_0(T)$, $F_1(T)$ and $F_2(T)$ are the parameters of the free energy of disordered carbide VC_y, see Eqn (8)]; $S_c = 3.132\ 10^{-3}$ kJ mol^{-1} K^{-1} is the configurational entropy of carbide $VC_{0.875}$; $\Delta H_{tr} = 3$ kJ mol^{-1} and $T_{tr} = 1380$ K are the heat and temperature of the $V_8C_7 \rightarrow VC_{0.875}$ transition estimated from experimental data.[25, 62, 69, 143]

The phase boundary between the homogeneity region of disordered carbide VC_y and the two-phase region ($VC_y + V_8C_7$) was determined using [27] the equation

$$F_{V_8C_7\,(VC_{0.875})}(T) = F(y,0,T) - (y - y_b)\frac{\partial F(y,0,T)}{\partial y}, \qquad (30)$$

where

$$F(y,0,T) - (y - y_b)\frac{\partial F(y,0,T)}{\partial y} = F_0(T) + y_bF_1(T) + \qquad (31)$$
$$+ y(2y_b - y)F_2(T) + kT\left[\ln(1-y) + y_b\ln\frac{y}{1-y}\right],$$

$y_b = 0.875$.

The position of the phase boundary between the homogeneity region of the ordered phase $V_{2t}C_{2t-1}$ (V_6C_5) and the two-phase region ($V_{2t}C_{2t-1} + V_8C_7$) was specified analogously

$$F_{V_8C_7\,(VC_{0.875})}(T) = F(y,\eta,T) - (y - y_b)\frac{\partial F(y,\eta,T)}{\partial y}, \qquad (32)$$

where

$$F(y,\eta,T) - (y - y_b)\frac{\partial F(y,\eta,T)}{\partial y} = F_0(T) + y_bF_1(T) + \qquad (33)$$
$$+ y(2y_b - y)F_2(T) + \frac{a^{(s)}}{4t^2}\eta_{eq}^2F_2(T) +$$
$$+ \frac{kT}{2t}\left\{\ln\left[n_1^{y_b}(1-n_1)^{(1-y_b)}\right] + (2t-1)\ln\left[n_2^{y_b}(1-n_2)^{(1-y_b)}\right]\right\}.$$

The parameters n_1, n_2, η_{eq}, t and $a^{(s)}$ (see below) refer to the phase $V_{2t}C_{2t-1}$ (V_6C_5).

In calculations of the phase equilibria involving lower disordered hexagonal carbide β-V_2C ($V_2C_{y'}$), its homogeneity region was not taken into account, and the composition of the lower carbide was interpreted as V_2C ($VC_{0.50}$). Calculations were carried out according to the equation

$$0.5\,F_{V_2C}(T) = F_0(T) + 0.5\,F_1(T) + y(1-y)F_2(T) + \qquad (34)$$
$$+ \frac{a^{(s)}}{4t^2}\eta_{eq}^2F_2(T) + \frac{kT}{4t}\left\{\ln\left[n_1(1-n_1)\right] + \right.$$
$$\left. + (2t-1)\ln\left[n_2(1-n_2)\right]\right\}_{\eta = eta_{eq}},$$

where $F_{V_2C}(T)$ is the free energy of lower hexagonal vanadium carbide β-V_2C described by Eqn (9).

Equations (33) and (34) include the parameters n_1, n_2, η_{eq}, t and $a^{(s)}$. The numerical coefficients t and $a^{(s)}$, which characterise the possible $M_{2t}C_{2t-1}$-type superstructures of cubic carbides MC_y, are given in Table 13. The parameters n_1 and n_2 are the probabilities of finding a carbon atom in a site of the vacancy and carbon sublattices of the ordered phase $M_{2t}C_{2t-1}$ (see Refs 3 and 4):

$$n_1 = y - \frac{\eta(2t-1)}{2t}, \qquad (35)$$
$$n_2 = y\frac{\eta}{2t}.$$

Table 13. Structural characteristics of possible ordered phases $M_{2t}C_{2t-1}$ of strongly nonstoichiometric compounds MC_y with the *B*1 basic structure (NaCl).[3, 4]

Type of the ordered phase	Space group	t	$a^{(s)}$	$2a^{(s)}/(2t-1)$
M_2C	*R*3*m*, *Fd*3*m*	1	0.2	0.4
M_2C	$I4_1/amd$	1	0.2	0.4
M_2C	*P*4/*mmm*	1	0.067 (1/15)	0.133 (2/15)
M_3C_2	*Immm*, *P*2	1.5	0.4	0.4
M_3C_2	$C222_1$	1.5	0.4	0.4
M_3C_2	$P\bar{3}m1$	1.5	−0.2	−0.2
M_4C_3	$Pm\bar{3}m$	2	0.2	0.133 (2/15)
M_4C_3	*I*4/*mmm*	2	0.467 (7/15)	0.311 (14/45)
M_6C_5	*C*2/*m*, $P3_1$, *C*2	3	1.0	0.4
M_8C_7	*Fm*3*m*, $P4_332$	4	1.0	0.286 (2/7)

The equilibrium long-range order parameter η_{eq} in the ordered phase $M_{2t}C_{2t-1}$ at the temperature T satisfies the equation [3, 4]

$$\frac{1}{\eta_{eq}}\ln\left[\frac{n_2(1-n_1)}{n_1(1-n_2)}\right]_{\eta=\eta_{eq}} = \frac{2a^{(s)}}{2t-1}\frac{F_2(T)}{kT}. \qquad (36)$$

The phase diagram of the V–C system published in the papers [27, 32] is shown in Fig. 23. Calculations demonstrated [27] that ordering of nonstoichiometric cubic carbide VC_y in different temperature and concentration ranges can give rise to three ordered phases, *viz.*, V_3C_2, V_6C_5 and V_8C_7.

The phase V_6C_5 is the main ordered vanadium carbide phase. This phase appears at a temperature lower than 1485 K, and its homogeneity region extends from $VC_{0.745}$ to $VC_{0.831}$ at 1100 K. This phase can also be observed in two-phase regions, *i.e.*, it exists almost throughout the homogeneity region of carbide VC_y (see Fig. 23). The ordered phase V_8C_7 is formed at a lower temperature (1380 K). At 1330 K, it can be observed along with V_6C_5 in the two-phase region extended from $VC_{0.83}$ to $VC_{0.875}$, which is consistent with experimental data.[47, 144, 146] The $V_6C_5 + V_8C_7$ two-phase region, where the ordered phase V_8C_7 exists, becomes narrower with decreasing temperature. The ordered phases V_6C_5 and V_8C_7 form an eutectic with $T_e = 1331$ K and $y_e = 0.852$. These parameters are close to the estimate obtained in the study:[48] $T_e \approx 1300$ K and $y_e \approx 0.852$. The calculations also demonstrated that the ordered phase V_3C_2, which has a narrow homogeneity region (from $VC_{0.667}$ to $VC_{0.710}$ at 800 K), can be generated in

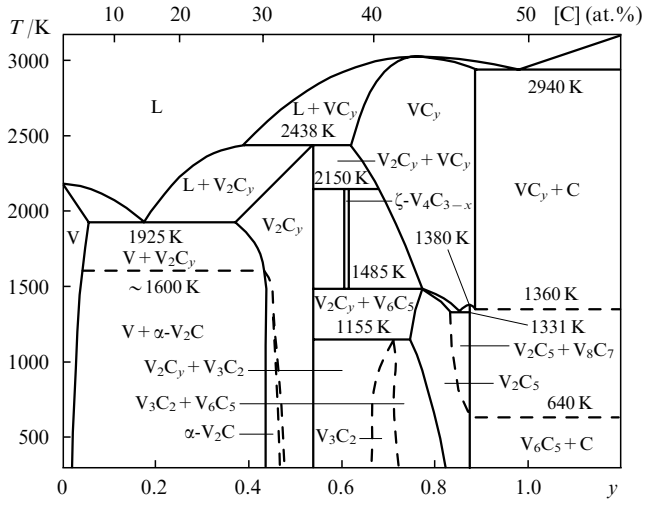


Figure 23. Phase diagram of the V – C equilibrium system, which was constructed taking into account the atomic ordering of nonstoichiometric cubic vanadium carbide VC_y.[27, 32]
The phase boundaries outside the ordering region are those published in the studies;[41, 147] the position of the phase ζ-V_4C_{3-x} is given according to the publication:[52] V_8C_7, V_6C_5 and V_3C_2 are the ordered phases of cubic carbide VC_y, α-V_2C is the ordered phase of lower hexagonal carbide $V_2C_{y'}$ (β-V_2C).

vanadium carbide at 1155 K (lower temperatures) under equilibrium conditions according to the peritectoid reaction

$$V_2C_y + V_6C_5 \longrightarrow V_3C_2 .$$

This phase has not been experimentally observed. According to the results of calculations,[27] the region of existence of the ordered phase V_3C_2 is close to the concentration range, in which the rhombohedral (trigonal) phase ζ-V_4C_{3-x} is actually observed, but its existence was not taken into account in calculations of ordering of carbide VC_y, because the thermodynamic characteristics of this phase are unknown. If the free energy of the ζ-phase at $T < 1150$ K is lower than that of the ordered phase V_3C_2, the phase V_3C_2 cannot exist. Taking into consideration this fact, the region of existence of the ordered phase V_3C_2 is shown hypothetically.

The position of the phase ζ-V_4C_{3-x} is given based on the results of the study.[52] The lowest temperature, at which it was detected after long-term annealing, is 1540 K. This temperature is close to the calculated maximum temperature of the disorder – order $VC_y - V_6C_5$ transition (1485 K) and is taken as the lower temperature boundary of existence of the phase ζ-V_4C_{3-x}.

In the homogeneity region of lower carbide $V_2C_{y'}$ (β-V_2C), the ordered orthorhombic phase α-V_2C (β_r-V_2C) is formed.[108–113] The precise temperature of ordering is unknown. According to the results of the studies,[41, 147] this temperature is lower than 1870 K. Magnetic susceptibility measurements of ordered carbide α-V_2C (β_r-V_2C) in the temperature range of 300 – 1300 K did not reveal the structural phase transition

$$\alpha\text{-}V_2C\ (\beta_r\text{-}V_2C) \longrightarrow V_2C_{y'}\ (\beta\text{-}V_2C)$$

up to 1300 K.[148] Taking into account this fact and the results of the investigation,[147] the temperature of the order – disorder phase transition in the phase diagram of the V – C system was assumed to be equal to ~1600 K (see Fig. 23). The new V_8C_{12} compound, which was discovered in 1992,[35] was omitted in the phase diagram of the V – C system published in the papers,[27, 32] because it is outside the range of the compositions under consideration.

All disorder – order transitions in vanadium carbide VC_y belong to first-order phase transitions (see Fig. 23). The same conclusion was drawn in the publications,[25, 69] where the changes in the heat capacities of carbides $VC_{0.79}$, $VC_{0.83}$ and $VC_{0.87}$ upon heating and cooling were considered.

The calculated[27] values of T_{tr}, ΔS_{tr} and ΔH_{tr} for phase transitions associated with ordering of nonstoichiometric carbide VC_y are listed in Table 14, which gives also experimental T_{tr} and ΔH_{tr} for comparison.[25, 69] For carbide $VC_{0.79}$, the calculated temperature T_{tr} and heat ΔH_{tr} of the $V_6C_5 \rightarrow VC_{0.79}$ transition are 1450 K and 2.84 kJ mol^{-1}, respectively; the experimental ΔH_{tr} value is somewhat lower, because a small amount of the

Table 14. Temperatures (T_{tr} /K), entropies (ΔS_{tr} /J mol^{-1} K^{-1}) and heats (ΔH_{tr} /kJ mol^{-1}) of order – order and order – disorder phase transitions in nonstoichiometric vanadium carbide VC_y.

y	$V_3C_2 - V_6C_5$ (calculation[25, 27])			$V_6C_5 - VC_y$					$V_8C_7 - VC_y$				
	T_{tr}	ΔS_{tr}	ΔH_{tr}	T_{tr}		ΔS_{tr} (calculation[25, 27])	ΔH_{tr}		T_{tr}		ΔS_{tr} (calculation[25, 27])	ΔH_{tr}	
				calculation[25, 27]	experiment[25, 69]		calculation[25, 27]	experiment[25, 69]	calculation[25, 27]	experiment[25, 69]		calculation[25, 27]	experiment[25, 69]
0.73	1138	1.38	1.57	–	–	–	–	–	–	–	–	–	–
0.74	993	1.17	1.16	–	–	–	–	–	–	–	–	–	–
0.75	728	0.82	0.60	–	–	–	–	–	–	–	–	–	–
0.76	–	–	–	–	–	–	–	–	–	–	–	–	–
0.77	–	–	–	1481	–	1.75	2.59	–	–	–	–	–	–
0.78	–	–	–	1466	–	1.85	2.72	–	–	–	–	–	–
0.79	–	–	–	1450	1430 ± 5	1.96	2.84	2.16 ± 0.1	–	–	–	–	–
0.80	–	–	–	1433	–	2.05	2.94	–	–	–	–	–	–
0.81	–	–	–	1413	–	2.13	3.01	–	–	–	–	–	–
0.82	–	–	–	1391	–	2.19	3.04	–	–	–	–	–	–
0.83	–	–	–	1366	1442 ± 5	2.21	3.02	1.26 ± 0.1 [a]	–	1334 ± 5	–	–	0.70 ± 0.1 [a]
0.84	–	–	–	1338	–	2.20	2.95	–	–	–	–	–	–
0.85	–	–	–	1307	–	2.15	2.81	–	–	–	–	–	
0.86	–	–	–	1272	–	2.06	2.62	–	–	–	–	–	–
0.87	–	–	–	–	–	–	–	–	–	1355 ± 5	–	–	2.30 ± 0.1
0.875	–	–	–	–	–	–	–	–	1380	–	2.17	3.00	–

[a] In the study,[69] the total thermal effect $\Delta H_{tr} = 2.11$ kJ mol^{-1}, which includes the thermal effects of two transformations, $VC_{0.83} \rightarrow V_6C_5$ ($\Delta H_{tr} \approx 1.37$ kJ mol^{-1}) and $VC_{0.83} \rightarrow V_8C_7$ ($\Delta H_{tr} \approx 0.75$ kJ mol^{-1}), is given for the transformation occurring in carbide $VC_{0.83}$ on cooling.

phase ζ-V_4C_{3-x} is present (which was demonstrated by calorimetric measurements [69]) in carbide $VC_{0.79}$.

Additional model calculations were carried out [27] to refine the phase diagram of the V–C system in the event that the phase V_8C_7 has a small homogeneity region. In these calculations, the free energy of the ordered phase V_8C_7 is represented as follows:

$$F_{V_8C_7\,(VC_{0.875})}(T) = F(T) - TS_c + \qquad (37)$$
$$+ \frac{\Delta H_{tr}(y)}{T_{tr}(y)}[T - T_{tr}^{max}(a + by + cy^2)],$$

where $F(T)$ and S_c are the same parameters as those in Eqn (29);

$$\frac{\Delta H_{tr}(y)}{T_{tr}(y)} \equiv \Delta S_{tr} = 2.174 \text{ J mol}^{-1}\text{ K}^{-1};$$

$T_{tr}^{max} = 1380$ K is the maximum temperature of the $V_8C_7 \rightarrow VC_y$ transition corresponding to $VC_{0.875}$; $a = 40.7455$, $b = -93.367$ and $c = 54.793$.

If the phase V_8C_7 has a homogeneity region, the boundaries of the $VC_y + V_8C_7$ two-phase region were calculated according to the following equations:[27]

$$y_1^2F_2(T) - kT\ln(1-y_1) = \qquad (38)$$
$$= y_2^2F_2(T) - kT\ln(1-y_2) - \Delta S_{tr}\left[T - (a - cy_2^2)T_{tr}^{max}\right],$$
$$y_1(2-y_1)F_2(T) + kT\ln y_1 =$$
$$= y_2(2-y_2)F_2(T) + kT\ln y_2 +$$
$$+\Delta S_{tr}\left[T - (a + b + 2cy_2 - cy_2^2)T_{tr}^{max}\right].$$

In the event that the phase V_8C_7 has a homogeneity region, the phase boundaries of the $V_6C_5 + V_8C_7$ two-phase region were determined analogously

$$y_1^2F_2(T) - \frac{a^{(s)}}{4t^2}\eta_{eq}^2F_2(T) - \qquad (39)$$
$$-\frac{kT}{2t}\left[\ln(1-n_1^{(d)}) + (2t-1)\ln(1-n_2^{(d)})\right]_{\eta=\eta_{eq}} =$$
$$= y_2^2F_2(T) - kT\ln(1-y_2) - \Delta S_{tr}\left[T - (a - cy_2^2)T_{tr}^{max}\right],$$
$$y_1(2-y_1)F_2(T) - \frac{a^{(s)}}{4t^2}\eta_{eq}^2F_2(T) +$$
$$-\frac{kT}{2t}\left[\ln n_1^{(d)} + (2t-1)\ln n_2^{(d)})\right]_{\eta=\eta_{eq}} =$$
$$= y_2(2-y_2)F_2(T) - kT\ln y_2 +$$
$$+\Delta S_{tr}\left[T - (a + b + 2cy_2 - cy_2^2)T_{tr}^{max}\right].$$

In Eqns (39), the parameters n_1, n_2, t, η_{eq} and $a^{(s)}$ refer to the ordered phase V_6C_5.

The fragment of the phase diagram of the V–C system calculated without considering the homogeneity region of the phase V_8C_7 is shown in Fig. 24, and the corresponding fragment, which was calculated taking into account this region, is presented in Fig. 25. Calculations [27] demonstrated that the homogeneity region of the phase V_8C_7 is very narrow (the maximum size is observed at 1340 K and corresponds to the compoisition range from $VC_{0.852}$ to $VC_{0.875}$). A decrease in the temperature from 1340 K leads to a further narrowing of the homogeneity region of the phase V_8C_7. At 1340 K, the phases V_6C_5 and V_8C_7 form an eutectic with $y_e \approx 0.8476$. The $V_6C_5 + V_8C_7$ two-phase region existing at $T < 1340$ K is almost half as wide as that observed in the first case. Otherwise the phase diagram of the V–C system remains unchanged. It is necessary to perform thorough experimental investigations of the structure of vanadium carbide in the narrow composition range, $VC_{0.85}$–$VC_{0.875}$, to give an unambiguous answer to the question as to whether the phase V_8C_7 has a homogeneity region.

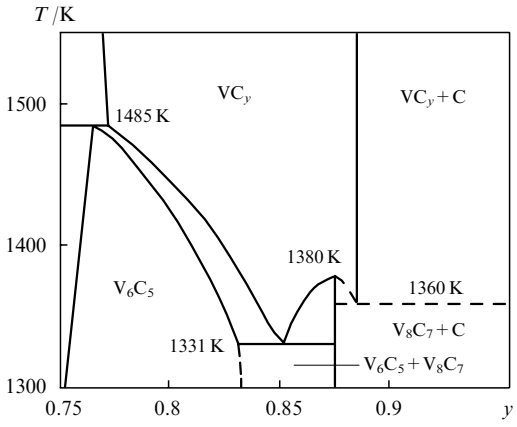


Figure 24. Fragment of the ordering region near the upper boundary of the homogeneity region of carbide VC_y (see Fig. 23).
Calculated on the assumption of the absence of the homogeneity region of the phase V_8C_7.

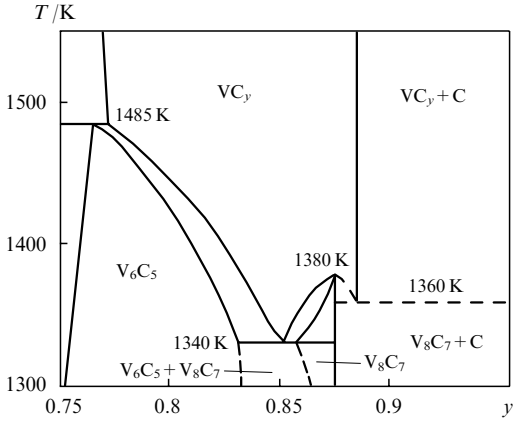


Figure 25. Fragment of the ordering region of carbide VC_y (see Fig. 23).
Calculated on the assumption of the presence of a narrow homogeneity region of the phase V_8C_7.

On the whole, the calculations [25–27, 32] well reproduced the formation of the monoclinic (or trigonal) phase V_6C_5 with the $VC_{0.75}$–$VC_{0.83}$ homogeneity region (or 1100 K), the cubic phase V_8C_7, which can co-exist with V_6C_5 in the two-phase region, and the ordered phase V_3C_2, which appears at $T < 1150$ K and exhibits a very narrow homogeneity region, upon ordering of VC_y. The temperatures of the $V_6C_5 \rightleftharpoons VC_y$ and $V_8C_7 \rightleftharpoons VC_{0.875}$ transitions are 1400–1450 and 1360–1380 K, respectively.

VI. Conclusion

Analysis of the results of investigations performed in the last 15 years demonstrated that a large number of compounds and phases are produced in the vanadium–carbon system. Their detection became possible due to the use of unconventional synthetic methods, studies of the phase equilibria in a low-temperature region and the use of highly sensitive diffraction and spectroscopic methods for analysing products of annealing and chemical reactions.

The phase V_6C_5, which can have monoclinic (space group $C2/m$ and $C2$) and trigonal (space group $P3_1$) symmetry, and the cubic (space group $P4_332$) phase V_8C_7 are the most well-known ordered phases of vanadium carbide. The phase V_6C_5 exists in the $VC_{0.75-0.77}-C_{0.82-0.86}$ range. The phase V_8C_7 was observed in vanadium carbide samples, whose compositions are close to the upper boundary of the homogeneity region of VC_y and was detected even in samples quenched from 1500 K.

Molecular clusters with compositions varying from $V_{14}C_{13}$, which, presumably, has a cubic structure, to V_8C_{12} with a dodecahedral structure and then to $V_{11}C_{21}$ and $V_{13}C_{22}$ were produced by the plasma-chemical synthesis using laser heating. Apparently, these compounds can be stabilised in the crystalline state in thin films by deposition of the molecular clusters onto supports.[149] A chemical modification of the support or thermal treatment of the deposited film provides additional possibilities of forming a particular structure of clusters.

X-Ray, neutron and electron diffraction techniques are the main experimental methods for the detection and investigation of new compounds and phases in the V–C system. The presence of model diffraction spectra for the phases under consideration in the V–C system substantially facilitates their identification and interpretation of experimental results.

Noteworthy is the applied aspect of investigations of nonstoichiometric carbides. Carbides of stoichiometric composition are generally used in the production of solid alloys with the aim of providing stability of their properties. However, interactions with matrix metal lead to complex chemical processes resulting in dissolution of matrix metal in carbide, depletion of the carbide phase in carbon and enrichment of matrix metal in metal from the carbide phase and (to a smaller degree) in carbon. Carbide grains in solid alloys have a ring structure with a non-uniform distribution of elements over the grain section. It is evident, even from this fact, that carbide phases in solid alloys are generally nonstoichiometric, and ordering and disordering processes can occur in these phases. Evidently, to provide stability of the properties of solid alloys during usage, *i.e.*, at temperatures from 600 to 900 °C, it is necessary that the solid nonstoichiometric carbide phase be in a thermodynamically stable structural state and do not undergo transformations under these conditions. That is why ordering of nonstoichiometric carbides is of applied interest.

Investigations of high-alloy vanadium-containing steels performed in the last decades demonstrated that the resulting vanadium carbide phases are ordered V_6C_5 phases and, more rarely, V_8C_7 phases. An understanding of the conditions of formation and isolation of these phases requires a knowledge of the disorder–order transformations in nonstoichiometric carbides.

Finally, recent investigations showed that ordering of nonstoichiometric vanadium carbide can be used to form nanocrystalline structures. Apparently, disorder–order transformations can be used to construct other nanostructured nonstoichiometric compounds and solid solutions.

On the whole, investigations of ordering of vanadium carbides and properties of these compounds in different structural states contribute to fundamental knowledge of nonstoichiometry and provides the basis for their practical use.

I thank Professor A I Gusev, who encouraged me to write this review. This review has been written with the financial support of the Russian Foundation for Basic Research (Project No. 03-03-32031).

References

1. A I Gusev *Fizicheskaya Khimiya Nestekhiometricheskikh Tugoplavkikh Soedinenii* (Physical Chemistry of Nonstoichiometric Refractory Compounds) (Moscow: Nauka, 1991)
2. A I Gusev *Usp. Fiz. Nauk* **170** 3 (2000) [*Physics-Uspekhi* **43** 1 (2000)]
3. A I Gusev, A A Rempel, A J Magerl *The Disorder and Order in Strongly Nonstoichiometric Compounds: Transition Metal Carbides Nitrides and Oxides* (Berlin, Heidelberg, New York, London: Springer, 2001)
4. A I Gusev, A A Rempel *Nestekhiometriya, Besporyadok i Poryadok v Tverdom Tele* (Nonstoichiometry, Disorder and Order in Solids) (Ekaterinburg: Urals Branch of the Russian Academy of Sciences, 2001)
5. P Pütz *Metallurgie (Paris)* **3** 649 (1906)
6. J O Arnold, H A Read *J. Iron Steel Inst. London* **85** 215 (1912)
7. A Osawa, M Oya *Sci. Rep. Tohoku Univ. First Ser.* **19** 95 (1930)
8. H Moissan *Compt. Rend.* **116** 1225 (1893)
9. A Morette *Bull. Soc. Chim. Fr.* **5** 1063 (1938)
10. E K Storms, R J McNeal *J. Phys. Chem.* **66** 1401 (1962)
11. E K Storms *The Refractory Carbides* (New York, London: Academic Press, 1967)
12. C H de Novion, N Lorenzelli, P Costa *C.R. Hebd. Seances Acad. Sci., Ser. B* **263** 775 (1966)
13. J D Venables, D Kahn, R G Lye *Philos. Mag.* **18** 177 (1968)
14. A I Gusev *Dokl. Akad. Nauk SSSR* **313** 887 (1990) [a]
15. C H de Novion, B Beuneu, T Priem, N Lorenzelli, A Finel, in *The Physics and Chemistry of Carbides, Nitrides and Borides* (Ed. R Freer) (Amsterdam: Kluwer Academic, 1990) p. 329
16. A I Gusev *Fiz. Tv. Tela* **32** 2752 (1990) [b]
17. A I Gusev, A A Rempel *Zh. Fiz. Khim.* **65** 625 (1991) [c]
18. A I Gusev *Dokl. Akad. Nauk* **322** 918 (1992) [a]
19. A A Rempel *Effekty Uporyadocheniya v Nestekhiometricheskikh Soedineniyakh Vnedreniya* (Effects of Ordering in Nonstoichiometric Interstitial Compounds) (Ekaterinburg: Nauka, 1992)
20. A I Gusev, A A Rempel *Dokl. Akad. Nauk* **332** 717 (1993) [a]
21. A I Gusev, A A Rempel *J. Phys. Chem. Solids* **55** 299 (1994)
22. A I Gusev, A A Rempel *Phys. Status Solidi A* **163** 273 (1997)
23. V N Lipatnikov, A Kottar, L V Zueva, A I Gusev *Fiz. Tv. Tela* **40** 1332 (1998) [b]
24. A I Gusev, A A Rempel, in *Materials Science of Carbides, Nitrides and Borides* (Eds Y G Gogotsi, R A Andrievski) (Dordrecht: Kluwer Academic, 1999) p. 47
25. V N Lipatnikov, A I Gusev, P Ettmayer, W Lengauer *J. Phys.: Condens. Matter* **11** 163 (1999)
26. V N Lipatnikov, A I Gusev, P Ettmaier, V Lengauer *Fiz. Tv. Tela* **41** 529 (1999) [b]
27. A I Gusev *Zh. Fiz. Khim.* **74** 600 (2000) [c]
28. V N Lipatnikov, A I Gusev *Uporyadochenie v Karbidakh Titana i Vanadiya* (The Ordering in Titanium and Vanadium Carbides) (Ekaterinburg: Urals Branch of the Russian Academy of Sciences, 2000)
29. V N Lipatnikov, A V Safonov, A I Gusev, A A Rempel, in *MSIT Workplace — Research Results* (Stuttgart: MSI, 2002) No. 50.10097.9.20.2002, p. 1
30. A I Gusev, S V Rempel, in *MSIT Workplace — Research Results* (Stuttgart: MSI, 2002) No. 50.12291.7.20.2002, p. 1
31. A I Gusev, A N Zyryanova, A A Rempel, in *MSIT Workplace — Research Results* (Stuttgart: MSI, 2002) No. 50.12273.5.20.2002, p. 1
32. A I Gusev, in *MSIT Workplace — Research Results* (Stuttgart: MSI, 2002) No. 50.10083.5.20.2002, p. 1
33. A I Gusev, A N Zyryanova, A A Rempel, in *MSIT Workplace — Research Results* (Stuttgart: MSI, 2002) No. 50.15740.9.20.2002, p. 1
34. A I Gusev, A N Zyryanova, A A Rempel, in *MSIT Workplace — Research Results* (Stuttgart: MSI, 2002) No. 50.12290.10.20.2002, p. 1
35. B C Guo, S Wei, J Purnell, S Buzza, A W Castleman *Science* **256** 515 (1992)
36. S Wei, B C Guo, J Purnell, S Buzza, A W Castleman *J. Phys. Chem.* **96** 4166 (1992)
37. E Rudy, S Windisch, C E Brukl, in *Ternary Phase Equilibria in Transition Metal–Boron–Carbon–Silicon Systems (Binary Systems) Tech. Report AFML-TR-65-2. Metals and Ceramics Division, Wright-Patterson Air Force Base, OH, 1967* Vol. XII, Pt. I, p. 1
38. E Rudy, S Windisch, C E Brukl *Planseeber. Pulvermet.* **16** 3 (1968)

39. E Rudy *Compendium of Phase Diagram Data. Final Tech. Report AFML TR-65-2. Metals and Ceramics Division, Air Force Materials Laboratory, Wright-Patterson Air Force Base, OH, 1969* Pt. V
40. W Huang *Z. Metallkd.* **82** 174 (1991)
41. O N Carlson, A N Ghaneya, J F Smith *Bull. Alloys Phase Diagrams* **6** 115 (1985)
42. E K Storms, in *Phase Equilibria Diagrams. Phase Diagrams for Ceramists* Vol. 10 (Ed. A E McHale) (Westerville, OH, 1994) p. 269
43. J Billingham, P S Bell, M H Lewis *Philos. Mag.* **25** 661 (1972)
44. E Rudy, C E Brukl *J. Am. Ceram. Soc.* **50** 265 (1967)
45. J Billingham, P S Bell, M H Lewis *Acta Crystallogr., Sect. A* **28** 602 (1972)
46. S I Alyamovskii, P V Gel'd, G P Shveikin, E N Shchetnikov *Zh. Neorg. Khim.* **13** 895 (1968) [d]
47. M P Arbuzov, B V Khaenko, V G Fak, Yu F Nosachev *Ukr. Fiz. Zh.* **22** 291 (1977)
48. T Athanassiadis, N Lorenzelli, C H de Novion *Ann. Chim. (Paris)* **12** 129 (1987)
49. D Rafaja, W Lengauer, P Ettmayer, V N Lipatnikov *J. Alloys Compd.* **269** 60 (1998)
50. E K Storms, A Lowe, E Baca, J Griffin *High Temp. Sci.* **5** 276 (1973)
51. B V Khaenko, V G Fak *Izv. Akad. Nauk SSSR, Neorg. Mater.* **14** 1294 (1978) [e]
52. H Wiesenberger, W Lengauer, P Ettmayer *Acta Mater.* **46** 651 (1998)
53. A I Gusev, A A Rempel *Strukturnye Fazovye Perekhody v Nestekhiometricheskikh Soedineniyakh* (Structural Phase Transitions in Non-stoichiometric Compounds) (Moscow: Nauka, 1988)
54. A A Rempel *Usp. Fiz. Nauk* **166** 33 (1996) [*Physic-Uspekhi* **39** 31 (1996)]
55. N M Volkova, P V Gel'd *Izv. Vyssh. Ucheb. Zaved., Tsvet. Metal.* (5) 89 (1963)
56. N M Volkova, P V Gel'd, in *Fiziko-khimicheskie Issledovaniya Soedinenii Redkikh Tugoplavkikh Elementov. Trudy Instituta Khimii UF Akad. Nauk SSSR* (Physicochemical Investigations of Compounds of Rare Refractory Elements. Proceedings of the Institute of Chemistry, Urals Branch of the Academy of Sciences of the USSR) (Sverdlovsk: Urals Branch of the Academy of Sciences of the USSR, 1966) No. 9, p. 23
57. W L Worrel, J Chipman *J. Phys. Chem.* **68** 860 (1964)
58. A I Gusev *Dokl. Akad. Nauk* **365** 644 (1999) [a]
59. O Kubashevski, A Evans, C B Alcock *Metallurgical Thermochemistry* (New York: Pergamon Press, 1958)
60. A I Gusev *Zh. Fiz. Khim.* **57** 1382 (1983) [c]
61. N M Volkova, P V Gel'd *Izv. Vyssh. Ucheb. Zaved., Tsvet. Metal.* (3) 77 (1965)
62. N M Volkova, P V Gel'd, in *Khimiya Soedinenii Redkikh Tugoplavkikh Elementov. Trudy Instituta Khimii UF AN SSSR* (The Chemistry of Compounds of Rare Refractory Elements. Proceedings of the Institute of Chemistry, Urals Branch of the Academy of Sciences of the USSR) (Sverdlovsk: Urals Branch of the Academy of Sciences of the USSR, 1967) No. 14, p. 41
63. A G Turchanin, E A Guseva, V V Morozov, A S Bolgar, V V Fesenko *Izv. Akad. Nauk SSSR, Neorg. Mater.* **10** 1619 (1974) [e]
64. L A Korolev, I I Spivak, M L Taubin *Izv. Akad. Nauk SSSR, Neorg. Mater.* **18** 54 (1982) [e]
65. V S Chernyaev, E N Shchetnikov, G P Shveikin, R P Krentsis, P V Gel'd *Izv. Akad. Nauk SSSR, Neorg. Mater.* **3** 789 (1967) [e]
66. V S Chernyaev, S M Letun, G P Shveikin, in *Fizicheskie Svoistva Metallov i Splavov. Trudy Ural'skogo Politekhnicheskogo Insituta* (Physical Properties of Metals and Alloys. Proceedings of Urals Polytechnic Institute) (Sverdlovsk: Urals Polytechnic Institute, 1970) No. 186, p. 167
67. V S Chernyaev, E N Shchetnikov, in *Khimiya Soedinenii Redkikh Tugoplavkikh Elementov. Trudy Instituta Khimii UF AN SSSR* (The Chemistry of Compounds of Rare Refractory Elements. Proceedings of the Institute of Chemistry, Urals Branch of the Academy of Sciences of the USSR) (Sverdlovsk: Urals Branch of the Academy of Sciences of the USSR, 1967) No. 14, p. 47
68. V N Lipatnikov, P Ettmayer, in *Proceedings of the 14th International Plansee Seminar* Vol. 2 (Eds G Kneringer, P Rödhammer, P Wilhartitz) (Reutte: Plansee AG, 1997) p. 485
69. V N Lipatnikov, W Lengauer, P Ettmayer, E Keil, G Groboth, E Kny *J. Alloys Compd.* **261** 192 (1997)
70. D H Lowndes, L Finegold, R G Lye *Philos. Mag.* **21** 245 (1970)
71. W L Worrel *J. Phys. Chem.* **68** 954 (1964)
72. V P Glushko (Ed.) *Termodinamicheskie Svoistva Individual'nykh Veshchestv* (Thermodynamic Properties of Pure Substances) (Moscow: Nauka, 1979)
73. R B Kotel'nikov, S N Bashlykov, Z G Galiakbarov, A I Kashtanov *Osobo Tugoplavkie Elementy i Soedineniya* (Extra Refractory Elements and Compounds) (Moscow: Metallurgiya, 1969)
74. A I Gusev *Usp. Khim.* **71** 507 (2002) [*Russ. Chem. Rev.* **71** 439 (2002)]
75. J P Hirth, G M Pound *Condensation and Evaporation-Nucleation and Growth Kinetics* (Oxford: Pergamon Press, 1963)
76. A I Gusev *Dokl. Akad. Nauk SSSR* **311** 631 (1990) [a]
77. A I Gusev *Teplofiz. Vysok. Temp.* **29** 695 (1991)
78. F J Kohl, C A Stearns *J. Phys. Chem.* **74** 2714 (1970)
79. S Fujishiro *Trans. Jpn. Inst. Met.* **1** 125 (1962)
80. S Fujishiro, N A Gokcen *J. Electrochem. Soc.* **109** 835 (1962)
81. A I Gusev *Teplofiz. Vysok. Temp.* **31** 216 (1993)
82. Yu A Izyumov, V E Naish, R P Ozerov *Neitronografiya Magnetikov* (Neutron Diffraction in Magnets) (Moscow: Atomizdat, 1981)
83. C Froidevaux, D Rossier *J. Phys. Chem. Solids* **28** 1197 (1967)
84. D Kahn, R G Lye *Bull. Am. Phys. Soc.* **14** 332 (1969)
85. A V Dmitriev, V K Kapustkin, R N Pletnev, V A Gubanov, Yu G Zainulin *Fiz. Tv. Tela* **25** 66 (1983) [b]
86. A V Dmitriev, R N Pletnev, V A Gubanov *Yadernyi Magnitnyi Rezonans i Defekty v Tugoplavkikh Soedineniyakh Vanadiya* (Nuclear Magnetic Resonance and Defects in Refractory Vanadium Compounds) (Sverdlovsk: Urals Scientific Cntre of Academy of Sciences of the USSR, 1983)
87. A A Rempel, A I Gusev *Phys. Status Solidi B* **130** 413 (1985)
88. A A Rempel, A I Gusev *Fiz. Met. Metalloved* **60** 847 (1985)
89. M Sauvage, E Parthe *Acta Crystallogr., Sect. A* **28** 607 (1972)
90. M Sauvage, E Parthe, W B Yelon *Acta Crystallogr., Sect. A* **30** 597 (1974)
91. C H de Novion, V Maurice *J. Phys. Colloq.* **38** 211 (1977)
92. K Hiraga, M Hirabayashi *J. Phys. Colloq.* **38** 224 (1977)
93. B V Khaenko *Izv. Akad. Nauk SSSR, Neorg. Mater.* **15** 1952 (1979) [e]
94. B V Khaenko *Poroshk. Metall.* (1) 71 (1978)
95. I Karimov, F Faizullaev, M Kalanov, A Emiraliev, A S Rakhimov, L Slepoi, V S Polishchuk *Dokl. Akad. Nauk Uzb.SSR* (2) 32 (1976)
96. I Karimov, F Faizullaev, M Kalanov, A Emiraliev, V S Polishchuk *Izv. Akad. Nauk Uzb.SSR, Ser. Fiz.-mat. Nauk* (4) 87 (1978)
97. I Karimov, F Faizullaev, M Kalanov, A Emiraliev, V S Polishchuk *Izv. Akad. Nauk Uzb.SSR, Ser. Fiz.-mat. Nauk* (4) 74 (1976)
98. R Kesri, S Hamar-Thibault *Acta Metall.* **36** 149 (1988)
99. A A Rempel, A I Gusev, V G Zubkov, G P Shveikin *Dokl. Akad. Nauk SSSR* **275** 883 (1984) [a]
100. A I Gusev, A A Rempel *Fiz. Tv. Tela* **26** 3622 (1984) [b]
101. A A Rempel, A I Gusev *Kristallografiya* **30** 1112 (1985) [f]
102. A I Gusev, A A Rempel *Phys. Status Solidi A* **93** 71 (1986)
103. D Kordes *Phys. Status Solidi* **26** K103 (1968)
104. A W Henfrey, B E F Fender *Acta Crystallogr., Sect. B* **26** 1882 (1970)
105. K Yvon, H Nowotny, R Kieffer *Monatsch. Chem.* **98** 34 (1967)
106. H Nowotny, F Benesovsky *Planseeber. Pulvermetall* **16** 204 (1968)
107. N Terao *C.R. Hebd. Seances Acad. Sci., Ser. C* **275** 1165 (1966)
108. I Karimov, F Faizullaev, I S Latergaus, V T Em *Izv. Akad. Nauk Uzb.SSR, Ser. Fiz.-mat. Nauk* (2) 65 (1988)
109. V T Em, I Karimov, F Faizullaev, I S Latergaus *Metallofizika* **10** 10 (1988)
110. M P Arbuzov, V G Fak, B V Khaenko *Izv. Akad. Nauk SSSR, Neorg. Mater.* **12** 846 (1976) [e]

111. K Yvon, W Rieger, H Nowotny *Monatsch. Chem.* **97** 689 (1966)
112. M P Arbuzov, B V Khaenko, V G Fak *Dokl. Akad. Nauk Ukr.SSR, Ser. A* (2) 153 (1977)
113. A Emiraliev, M Patiev, F Faizullaev, I Karimov *Izv. Vyssh. Ucheb. Zaved., Fiz.* (10) 34 (1986)
114. G L Dunlop, D A Porter *Scand. J. Metall.* **6** 19 (1977)
115. J D Venables, R G Lye *Philos. Mag.* **19** 565 (1969)
116. A G Khachaturyan *Teoriya Fazovykh Prevrashchenii i Struktura Tverdykh Rastvorov* (Theory of Phase Transformations and Structure of Solid Solutions) (Moscow: Nauka, 1974)
117. A I Gusev, A A Rempel *Phys. Status Solidi A* **135** 15 (1993)
118. A I Gusev, A A Rempel *J. Phys. C: Solid State Phys.* **20** 5011 (1987)
119. K Yvon, E Parthe *Acta Crystallogr., Sect. B* **26** 149 (1970)
120. A I Gusev *Usp. Fiz. Nauk* **168** 55 (1998) [*Physics-Uspekhi* **41** 49 (1998)]
121. A S Edelstein, R C Cammarata (Eds) *Nanomaterials: Synthesis, Properties and Applications* (Baltimor: The Johns Hopkins University, 1998)
122. A I Gusev *Nanokristallicheskie materialy: metody polucheniya i svoistva* (Nanocrystalline Materials: Methods of Production and Properties) (Ekaterinburg: Urals Branch of the Russian Academy of Sciences, 1998)
123. A I Gusev, A A Rempel *Nanokristallicheskie Materialy* (Nanocrystalline Materials) (Moscow: Fizmatlit-Nauka, 2000)
124. J Yi-Ru Ying (Ed.) *Nanostructured Materials* (New York: Academic Press, 2001)
125. A I Gusev, A A Rempel *Nanocrystalline Materials* (Cambridge: Cambridge Int. Sci. Publ., 2004)
126. A I Gusev, in *Dekker Encyclopedia of Nanoscience and Nanotechnology* (Eds H S Nalwa, J A Schwarz, C Contescu, K Putyera) (Austin: American Scientific Publ., 2004) p. 2289
127. A A Rempel, A I Gusev *Pis'ma Zh. Eksp. Teor. Fiz.* **69** 436 (1999) [g]
128. A A Rempel, O V Makarova, S Z Nazarova, A I Gusev, in *Ul'tradispersnye Poroshki, Nanostruktury, Materialy* (Superdispersed Powders, Nanostructurs, Materials) (Krasnoyarsk: Krasnoyarsk State Technological University, 1999) p. 168
129. A A Rempel, A I Gusev, O V Makarova, S Z Nazarova *Perspektiv. Mater.* (6) 9 (1999)
130. A I Gusev, A A Tulin, V N Lipatnikov, A A Rempel *Zh. Obshch. Khim.* **72** 1067 (2002) [h]
131. A I Gusev, A A Rempel, in *Nanostructures: Synthesis, Functional Properties and Applications (NATO Science Series II: Mathematics, Physics and Chemistry)* (Eds T Tsakalakos, I A Ovid'ko, A K Vasudevan) (Dordrecht, Boston, London: Kluwer Academic Publ., 2003) Vol. 128, p. 313
132. A A Rempel, M Foster, G-E Shefer *Dokl. Akad. Nauk* **326** 91 (1992) [a]
133. A A Rempel, M Forster, H-E Schaefer *J. Phys.: Condens. Matter* **5** 261 (1993)
134. A A Rempel, L V Zueva, V N Lipatnikov, H-E Schaefer *Phys. Status Solidi A* **169** R9 (1998)
135. A L Ivanovskii, A A Sofronov, Yu N Makurin *Teor. Eksp. Khim.* **35** 289 (1999) [i]
136. B C Guo, K P Kerns, A W Castleman *Science* **255** 1411 (1992)
137. J S Pilgrim, M A Duncan *J. Am. Chem. Soc.* **115** 6958 (1993)
138. S Wei, B C Guo, H T Deng, K Kerns, J Purnell, S Buzza, A W Castleman *J. Am. Chem. Soc.* **116** 4475 (1994)
139. S Wei, B C Guo, J Purnell, S Buzza, A W Castleman *Science* **256** 818 (1992)
140. A I Gusev, A A Rempel *Phys. Status Solidi B* **131** 43 (1985)
141. A I Gusev, A A Rempel *Phys. Status Solidi B* **140** 335 (1987)
142. A I Gusev *Philos. Mag. B* **60** 307 (1989)
143. N M Volkova, P V Gel'd, S I Alyamovskii *Zh. Neorg. Khim.* **10** 1758 (1965) [d]
144. G H Emmons, W S Williams *J. Mater. Sci.* **18** 2589 (1983)
145. L W Shacklette, W S Williams *Phys. Rev. B* **7** 5041 (1973)
146. K Hiraga *Philos. Mag.* **27** 1301 (1973)
147. J F Smith, in *Phase Diagrams of Binary Vanadium Alloys* (Ed. J F Smith) (Metals Park, OH: ASM Int. Publ., 1989) p. 33
148. V N Lipatnikov, A I Gusev, in *Tezisy Dokladov 5-go Vsesoyuznogo Soveshchaniya po Khimii, Tekhnologii i Primeneniyu Vanadievykh Soedinenii* (Abstracts of Reports of the 5th All-Union Meeting on Chemistry, Technology and Applications of Vanadium Compounds) (Ed. A V Chentsov) (Sverdlovsk: UNTs AN SSSR, 1987) Pt. 1, p. 166
149. R B King *Izv. Akad. Nauk, Ser. Khim.* 862 (1998) [j]

[a] — *Dokl. Chem. (Engl. Transl.)*
[b] — *Phys. Solid State (Engl. Transl.)*
[c] — *Russ. J. Phys. Chem. (Engl. Transl.)*
[d] — *Russ. J. Inorg. Chem. (Engl. Transl.)*
[e] — *Inorg. Mater. (Engl. Transl.)*
[f] — *Crystallogr. Rep. (Engl. Transl.)*
[g] — *J. Exp. Theor. Phys. Lett. (Engl. Transl.)*
[h] — *Russ. J. Gen. Chem. (Engl. Transl.)*
[i] — *Theor. Exp. Chem. (Engl. Transl.)*
[j] — *Russ. Chem. Bull., Int. Ed. (Engl. Transl.)*